

IRIDIUM-CATALYZED REDUCTION OF C-X BONDS (X = F, Cl, Br, I, O)
BONDS WITH TRIETHYLSILANE

Jian Yang

A dissertation submitted to the faculty of the University of North Carolina at Chapel Hill in partial fulfillment of the requirements for the degree of Doctor of Philosophy in the Department of Chemistry.

Chapel Hill
2008

Approved by:

Professor M. S. Brookhart

Professor M. R. Gagné

Professor C. K. Schauer

Professor J. L. Templeton

Professor V. S. Ashby

© 2008
Jian Yang
ALL RIGHTS RESERVED

ABSTRACT

JIAN YANG: Iridium-Catalyzed Reduction of C-X Bonds (X= F, Cl, Br, I, O) with Triethylsilane

(Under the direction of Professor Maurice Brookhart)

Alkyl halides are generally reduced with trialkyl tin hydrides via a radical chain mechanism. Alternative reduction procedures are desired owing to the toxicity of the tin reagents and problems separating tin byproducts from reduction products. We have discovered and developed a highly efficient and environmental friendly procedure for the reduction of a broad range of alkyl halides by triethylsilane reagents with cationic iridium pincer catalysts.

In-depth mechanistic studies have been carried out which have revealed a unique catalytic cycle. The electrophilic iridium hydride complex binds and activates the silane. This complex transfers “Et₃Si⁺” to the halide forming a highly active bridged halonium ion which is rapidly reduced by the iridium dihydride remaining following silyl transfer and the cationic iridium hydride complex is thus regenerated. All key intermediates have been identified by in situ NMR monitoring and kinetic studies have been completed. The key Ir(silane) intermediate has even been isolated and fully characterized by NMR spectroscopy and X-ray crystallography, which shows an unprecedented example of a cationic transition metal η^1 -silane complex.

In application of this novel chemistry to other organic functional groups, we have been particularly drawn to the cleavage and reduction of alkyl ethers, due to its several potential

applications. We have found that these cationic iridium pincer catalysts are highly active for the room-temperature cleavage and reduction of a wide variety of unactivated alkyl ethers with triethylsilane. For example, diethyl ether can be readily converted to two equivalents of ethane and $\text{Et}_3\text{SiOSiEt}_3$. Poly(ethylene glycol) can be readily degraded to $\text{Et}_3\text{SiOCH}_2\text{CH}_2\text{OSiEt}_3$ and ethane. Mechanistic studies have revealed the full details of the catalytic cycle with the resting state(s) depending on the basicity of the alkyl ether. The key intermediate diethyl(triethylsilyl)oxonium ion has been isolated and fully characterized by low temperature NMR spectroscopies and X-ray crystallography.

To: Lily

ACKNOWLEDGMENTS

I am now trying to catch up the graduate school deadline to submit this dissertation, and the only part left is acknowledgement. Nevertheless, this is the last but the most important part because without those people I acknowledge below I would not reach here.

Upon looking back, I always feel fortunate that I have made wonderful choices to come to North Carolina, join Brookhart group, and marry my wife, Lily. There are lucky and unlucky moments in graduate research, but Brook has always been a great advisor. He teaches me, encourages me, leads me into the area of organometallic chemistry, and helps me understand the arts and sciences of homogeneous catalysis. At this moment I sincerely thank him for invaluable guidance for last five years. I would also like to thank my undergraduate advisor, Prof. Dongyuan Zhao, for getting me started in chemical research. I am also grateful to my high school teacher, Mrs Guoyong Chen, who sparked my interest in chemistry, encouraged me to attend the Final of Chinese National Chemistry Olympiad and get the first prize award.

I am indebted to Dr. Peter White, a very nice person, who has solved a few very important crystal structures for me. Drs. David Harris and Dr. Marc ter Horst have also given me invaluable help in finding solutions for NMR problems I have met. I am grateful to Prof. Cindy Schauer for such an excellent teacher and collaborator. I would also like to thank other committee members, Profs. Joe Templeton, Mike Gagné, Ed Samulski and Valerie Ashby.

Importantly I would like to take this opportunity to thank all of my group members: Marc, Andy, Wes, Zheng, Stephanie, Azi, Nick, Michel, Eleanor, and Abby (I still consider you as a current group member!). I also thank all of the past members of Brookhart lab, especially Alison, Amy, Mark, Lei, Becky, Emily, Rick, James, Henri, Tom, Julia and Vasily. You guys have made a nice research environment and atmosphere for last five years. Particularly I am grateful to Marc and Mark, Alison and Amy, Rick and James who taught me most of my organometallic techniques in the lab.

Last but not least, I sincerely thank the constant support of my family, both in China and Chapel Hill. They have always been together with me and are those I can rely on. Of course, my wife Lily, marrying whom is the most fortunate thing that could happen to me.

PREFACE

The history of chemistry is a history of discovery and development, from the discovery of each element to the make of new element, from the discovery of active compounds to design of new drugs, etc. More specific and related (to organometallic chemistry) examples include but not limited to, from the discovery of Ziegler-Natta olefin polymerization catalysts to the development of homogeneous early metal metallocene catalysts and late metal Brookhart α -diimine catalysts, from the discovery of early metal olefin metathesis to the development of Ru Grubbs catalyst, from the discovery of a metal dihydrogen complex and agostic interactions to the later numerous examples of inter- and intramolecular σ -complexes.

The history of chemistry also teaches us that nothing is impossible. The enormous revival of late metal olefin polymerization catalysts in last decade tells a story of “it is all about ligands”. The intense debate and studies of silicon cation chemistry tells us “it is all about counteranions and nothing is non-coordinating”. The discovery and development of coordination chemistry of saturated molecules shows that “it is all about metals and coordination environments”. Developments from the first discoveries of C-H oxidative addition on iridium center to alkane dehydrogenation with thousands of turnovers tell that “It not only can be done but also can be done very efficiently”.

In this dissertation, the author wishes to tell a story of the discovery and development of a novel catalytic reduction chemistry, which constitutes majority of his graduate work, may only add a tiny example to the chemistry discovery and development though.

TABLE OF CONTENTS

LIST OF TABLES.....	xii
LIST OF SCHEMES.....	xiii
LIST OF FIGURES.....	xv
ABBREVIATIONS AND SYMBOLS.....	xvii

Chapter

I. Iridium-Catalyzed Reduction of Alkyl Halides with Triethylsilane: Discovery, Development, Mechanistic Studies and Application.....	1
1) Background and Introduction.....	1
2) Research Goals and Achievements.....	5
3) Results and Discussion.....	6
A. Synthesis of Cationic Iridium Bis(phosphinite) Pincer Catalyst: a Dichloromethane Complex, 2	6
B. Synthesis of a More Active and Stable Catalyst: The Cationic Iridium Acetone Complex, 3	7
C. Reduction of Alkyl Halides by Et ₃ SiH Catalyzed by Iridium Acetone Complex 3	8
D. Competition Experiments to Determine Relative Reactivities: Comparison with Conventional Radical-Based Reduction Chemistry.....	12
E. Comparison of Ir-Catalysis with AlCl ₃	15
F. Comparison of Ir-Catalysis with [Ph ₃ C][B(C ₆ F ₅) ₄].....	16

G.	In situ ^{31}P and ^1H NMR Monitoring of the Working Catalyst System: Identification of the Catalytic Resting State(s) and Key Intermediates.....	18
H.	Proposed Catalytic Cycle.....	20
I.	Preliminary Studies on In situ Generation of Triethylsilyl Iodonium Ion $[\text{Et}_3\text{Si-I-CH}_3]^+$, 14	23
J.	Reduction of (Chloromethyl)cyclopropane.....	24
K.	Application to Other Functional Groups.....	25
L.	Iridium-Catalyzed Hydrosilation of Acetone.....	26
M.	Auto-catalysis: Catalytic Hydrodechlorination of 1a with Et_3SiH	27
4)	Summary.....	28
5)	Experimental Section.....	30
6)	References.....	45
II.	Scope and Mechanism of the Iridium-Catalyzed Cleavage of Alkyl Ethers with Triethylsilane.....	47
1)	Introduction.....	47
2)	Results and Discussion.....	50
A.	Cleavage of Alkyl Ethers with Et_3SiH Catalyzed by Iridium Complex 1	50
B.	In situ ^{31}P and ^1H NMR Spectroscopic Monitoring of the Working Catalyst System for Et_2O Reduction: Identification of the Catalytic Resting State and Key Intermediates.....	53
C.	Effect of Adding Additional Iridium Dihydride, 5	57
D.	Generation, Spectroscopic and Structural Characterization and Dynamic Behavior of diethyl(triethylsilyl)oxonium and its Reactivity towards 5	58
E.	Catalytic Cleavage of Less Basic PhOCH_3 with Et_3SiH	60

F. Comparison of Ir-catalysis with $[\text{Ph}_3\text{C}][\text{B}(\text{C}_6\text{F}_5)_4]$ for Alkyl Ether Cleavage.....	64
3) Summary.....	67
4) Experimental Section.....	69
5) References.....	78
III. Structural and Spectroscopic Characterization and Dynamics of an Unprecedented Cationic Transition Metal η^1 -Silane Complex.....	81
1) Introduction.....	81
2) Results and Discussion.....	84
A. In Situ Generation and Spectroscopic Characterization of the Iridium σ - Et_3SiH complex $[(\text{POCOP})\text{Ir}(\text{H})(\text{Et}_3\text{SiH})]^+[\text{B}(\text{C}_6\text{F}_5)_4]^-$	84
B. X-ray Crystallography of 2	85
C. Density Functional Theory (DFT) Studies of Structure and Bonding of 2	87
D. Dynamics of 2 and Hydride Exchange Mechanisms.....	91
3) Summary.....	95
4) Experimental Section.....	96
5) References.....	100

LIST OF TABLES

Table

1.1	Iridium-catalyzed reduction of benzyl halides by Et ₃ SiH.....	9
1.2	Iridium-catalyzed reduction of primary alkyl halides by Et ₃ SiH.....	10
1.3	Iridium-catalyzed reduction of secondary and tertiary alkyl halides by Et ₃ SiH.....	11
1.4	Solvent-free reduction of alkyl halides with Et ₃ SiH catalyzed by 1	12
1.5	Competition experiments to determine the relative reactivities of primary alkyl chloride, bromide and iodide.....	14
1.6	X-ray crystal structure data for complex 3	33
2.1	Cleavage of alkyl ethers with Et ₃ SiH catalyzed by 1	51
2.2	X-ray crystal structure data for complex 7	74
3.1	Selected bond lengths (Å) and angles (°) and energies from DFT studies.....	88
3.2	Natural charges and NBO populations in the silane complexes.....	90
3.3	X-ray crystal structure data for complex 2	99

LIST OF SCHEMES

Scheme

1.1	Two-step chain process for the reduction of RX by organotin reagents.....	1
1.2	Proposed mechanism for reduction of alkyl fluorides with the $[\text{Ph}_3\text{C}][\text{B}(\text{C}_6\text{F}_5)_4]/\text{Et}_3\text{SiH}$ system.....	3
1.3	Unexpected iridium-catalyzed reduction of CD_2Cl_2 to CD_2H_2 by Et_3SiH	4
1.4	Chemoselectivity for alkyl halide reductions observed in the 3 / Et_3SiH system compared with conventional radical-based reductions.....	14
1.5	Comparison of Ir-catalysis with AlCl_3 catalysis.....	16
1.6	Methods for generating potential intermediates independently.....	19
1.7	Proposed catalytic cycle for iridium-catalyzed reduction of RX by Et_3SiH	21
1.8	Rearrangements of the Cyclopropylcarbinyl Radical (A) and the Cyclopropylcarbinyl Cation (B).....	25
1.9	Application of 3 / Et_3SiH to the reduction of other functional groups.....	26
2.1	Proposed catalytic cycle for iridium-catalyzed reduction of alkyl halides by triethylsilane.....	49
2.2	Fragmentation of poly(ethylene glycol) with 1 / Et_3SiH system.....	53
2.3	Proposed catalytic cycle for cleavage of Et_2O with 1 / Et_3SiH	56
2.4	Reaction of 7 with 5 at $-40\text{ }^\circ\text{C}$	60
2.5	Two mechanistic proposals for Ir-catalyzed cleavage of anisole with Et_3SiH	61
2.6	Proposed catalytic cycle for cleavage of PhOMe	63
2.7	Proposed catalytic cycle for Et_2O cleavage with $[\text{Ph}_3\text{C}][\text{B}(\text{C}_6\text{F}_5)_4]/\text{Et}_3\text{SiH}$	66
3.1	Interactions of R_3SiH with transition metal complexes.....	82
3.2	Proposed catalytic cycle for iridium-catalyzed reduction of C-X bonds.....	83
3.3	A proposed pathway for the reaction of silanes with metal fragment.....	87

3.4	Possible mechanisms of scrambling hydrides in 2	92
-----	--	----

LIST OF FIGURES

Figure

1.1	ORTEP diagram of complex 3	8
1.2	Plot of substrate concentration vs time for reduction of alkyl halides catalyzed by catalyst a : [Ph ₃ C][B(C ₆ F ₅) ₄] (top), and by catalyst b : iridium complex 3 (bottom).....	17
1.3	Characteristic ³¹ P NMR shifts used to identify key Ir species.....	18
1.4	Plot of the initial rate, V _i , vs. complex 3 concentration at 23 °C.....	21
1.5	Plot of the initial rate, V _i , vs. Et ₃ SiH concentration at 23 °C.....	22
1.6	Plot of the initial rate, V _i , vs. CH ₃ I concentration at 23 °C.....	22
1.7	Preliminary variable-temperature ¹³ C{ ¹ H} NMR studies of 14	24
1.8	Plot of concentration vs. time for the reduction of 1-chloropentane (0.54 M) and 2-chloropentane (0.54 M) with Et ₃ SiH (3.22 M) and complex 3 (5.4 mM) in C ₆ D ₄ Cl ₂ at 23 °C.....	35
1.9	Linear portions of the concentration vs. time curve used to determine the initial rates for the reduction of 1-chloropentane and 2-chloropentane.....	35
1.10	Plot of concentration vs. time for the reduction of 1-bromopentane (0.54 M) and 2-bromopentane (0.54 M) with Et ₃ SiH (3.22 M) and complex 3 (2.7 mM) in C ₆ D ₄ Cl ₂ at 23 °C.....	36
1.11	Linear portions of the concentration vs. time curve used to determine the initial rates for the reduction of 1-bromopentane and 2-bromopentane.....	36
1.12	Plot of concentration vs. time for the reduction of 1-iodobutane (0.54 M) and 2-iodobutane (0.54 M) with Et ₃ SiH (3.22 M) and complex 3 (5.4 mM) in C ₆ D ₄ Cl ₂ at 23 °C.....	37
1.13	Linear portions of the concentration vs. time curve used to determine the initial rate for the reduction of 1-iodobutane and 2-iodobutane.....	37
1.14	Plot of concentration vs. time during the first half life for the reduction of CH ₃ I (0.39 M) with Et ₃ SiH (1.18 M) and complex 3 (7.9 mM) in C ₆ D ₄ Cl ₂ at 23 °C.....	40

2.1	Plot of Et ₂ O concentration vs time for the cleavage of Et ₂ O with and without adding additional 5	57
2.2	An ORTEP diagram of the cation in 7	59
2.3	(Left): plot of PhOMe concentration vs time for the anisole cleavage catalyzed by 1 and 5 ; (right): plot of the initial rate, V _i , vs. concentration of 5 for the cleavage of anisole catalyzed by 1 and 5	61
2.4	Plot of the initial turnover frequency (TOF) vs. Et ₃ SiH concentration for the cleavage of anisole catalyzed by 1 and 5	62
2.5	Plot of PhOMe concentration vs time for anisole cleavage reactions catalyzed by catalyst a: [Ph ₃ C][B(C ₆ F ₅) ₄] and by catalyst b: complex 1	65
2.6	Plot of Et ₂ O concentration vs time for Et ₂ O cleavage reactions catalyzed by catalyst a: [Ph ₃ C][B(C ₆ F ₅) ₄] and by catalyst b: complex 1	65
3.1	An ORTEP diagram of the cation in 2 (hydrogens omitted).....	86
3.2	Selected minima for 3 and 4 , and corresponding space-filling diagrams (top view).....	89
3.3	Relevant orbitals for interaction between silane and iridium in 2	91
3.4	Variable temperature stacked ¹ H NMR spectra of 2 (hydride region).....	93
3.5	Calculated lowest energy transition state for exchange of the terminal and bridging hydrides in the trimmed complex 4	94

ABBREVIATIONS AND SYMBOLS

\ddagger	denotes transition state
σ	sigma bonding
π	pi bonding
$^{\circ}$	degrees
\AA	Angstrom
$^{\circ}\text{C}$	degrees Celsius
δ	chemical shift
μL	microliter
ΔG	change in free energy
Ar	aryl
br	broad
Cat.	Catalyst
Conv.	Conversion
d	doublet
DEPT	Double Excitation by Polarization Transfer
eq	equation
equiv.	equivalents
GC	gas chromatography
h	hour
Hz	hertz
<i>i</i> -Pr	isopropyl, $-\text{CH}(\text{CH}_3)_2$
J	scalar coupling constant

K_{eq}	equilibrium constant
kcal	kilocalorie
M	moles solute/liter solution
m	multiplet
min	minute
mol	moles
<i>n</i> -Bu	normal butyl, $-(CH_2)_3CH_3$
NMR	nuclear magnetic resonance
POCOP	2,6-(OP <i>t</i> Bu ₂) ₂ C ₆ H ₃
Ph	phenyl
ppm	parts per million
RX	alkyl halides
s	singlet
t	triplet
<i>t</i> -Bu	tertiary butyl, $-C(CH_3)_3$
TO	turnover
TOF	turnover frequency
TTMSS	tris(trimethylsilyl)silane
Vi	initial rate
vt	virtual triplet

CHAPTER ONE

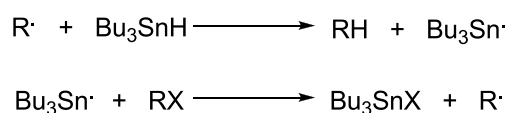
Iridium-Catalyzed Reduction of Alkyl Halides with Triethylsilane: Discovery, Development, Mechanistic Studies and Application.

(Part of this chapter has been adapted with permission from: Yang, J., Brookhart, M. *J. Am. Chem. Soc.* **2007**, *129*, 12656-12657. Copyright 2007 American Chemical Society.)

Background and Introduction

Reduction of alkyl halides to alkanes is a frequently practiced synthetic transformation. The most common method employed is the use of Bu_3SnH in a radical chain process.¹ While this is an efficient two-step chain process (Scheme 1.1), alternative reduction methods are desired owing to the toxicity of the tin reagents and difficulties in work-up and separation of tin halide by-products from the organic products.² The desired products are frequently contaminated by trace amounts of organotin complexes which prohibits their application in the synthesis of pharmaceuticals. Thus, replacing these highly toxic organotin reducing agents by environmentally benign alternatives is of increasing importance.

Scheme 1.1. Two-step Chain Process for the Reduction of RX by Organotin Reagents.



Other organometallic compounds such as Bu_3GeH and RHgH complexes have been explored as alternatives to Bu_3SnH as halide reducing agents, but they are not viable options for industrial applications due to high costs or high toxicities.^{2,3}

Although thermodynamically feasible, the use of readily available and cheap trialkyl silanes in place of tin hydrides for reduction is not effective due to the high bond energy of the Si-H bond which will not support a radical chain process. It was demonstrated that silicon-hydrogen bonds can be weakened dramatically by successive substitution of silyl groups at the Si-H function. Tris(trimethylsilyl)silane (TTMSS), therefore, is an efficient hydrogen donor and was used by Chatgililoglu et al. as a new free radical reducing reagent.² However, this TTMSS reagent is not economically attractive and also not easily made.

The success of TTMSS led to the exploration of other organosilanes as new radical-based reducing agents, including $(\text{Me}_3\text{Si})_2\text{SiHMe}$, $(\text{MeS})_3\text{SiH}$ and $(i\text{-PrS})_3\text{SiH}$.² These compounds are effective reducing agents for a variety of organic functionalities. The silanethiols $(\text{Me}_3\text{Si})_2\text{Si}(\text{SH})\text{Me}$ and $(\text{Me}_3\text{Si})_3\text{SiSH}$, which allow the transformation of a thiyl to a silyl radical via a fast intramolecular rearrangement, are also found to reduce alkyl halides through a radical mechanism.^{2,4} It has also been reported that Et_2SiH_2 and Et_3SiH can reduce alkyl halides to the corresponding alkanes in the presence of a suitable initiator and alkanethiols as polarity reversal catalysts.^{2,5}

Moreover, high loadings of strong Lewis acids like AlCl_3 have also been explored to mediate the reduction of alkyl halides by Et_3SiH .^{6a} Extensive skeletal rearrangements or Friedel-Crafts alkylation can occur accompanying this reduction chemistry.

Combination of $[\text{Ph}_3\text{C}][\text{B}(\text{C}_6\text{F}_5)_4]$ and Et_3SiH was recently demonstrated by Ozerov and co-workers to be capable of catalytic reduction of $\text{C}(\text{sp}^3)\text{-F}$ bonds via a mechanism involving

generation of carbocations through fluoride abstraction by Et_3Si^+ followed by hydride transfer to the carbocation by Et_3SiH (Scheme 1.2).^{7a} Similar chemistry has been described using a bisilylated onium salt.^{7b}

Scheme 1.2. Proposed Mechanism for Reduction of Alkyl Fluorides with the $[\text{Ph}_3\text{C}][\text{B}(\text{C}_6\text{F}_5)_4]/\text{Et}_3\text{SiH}$ System^{7a}

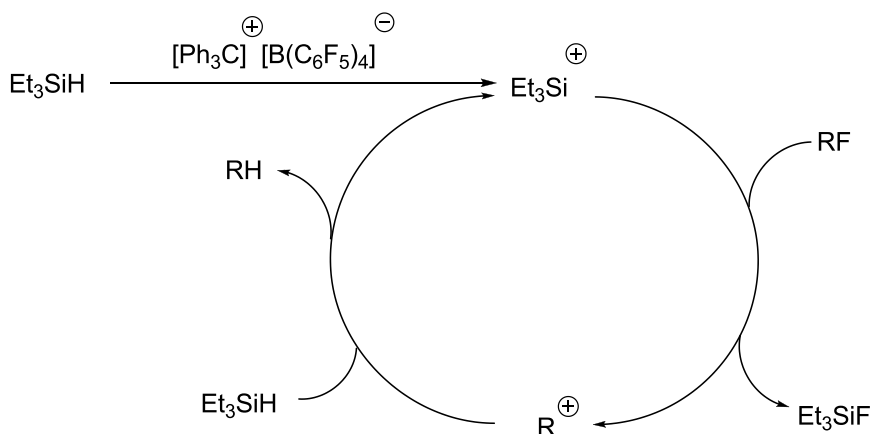
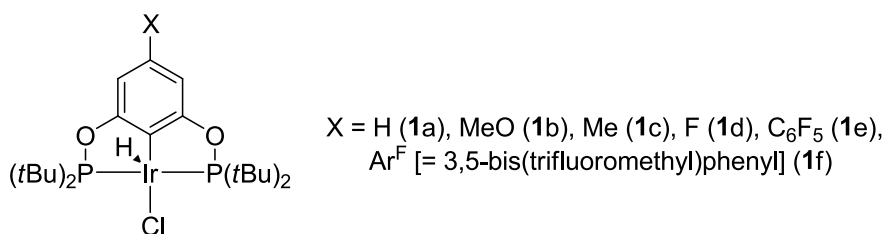


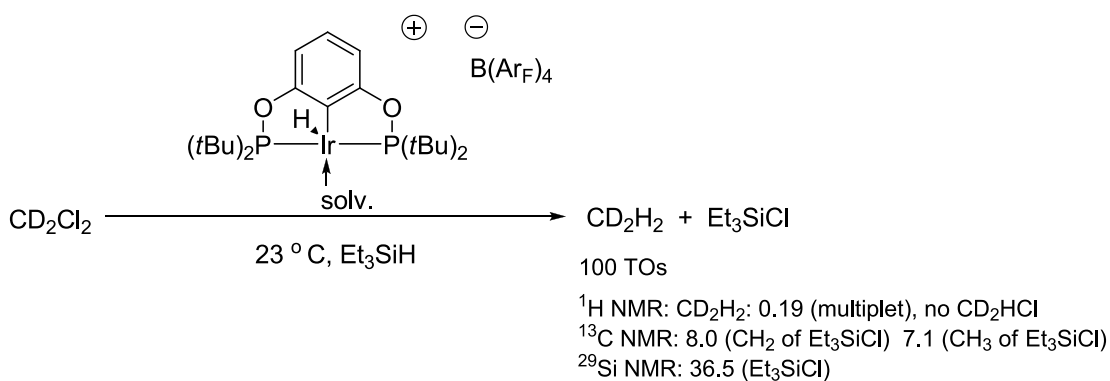
Chart 1.1. Iridium Bis(phosphinite) Pincer Complexes



Previously in our lab, iridium bis(phosphinite) pincer complexes (Chart 1.1) have been shown to be precursors to highly active catalysts for the transfer dehydrogenation of alkanes⁸ and are capable of N-H bond activation.⁹ By abstracting the chloride from $(\text{POCOP})\text{Ir}(\text{H})(\text{Cl})$ with $\text{NaB}(\text{Ar}_\text{F})_4$ [$\text{Ar}_\text{F} = 3, 5\text{-(CF}_3)_2\text{C}_6\text{H}_3$], a cationic iridium monohydride complex is generated. This in situ formed species was tested as a catalyst for dehydropolymerization of

silanes. Rather than dehydrocoupling of Et₃SiH, this cationic iridium complex was found to catalyze the reduction of methylene chloride to methane by Et₃SiH at room temperature with at least 100 turnovers (TOs) (Scheme 1.3).

Scheme 1.3. Unexpected Iridium-Catalyzed Reduction of CD₂Cl₂ to CD₂H₂ by Et₃SiH



More interestingly, since CD₂HCl should be the initial reduction product of CD₂Cl₂, the observation that only traces of CD₂HCl were identified during the reduction of CD₂Cl₂ indicates that the reduction of CD₂HCl is much more rapid than CD₂Cl₂. This observation suggests that this reduction chemistry probably does not go through the conventional radical-based process.

Research Goals and Achievements

The combination of a novel mechanism and practical utility strongly encouraged us to explore the scope, selectivities and mechanism of this reduction chemistry. Furthermore, we were also interested in application of the mechanistic understanding of alkyl halide reduction chemistry to the reduction of other organic functional groups.

Thus the remainder of this Chapter describes the development of these highly active cationic iridium hydride complexes for the reduction of primary, secondary and tertiary chlorides and bromides, primary iodides and even several types of alkyl fluorides. In-depth mechanistic studies have been carried out which have revealed a unique catalytic cycle. All key intermediates have been identified by NMR spectroscopy and kinetic studies have been completed.

Chapter Two details the use of these cationic iridium pincer catalysts for the room-temperature cleavage and reduction of a broad range of alkyl ethers with triethylsilane, as well as mechanistic details of these novel catalytic transformations including *isolation* and characterization of the key intermediate in the reduction of diethyl ether, diethyl(triethylsilyl)oxonium ion.

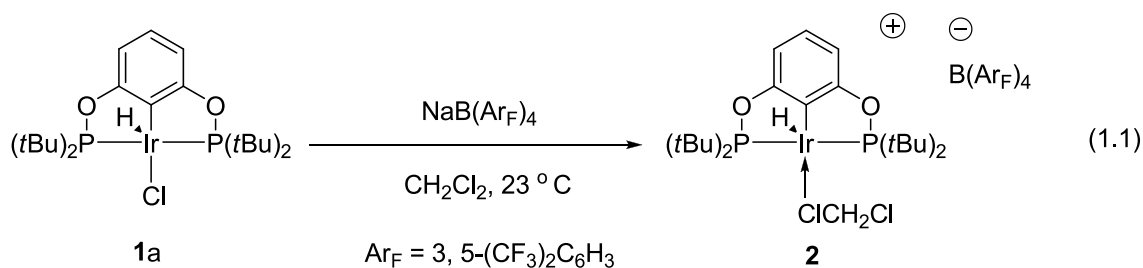
Chapter Three focuses on the isolation and complete characterization of the key cationic σ -silane intermediate for this reduction chemistry. X-ray crystallography in combination with DFT studies shows it to be an unprecedented example of the transition metal η^1 -silane complex with a unique dynamic process for scrambling hydrides.

Results and Discussion

A. Synthesis of Cationic Iridium Bis(phosphinite) Pincer Catalyst: a Dichloromethane Complex, **2**.

First of all, the inactivity of Ir(POCOP)HCl **1a** under identical conditions for reduction of CD₂Cl₂ excludes the possibility of Ir(POCOP)HCl as the catalytically active species for this reduction. NaB(Ar_F)₄ [Ar_F = 3, 5-(CF₃)₂C₆H₃] does not catalyze the reduction of CD₂Cl₂ either. Thus the catalytically active species must be the cationic monohydride complex generated from the reaction between Ir(POCOP)HCl and NaB(Ar_F)₄.

Catalysis with the in situ generated cationic catalyst often produces inconsistent results; therefore, the isolation of the active catalyst is crucial. The cationic iridium dichloromethane complex, **2**, was then synthesized and isolated by treatment of **1a** with slightly excess of NaB(Ar_F)₄ in dichloromethane (eq 1.1). Complex **2** was fully characterized by NMR spectroscopies and elemental analysis (see experimental section).

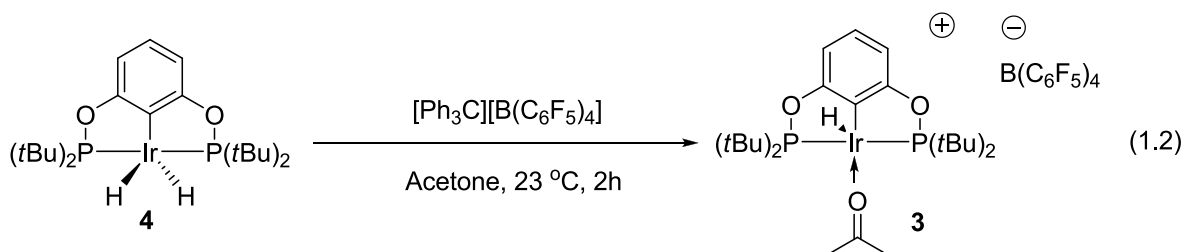


This cationic iridium dichloromethane complex, **2**, was found to be an efficient catalyst for the reduction of a variety of alkyl chlorides and bromides. However, at higher reaction temperatures (60 °C or 110 °C) with certain substrates, a small amount of Et₃SiF was identified by ¹³C and ¹⁹F NMR, which presumably due to the attack of “Et₃Si⁺” on B(Ar_F)₄[−].

counteranion. Therefore, in order to get a more stable and active catalyst, we turn to the $\text{B}(\text{C}_6\text{F}_5)_4^-$ counteranion.

B. Synthesis of a More Active and Stable Catalyst: The Cationic Iridium Acetone Complex, **3**.

Synthesis and isolation of **2** possessing a $\text{B}(\text{C}_6\text{F}_5)_4^-$ counteranion is not straight forward. The chloride abstraction route analogous to that described in eq 1 does not work presumably due to the poor solubility of $\text{KB}(\text{C}_6\text{F}_5)_4$ salts in a variety of solvents and the strong iridium-chlorine bond. Another synthetic route was then employed. The synthesis of **3** is readily achieved in 94% isolated yield by treatment of dihydride **4**¹⁰ with $[\text{Ph}_3\text{C}][\text{B}(\text{C}_6\text{F}_5)_4]$ in acetone (eq 1.2). Catalyst **3** is very stable because acetone binds tightly to the cationic Ir(III) center. Exposure of **3** to Et_3SiH results in rapid hydrosilation of acetone and forms noncoordinating $(\text{CH}_3)_2\text{CHOSiEt}_3$ and the highly reactive solvated complex which initiates reduction reactions.¹¹



Complete spectroscopic characterization is described in the experimental section. Crystals of iridium complex **3** were grown from slow diffusion of pentane into an acetone solution of complex **3**. The ORTEP diagram of **3** is shown in Figure 1.1. Acetone is coordinated through oxygen to the iridium(III) center *trans* to the *ipso* carbon of the tridentate POCOP ligand backbone. The hydrogen bound to Ir was not located in the X-ray diffraction experiment, but

was placed in a calculated position based on a square-pyramidal geometry at Ir assigned on the basis of the ^1H NMR data.

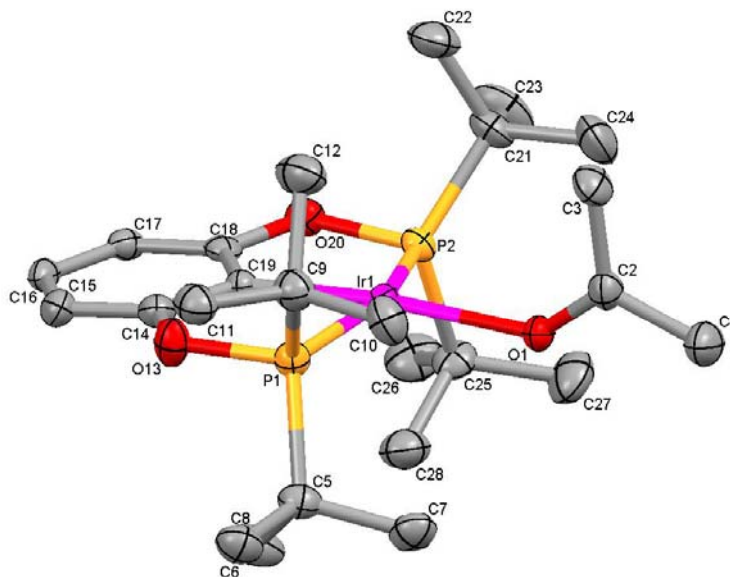


Figure 1.1. ORTEP diagram of complex **3** (the iridium hydride observed by ^1H NMR spectroscopy not located; $\text{B}(\text{C}_6\text{F}_5)_4^-$ not shown for clarity). Key bond distances (\AA) and bond angles (deg): $\text{Ir}(1)\text{-C}(19) = 2.018(4)$, $\text{Ir}(1)\text{-O}(1) = 2.178(3)$, $\text{Ir}(1)\text{-P}(2) = 2.3025(11)$, $\text{Ir}(1)\text{-P}(1) = 2.3253(10)$, $\text{P}(1)\text{-O}(13) = 1.656(3)$, $\text{P}(2)\text{-O}(20) = 1.654(3)$, $\text{O}(1)\text{-C}(2) = 1.235(5)$; $\text{C}(19)\text{-Ir}(1)\text{-O}(1) = 172.99(13)$, $\text{C}(19)\text{-Ir}(1)\text{-P}(2) = 79.98(12)$, $\text{O}(1)\text{-Ir}(1)\text{-P}(2) = 99.34(8)$, $\text{C}(19)\text{-Ir}(1)\text{-P}(1) = 79.78(12)$, $\text{O}(1)\text{-Ir}(1)\text{-P}(1) = 100.25(8)$, $\text{P}(2)\text{-Ir}(1)\text{-P}(1) = 159.37(4)$.

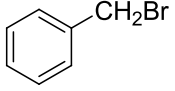
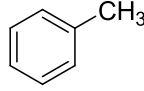
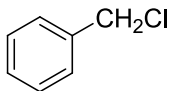
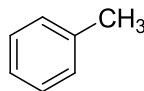
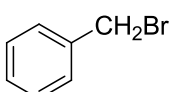
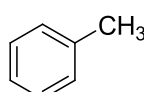
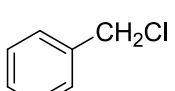
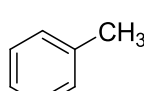
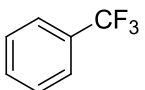
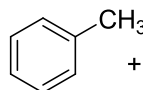
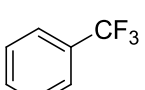
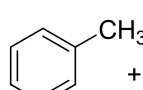
C. Reduction of Alkyl Halides by Et_3SiH Catalyzed by Iridium Acetone Complex **3**.

A broad spectrum of alkyl halides are conveniently reduced by triethylsilane in the presence of a catalytic amount of **3** in chlorobenzene. Fluorobenzene, dichlorobenzene and neat alkyl halides (see below) have also proved to be suitable solvents. Catalyst loadings of

0.5 mol% are generally used (but can be much lower, see below) together with 3 equiv. of Et₃SiH; temperatures of 23-60 °C are employed depending on substrate.

Table 1.1. Iridium-Catalyzed Reduction of Benzyl Halides by Et₃SiH^a

$$\text{PhCH}_2\text{X} + \text{Et}_3\text{SiH} \xrightarrow[23-100\text{ }^\circ\text{C}]{0.01-0.5\text{ mol\% } \mathbf{3}} \text{PhCH}_3 + \text{Et}_3\text{SiX}$$

Entry	Cat. mol %	RX	T °C	Solv. ^b	t h	Conv. ^c %	Product
1	0.5		23	A	0.3	>99	
2	0.5		23	A	0.3	>99	
3	0.075		23	A	2.5	>99	
4	0.01		23	B	29	32	
5 ^d	0.5		60	A	64	9	 + alkylation products
6 ^d	0.5		100	A	5	10	 + alkylation products

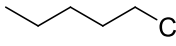
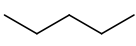
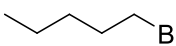
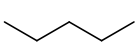
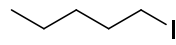
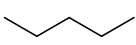
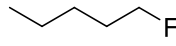
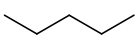
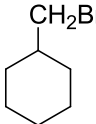
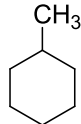
^a Reaction conditions: 3 equiv. of Et₃SiH. ^b Solvent: A, C₆D₅Cl; B, C₆D₄Cl₂. ^c Determined by loss of alkyl halides by NMR. ^d conversions were determined by formation of Et₃SiF by ¹⁹F NMR spectroscopy; reduction products were not fully identified.

Benzyl halides were first explored as reduction substrates. Results of typical reductions are illustrated in Table 1.1. Conversions were determined by ¹H NMR spectroscopy (conversions for alkyl fluoride reductions were determined by ¹⁹F NMR spectroscopy). Entries 1-2 show that benzyl chloride and benzyl bromide are rapidly reduced at 23 °C, 0.5% catalyst loading.

With 0.075% loading, complete reduction of benzyl bromide (1330 TOs) is accomplished in 2.5 h at 23 °C. At 0.01% loading 3200 TOs for reduction of benzyl chloride are achieved after 29 h. Entries 5-6 show that α, α, α -trifluorotoluene can also be reduced at either 60 °C or 100 °C but with limited efficiency (up to 20 TOs based on loss of C-F bonds) and poor selectivity (alkylation products in addition to toluene are observed).

Table 1.2. Iridium-Catalyzed Reduction of Primary Alkyl Halides by Et₃SiH^a

$$\text{RX} + \text{Et}_3\text{SiH} \xrightarrow[23-60\text{ }^\circ\text{C, chlorobenzene-d}^5]{0.5-2.0\text{ mol\% } \mathbf{3}} \text{RH} + \text{Et}_3\text{SiX}$$

Entry	Cat. mol %	RX	T/ °C	t/ h	Conv. ^b / %	Product
1	0.5		60	7	>99	
2	0.5		60	1.5	>99	
3	0.5		60	48	>99	
4 ^c	2.0		60	50	92	
5	1.0		23	51	>99	

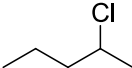
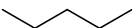
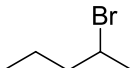
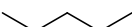
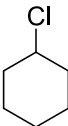
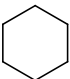
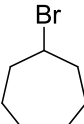

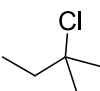
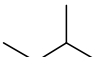
^a Reaction conditions: 3 equiv. of Et₃SiH. ^b Determined by loss of alkyl halides by NMR.

^c Products in addition to pentane are observed.

Results of reduction of simple primary alkyl halides are shown in Table 1.2. Rapid reduction of 1-bromopentane occurs at 60 °C (0.5% **3**) while under similar conditions 1-chloropentane requires ca. 7 h for complete reduction. Surprisingly, reduction of iodides is very slow and it takes about 48 h for complete conversion of 1-iodopentane to pentane at 60 °C with 0.5% loading of **3**. Entry 6 shows that 1-fluoropentane can also be reduced at 2% catalyst loading at 60 °C although with reduced efficiency (46 TOs based on loss of C-F

bonds) and selectivity (unidentified products in addition to pentane are observed). (Bromomethyl)cyclohexane can also be reduced to methyl cyclohexane with 0.5% catalyst loading at 23 °C (entry 5).

Table 1.3. Iridium-Catalyzed Reduction of Secondary and Tertiary Alkyl Halides by Et₃SiH^a

$\text{RX} + \text{Et}_3\text{SiH} \xrightarrow[23-60\text{ }^\circ\text{C, chlorobenzene-d}^5]{0.5\text{ mol\% } \mathbf{3}} \text{RH} + \text{Et}_3\text{SiX}$						
Entry	Cat. mol %	RX	T/ °C	t/ h	Conv. ^b / %	Product
1 ^c	0.5		60	2.3	>99	
2 ^c	0.5		60	0.7	>99	
3 ^c	0.5		60	16	>99	
4 ^c	0.5		23	0.3	>99	
5 ^c	0.5		23	0.3	>99	
6	0.5	Ph ₃ CCl	23	0.3	>99	Ph ₃ CH

^a Reaction conditions: 3 equiv. of Et₃SiH. ^b Determined by loss of alkyl halides by NMR.

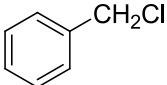
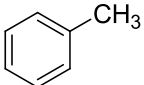
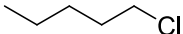
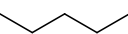
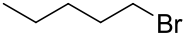
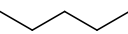
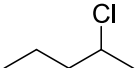
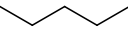
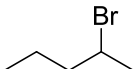
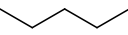
^c In addition to alkane, traces of olefin and H₂ were observed and converted to alkanes at longer reaction times.

Reductions of simple secondary halides are shown in entries 1-4 of Table 1.3. Like the primary halides, efficient reductions can be accomplished in chlorobenzene or in neat alkyl halide at either 60 or 23 °C and bromides are reduced more rapidly than chlorides. Bromocycloheptane is efficiently and selectively reduced to cycloheptane without

observation of the skeletal rearrangement product, methyl cyclohexane (entry 4). The tertiary chlorides, trityl chloride and *tert*-pentyl chloride, are reduced rapidly at 23 °C (entries 5-6).

The catalytic reduction can also be carried out in a solvent-free manner as illustrated in Table 1.4. Thus reduction of neat benzyl chloride can be achieved with 200 TOs in less than 20 minutes at room temperature (entry 1). Similarly, primary and secondary chlorides and bromides are reduced efficiently at 23 °C without a solvent (entry 2-5).

Table 1.4. Solvent-Free Reduction of Alkyl Halides with Et₃SiH Catalyzed by **1**^a

$\text{RX} + \text{Et}_3\text{SiH} \xrightarrow[23\text{ }^\circ\text{C, neat condition}]{0.5\text{ mol\% } \mathbf{3}} \text{RH} + \text{Et}_3\text{SiX}$				
Entry	RX	t/ h	Conv. ^b / %	Product
1		0.3	99	
2		20	86	
3		3.3	98	
4 ^c		9	99	
5 ^c		3.3	98	

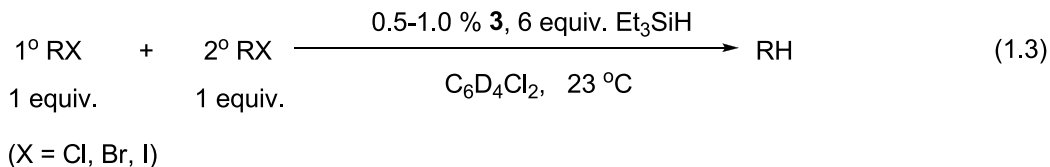
^a Reaction conditions: 3 equiv. of Et₃SiH. ^b Determined by loss of alkyl halides by NMR.

^c In addition to alkane, traces of olefin and H₂ were observed and converted to alkanes at longer reaction times.

D. Competition Experiments to Determine Relative Reactivities: Comparison with Conventional Radical-Based Reduction Chemistry.

To determine relative reactivities of primary and secondary halides, competition experiments were performed by treating a 1:1 molar ratio of the two pentyl halides in C₆D₄Cl₂ with 6 equiv Et₃SiH and 1% **3** and monitoring initial rates of reduction of the halides

at 23°C by ^1H NMR (eq 1.3). The following relative rates were determined: 1-chloropentane:2-chloropentane = 2.6:1.0, 1-bromopentane:2-bromopentane = 2.0:1.0 and 1-iodobutane:2-iodobutane = 1.6:1.0.



Results in Table 1.2 and 1.3 show that, qualitatively, reactivities follow the order $\text{RBr} > \text{RCl} > \text{RI}$ when reductions are carried out in separate flasks. Quite different results are seen when two different halides compete for reduction in the same flask. The experimental protocol is summarized in eq 1.4 and results are shown in Table 1.5. In a representative experiment, 1-iodoheptane (1 equiv) and 1-bromohexane (80 equiv) were treated with 30 equiv. of Et_3SiH and 5% **3**. Analysis of heptane and hexane very early in the reaction (less than 12.5% conversion of 1-iodoheptane) established a relative reactivity ratio of 80:1 for primary iodide: primary bromide. Bromide vs. chloride and iodide vs. chloride values are shown in the Table 1.5 and establish that in head-to-head competition $\text{RI} > \text{RBr} > \text{RCl}$. These results show that highly chemoselective reductions can be achieved.

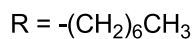
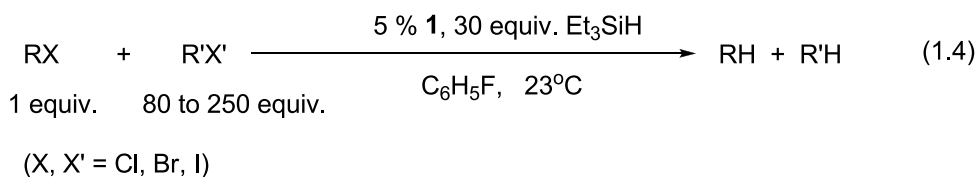


Table 1.5. Competition Experiments to Determine the Relative Reactivities of Primary Alkyl Chloride, Bromide and Iodide.

entry	RX	R'X'	R'X'/RX	relative reactivities (RX/R'X')
1	1-Iodoheptane	1-Chlorohexane	250	1200
2	1-Bromoheptane	1-Chlorohexane	200	260
3	1-Iodoheptane	1-Bromohexane	80	80

Thus the reduction selectivities found for the **3**/Et₃SiH system are very different from those based on the radical chain process,^{1,2} where general reactivities of RI>RBr>RCl and 2° RX>1° RX (2° RX = secondary alkyl halides; 1° RX = primary alkyl halides) are typically observed (Scheme 1.4). Only traces of CD₂HCl were observed during the reduction of CD₂Cl₂ by **3**/Et₃SiH which shows that CD₂HCl is reduced much faster than CD₂Cl₂, a result of which is also inconsistent with a radical mechanism.

Scheme 1.4. Chemoselectivity for Alkyl Halide Reductions Observed in the **3**/Et₃SiH System Compared with Conventional Radical-Based Reductions

Conventional Bu₃SnH based method:

RI > RBr > RCl

RF no reaction

3° RX > 2° RX > 1° RX

CCl₄ > CCl₃H > CH₂Cl₂ > CH₃Cl

Ir / Et₃SiH process:

RI > RBr > RCl (head-to-head competition)

RBr > RCl > RI (separate flasks)

1° RX > 2° RX (head-to-head competition)

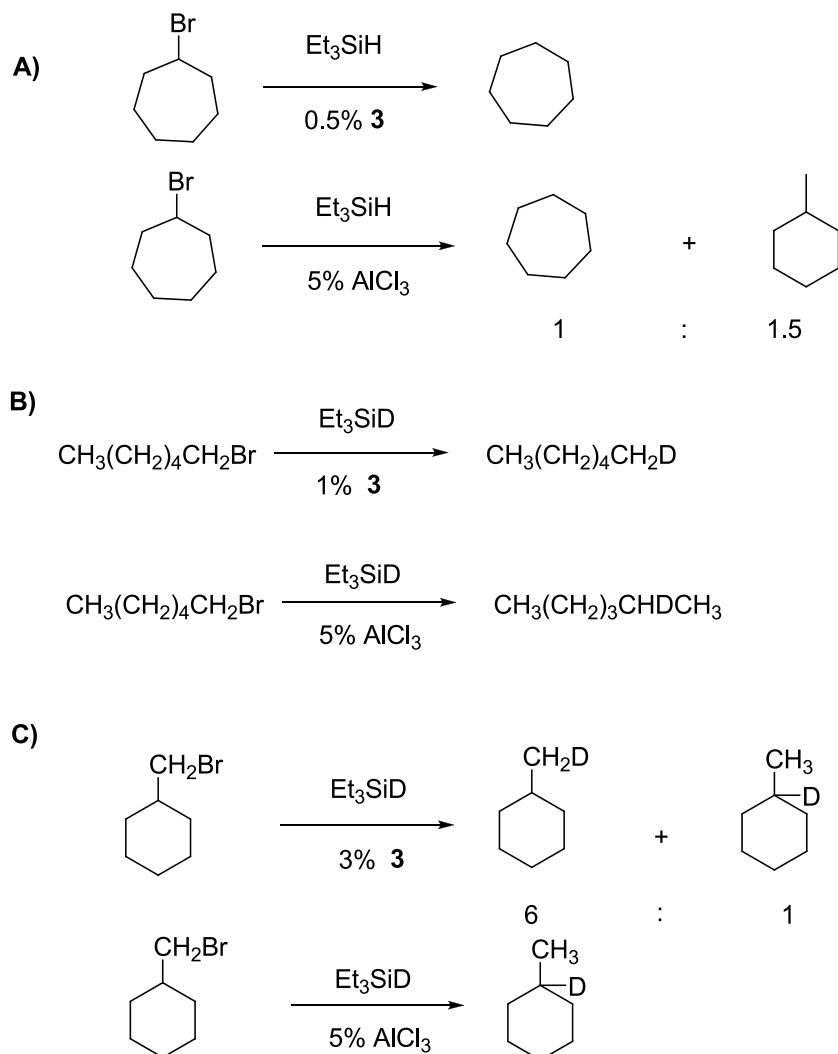
CH₃Cl > CH₂Cl₂

E. Comparison of Ir-Catalysis with AlCl_3 .

Strong Lewis acid AlCl_3 was explored about three decades ago by Doyle et al. to mediate the reduction of alkyl halides by Et_3SiH .^{6a} No major difference in reactivity was found between comparable alkyl bromides and chlorides. Reduction by triethylsilane was often accompanied by extensive skeletal rearrangements or Friedel-Crafts alkylation reactions (Scheme 1.5). The rearrangement to 1-bromo-1-methylcyclohexane was observed in the reduction of bromocycloheptane. Formation of 2-deuteriohexane or 1-deuterio-1-methylcyclohexane from reductions of 1-bromohexane and (bromomethyl)cyclohexane, respectively, using $\text{AlCl}_3/\text{Et}_3\text{SiD}$ suggests a mechanism involving carbocation-like intermediates in which the carbocation rearrangement precedes the reduction event.

In contrast to the AlCl_3 -catalyzed process, we observed quite different chemistry for the **3**/ Et_3SiH system (Scheme 1.5). Cycloheptane was the only observable reduction product (>99% conversion) from bromocycloheptane. When treated with Et_3SiD , 1-bromohexane yielded solely 1-deuteriohexane while (bromomethyl)cyclohexane gave (deuteriomethyl)cyclohexane as the major reduction product and 1-deuterio-1-methylcyclohexane as the minor product (ca. 6:1 ratio as determined by $^{13}\text{C}\{^1\text{H}\}$ NMR spectroscopy). These results suggest that the two catalytic systems behaved differently.

Scheme 1.5. Comparison of Ir-Catalysis with AlCl₃ Catalysis^{6a}



F. Comparison of Ir-Catalysis with [Ph₃C][B(C₆F₅)₄].

The combination of [Ph₃C][B(C₆F₅)₄]/Et₃SiH was recently reported to catalytically cleave alkyl fluorides via a mechanism involving generation of carbocations through fluoride abstraction by Et₃Si⁺ followed by hydride transfer to the carbocation by Et₃SiH.^{7a} To gain more insight into the **3**/Et₃SiH system, we compared the catalytic reactivities of **3** with [Ph₃C][B(C₆F₅)₄] for alkyl chloride reductions. Thus a mixture of a 1:1 molar ratio of 1-

chloropentane and 2-chloropentane was treated with 6 equiv. of Et_3SiH and 1% catalyst (**a**: $[\text{Ph}_3\text{C}][\text{B}(\text{C}_6\text{F}_5)_4]$; **b**: complex **3**) and the reaction was monitored by ^1H NMR spectroscopy (eq 1.5).

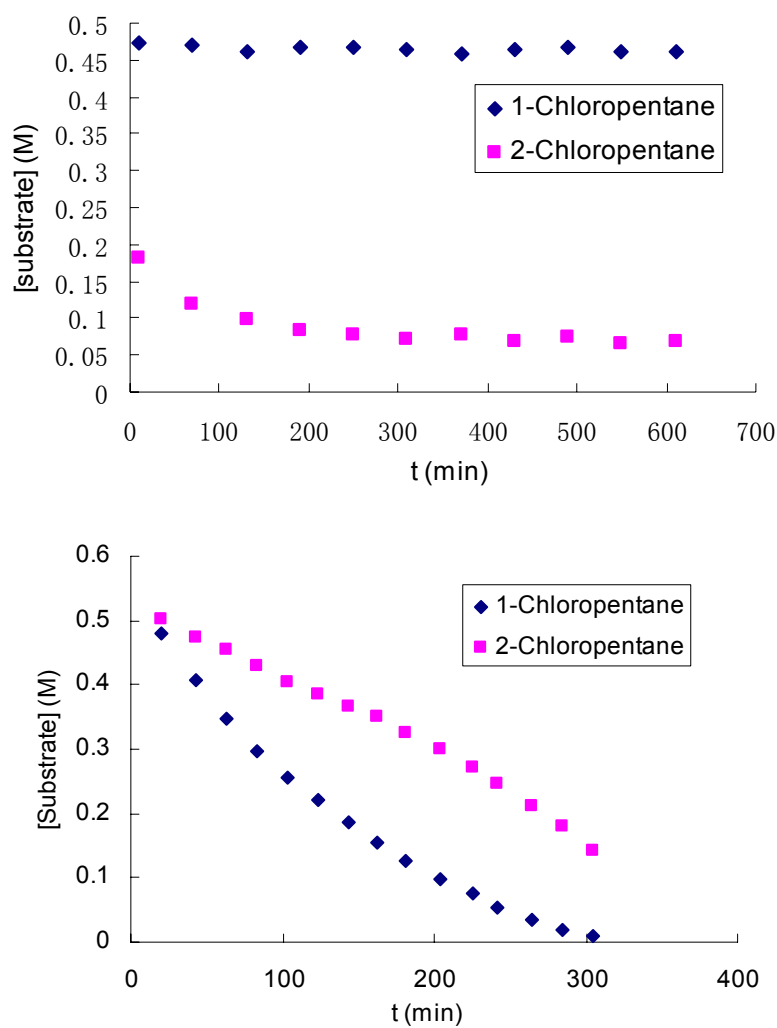
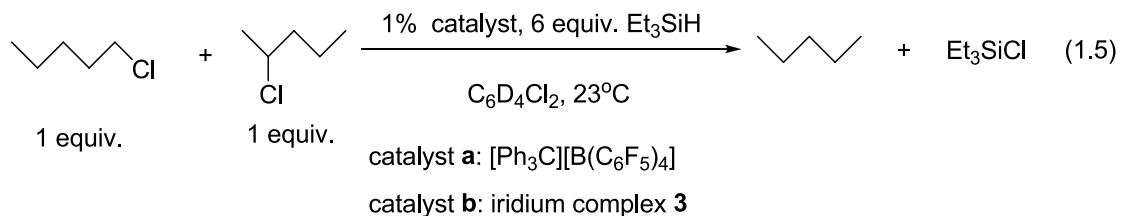


Figure 1.2. Plot of substrate concentration vs time for reduction of alkyl halides catalyzed by catalyst **a**: $[\text{Ph}_3\text{C}][\text{B}(\text{C}_6\text{F}_5)_4]$ (top), and by catalyst **b**: iridium complex **3** (bottom).

As shown in Figure 1.2a, in the $[\text{Ph}_3\text{C}][\text{B}(\text{C}_6\text{F}_5)_4]/\text{Et}_3\text{SiH}$ system, the secondary chloride was reduced more rapidly but only up to 80% conversion presumably due to the decomposition of the catalyst. If formation of a carbocation is rate-determining, then this is the expected order. In contrast, in the reduction system based on **3** (Figure 1.2b), head-to-head competition establishes that the primary chloride is more reactive than the secondary chloride, which is inconsistent with rate-determining formation of a carbocation or carbocation-like intermediate.

G. In situ ^{31}P and ^1H NMR Monitoring of the Working Catalyst System: Identification of the Catalytic Resting State(s) and Key Intermediates.

Substantial mechanistic details were uncovered by *in situ* ^1H and ^{31}P NMR monitoring of working catalyst systems, with ^{31}P NMR data being the more useful. First, potential intermediates were generated independently and their ^{31}P NMR spectra recorded. The ^{31}P chemical shifts for these species are summarized in Figure 1.3 and the means of generating them are described in Scheme 1.6.

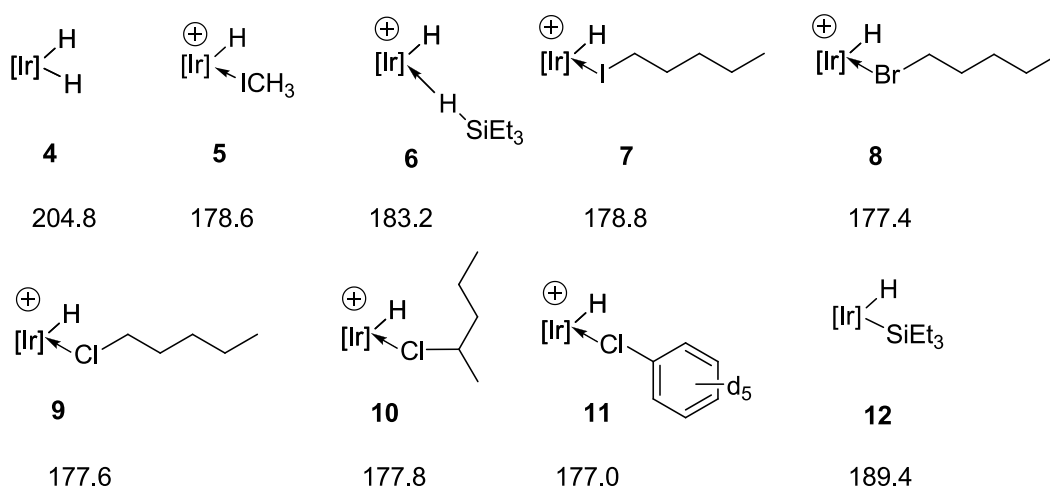
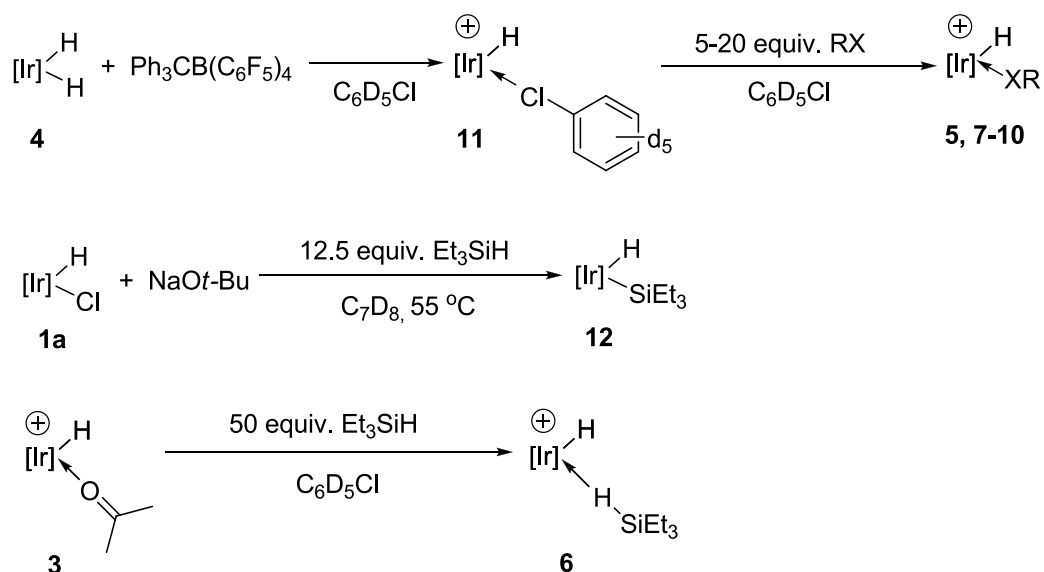


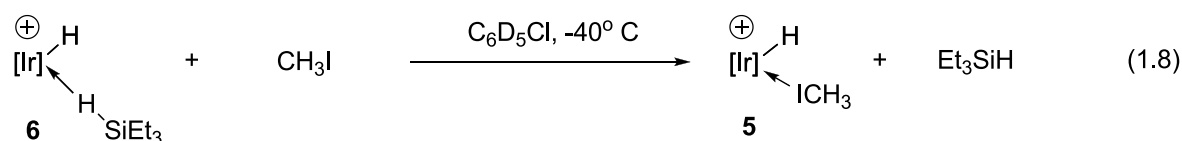
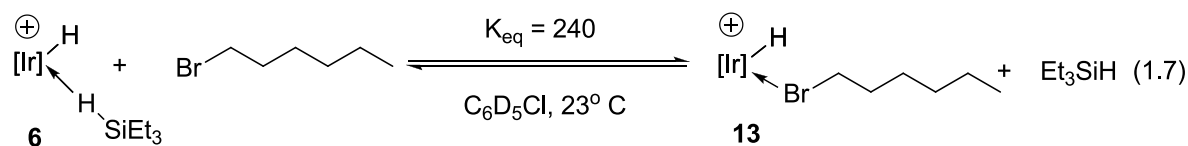
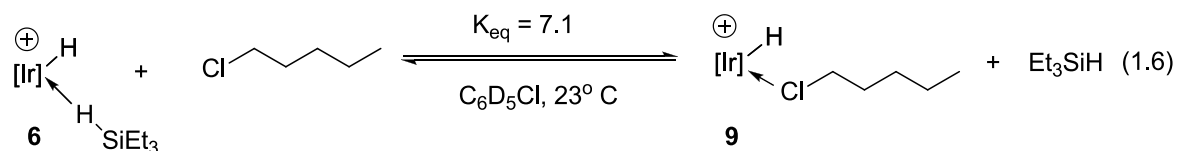
Figure 1.3. Characteristic ^{31}P NMR Shifts Used to Identify Key Ir Species.

Scheme 1.6. Methods for Generating Potential Intermediates Independently



To identify the potential catalyst resting state and key intermediates for this process, the reduction of alkyl halides was performed under catalytic conditions and monitored by ^1H , $^{13}\text{C}\{^1\text{H}\}$ and $^{31}\text{P}\{^1\text{H}\}$ NMR spectroscopy. Exposure of the acetone complex **3** to Et_3SiH results in rapid formation of $(\text{CH}_3)_2\text{CHOSiEt}_3$ and a highly reactive solvated complex which initiates the reaction.

The catalyst resting states were found to depend on the relative binding affinities of the silane and the alkyl halide. Following the in situ reduction of CH_3I at 23°C shows that the only Ir species present is the CH_3I complex, **5**. However, monitoring the reduction of either 1-chloropentane or 1-bromohexane shows that the Ir species exist as an equilibrium mixture of the halide complex (**9** or **13**) and the silane complex **6** with the ratio depending on the ratio of silane: halide and the nature of the halide (eq 1.6 and 1.7). A low temperature NMR experiment also shows that the reaction between silane complex and iodomethane is rapid relative to reduction (eq 1.8).



H. Proposed Catalytic Cycle.

A plausible catalytic cycle accounting for all observations has been proposed (Scheme 1.6). The cationic iridium hydride binds and activates the silane. Then the cationic silane complex, $(\text{POCOP})\text{Ir}(\text{H})(\text{Et}_3\text{SiH})^+$, serves as a potent silylating reagent to generate silyl halonium ions, Et_3SiXR^+ , which are then reduced by the neutral iridium dihydride to yield alkane product and regenerate the cationic $(\text{POCOP})\text{IrH}^+$ and close the cycle. Kinetic studies of the reduction of CH_3I (Figures 1.4-1.6) show that the turnover frequency is zero-order in $[\text{CH}_3\text{I}]$ and first-order in $[\text{Et}_3\text{SiH}]$, consistent with the proposed catalytic cycle where **A**, $[\text{Ir}]\text{H}(\text{ICH}_3)^+$, is the dominant resting state. The proposed mechanism explains the differing relative reactivities of halides in separate flasks versus the same flask. Alkyl iodides bind tightly to Ir and result in very low equilibrium concentrations of the σ -silane complex thus retarding the overall rate, but the silane complex reacts preferentially with iodides when carried out in the “same flask” experiments. Kinetic studies can not distinguish step I

(silylation) or step II (hydride transfer) as the turnover-limiting step, and this may well depend on the nature of the substrate.

Scheme 1.7. Proposed Catalytic Cycle for Iridium-Catalyzed Reduction of RX by Et₃SiH

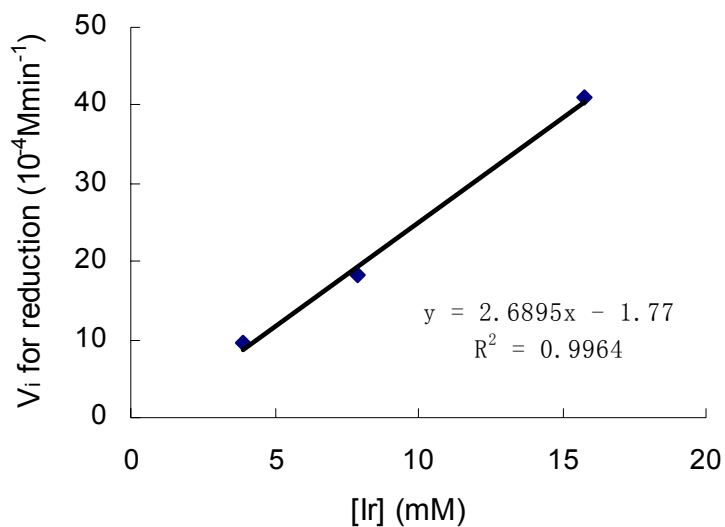
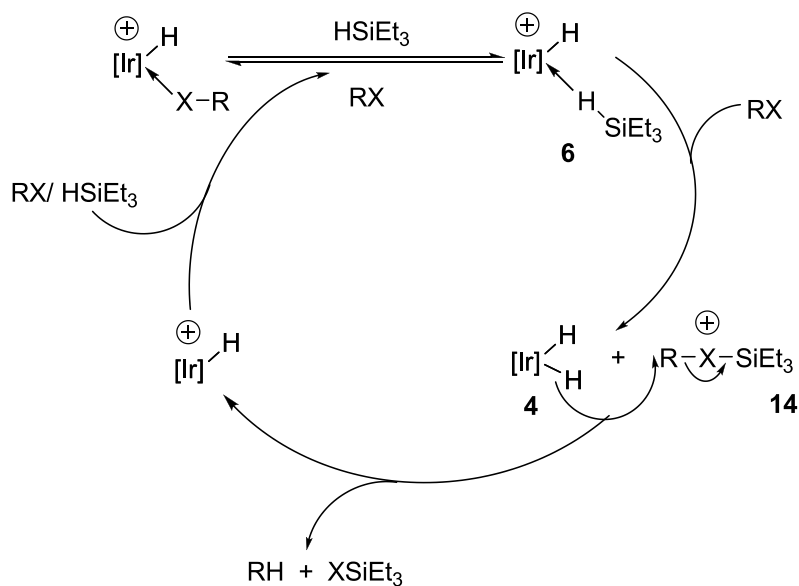


Figure 1.4. Plot of the initial rate, V_i , vs. complex **3** concentration at 23 °C.

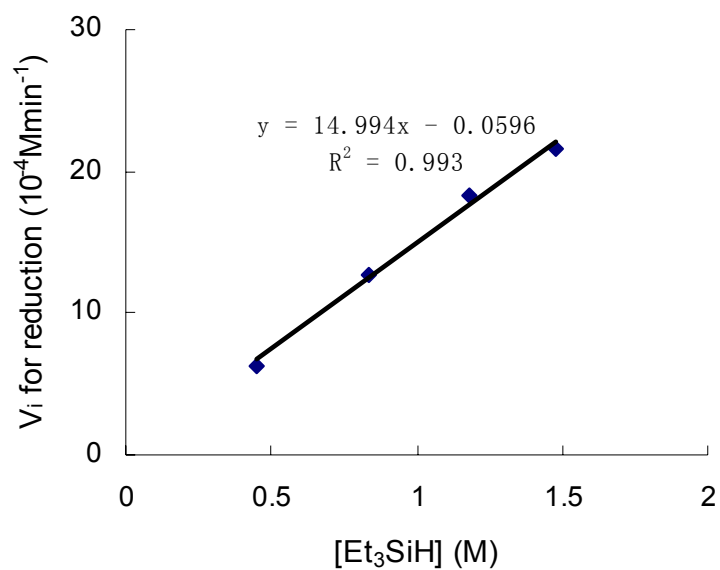


Figure 1.5. Plot of the initial rate, V_i , vs. Et_3SiH concentration at 23 °C.

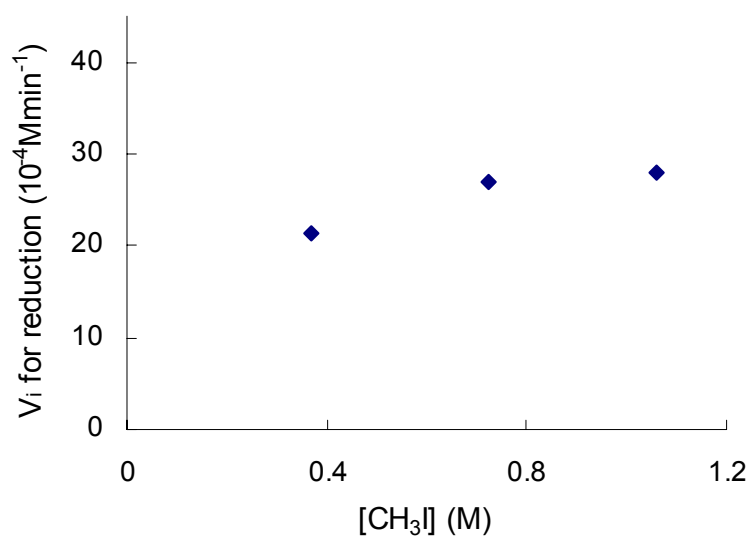
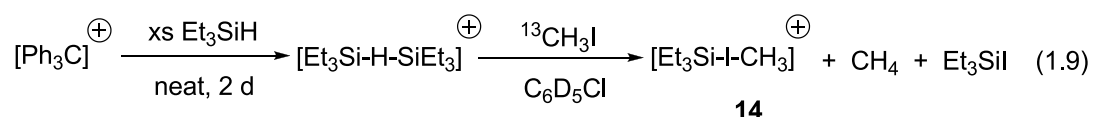


Figure 1.6. Plot of the initial rate, V_i , vs. CH_3I concentration at 23 °C.

The relatively small difference in competitive rates of reduction of 1° and 2° halides and the trend observed with different halides (1° RX : 2° RX = 2.6(Cl), 2.0(Br) 1.6(I)) is consistent with a S_N2 reaction in step II in which RXSiR₃⁺ may bear a high positive charge at C_α. This appreciable carbocationic character at C_α might also explain the minor carbocation rearrangement products in the reduction of (bromomethyl)cyclohexane as well as some minor elimination products seen in secondary halide reductions.

I. Preliminary Studies on In situ Generation of Triethylsilyl Iodonium Ion [Et₃Si-I-CH₃]⁺, **14**.

To test the chemical viability of the triethylsilyl halonium ion, [Et₃Si-X-R]⁺ (X = Cl, Br, I), and gain more insights about the silylation and hydride transfer steps, the proposed catalytic reaction intermediate **14** has been independently generated by treating the Et₃SiH stabilized triethylsilyl cation [Et₃Si-H-SiEt₃]⁺[B(C₆F₅)₄]⁻ with 1-2 equiv. of ¹³CH₃I in C₆D₅Cl at -40 °C (eq 1.9).¹²



Preliminary studies show the formation of **14** together with ¹³CH₄. Line broadening of the methyl resonance attributed (tentatively) to **14**, Et₃SiI-CH₃⁺, is observed in the ¹³C NMR spectra (Figure 1.7) which we propose (tentatively) indicates rapid dynamic exchange between **14** and free ¹³CH₃I (eq 1.10). Work on the in situ generation of **14** by treating the C₆D₆-stabilized triethylsilyl cation [Et₃Si(C₆D₆)]⁺[B(C₆F₅)₄]⁻¹³ (Chapter two) with CH₃I, its variable-temperature dynamics and reactivity towards dihydride **4** is currently underway.

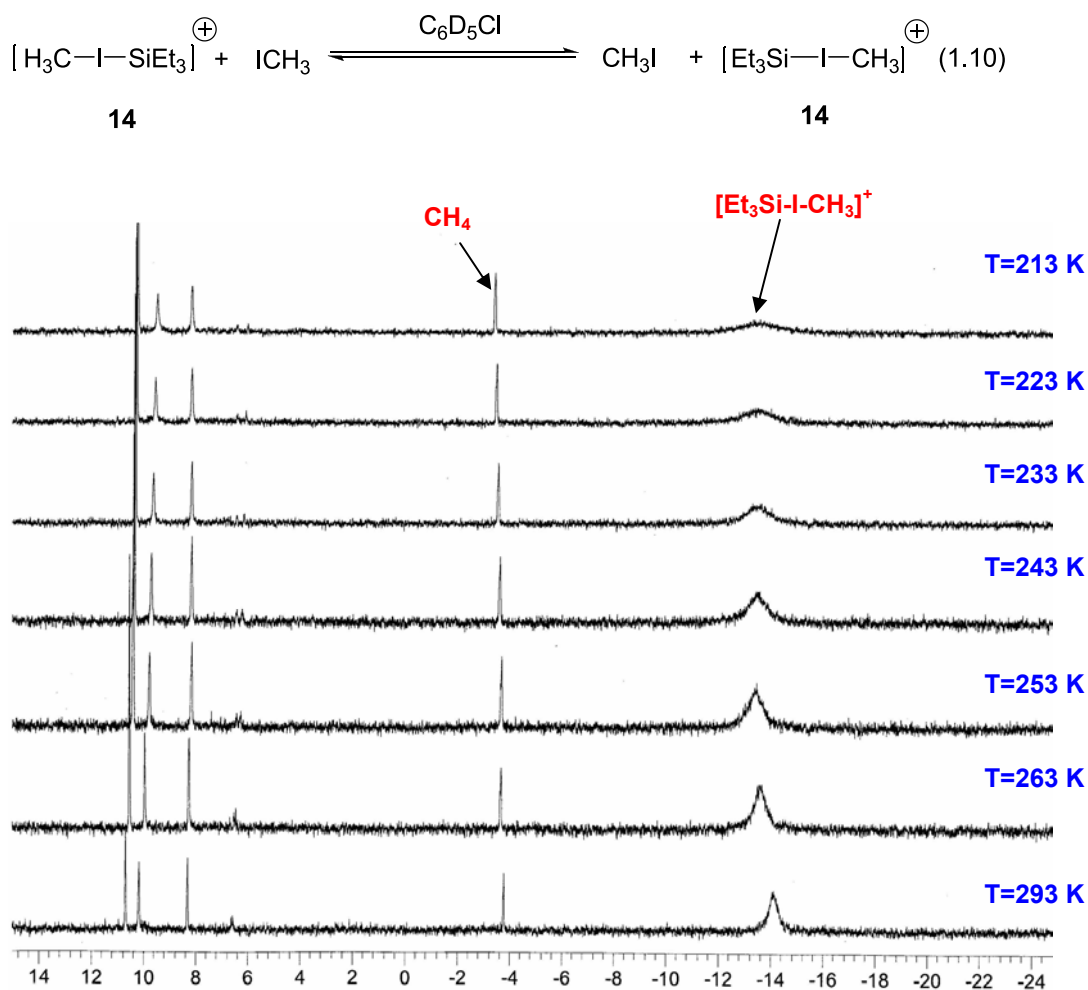
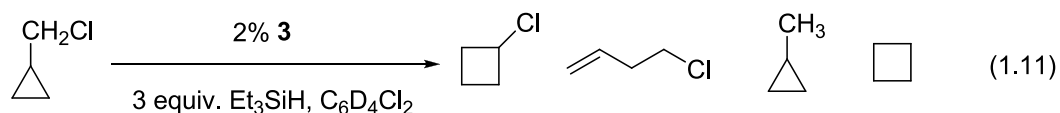


Figure 1.7. Preliminary Variable-Temperature $^{13}\text{C}\{^1\text{H}\}$ NMR Studies of **14**.

J. Reduction of (Chloromethyl)cyclopropane.

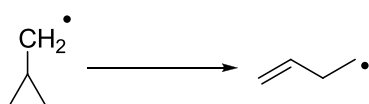
(Chloromethyl)cyclopropane was employed as a radical clock¹⁴ (Scheme 1.8, A) to further probe the intermediacy of free radicals in this iridium-catalyzed reduction of alkyl halides. A mixture of a variety of products were observed and identified by ^1H and $^{13}\text{C}\{^1\text{H}\}$ NMR (eq 1.11).



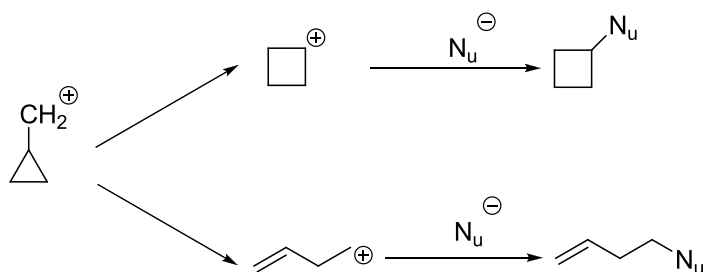
The observation of both chlorocyclobutane and 4-chloro-1-butene is well expected and implies a complication in this system: silyl-substituted halonium ion intermediate bears a high positive charge at C_α and thus could also rearrange under the reaction conditions (Scheme 1.8, B).¹⁵

Scheme 1.8. Rearrangements of the Cyclopropylcarbiny Radical (A) and the Cyclopropylcarbiny Cation (B).¹⁵

A: Rearrangement of the Cyclopropylcarbiny Radical



B: Rearrangement of the Cyclopropylcarbiny Cation

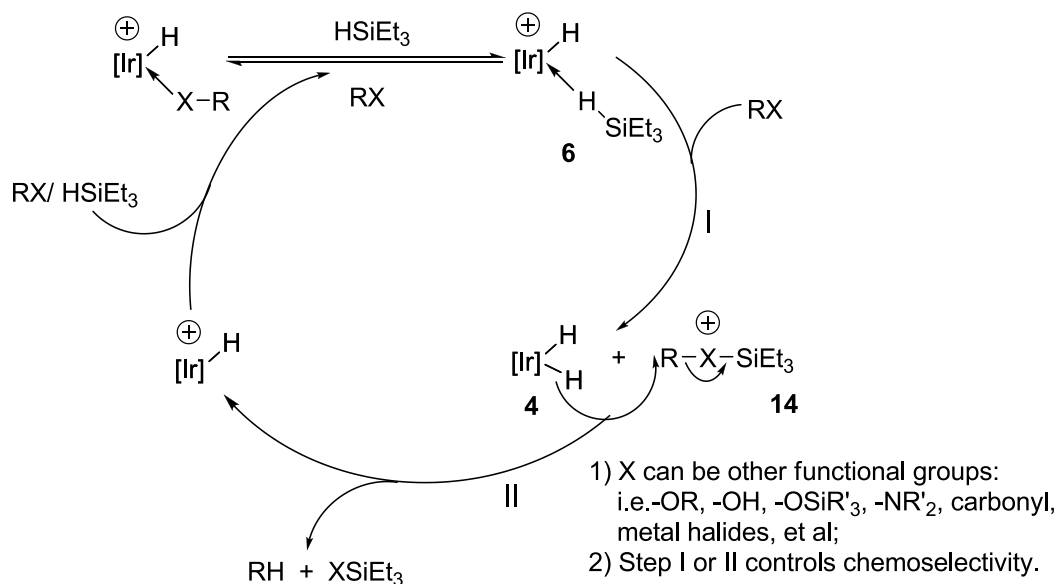


K. Application to Other Functional Groups.

The new catalytic cycle discovered can be generalized to other processes (Scheme 1.9). Indeed **3** catalyzes the reduction of other functional groups. We will discuss in Chapter Two the catalytic cleavage of the carbon-oxygen bonds, a functional group much harder to reduce.

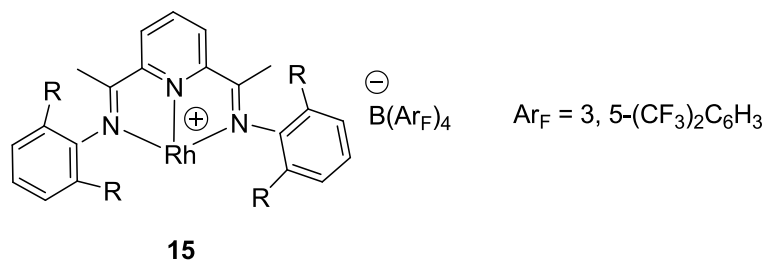
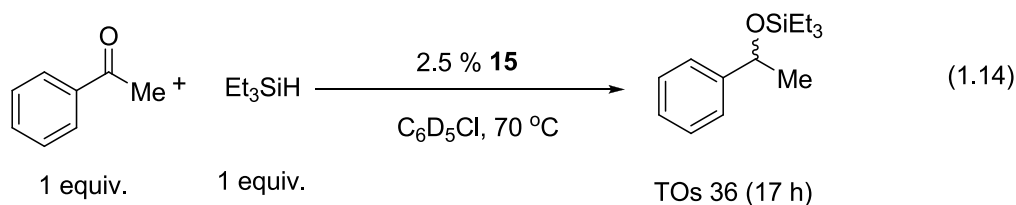
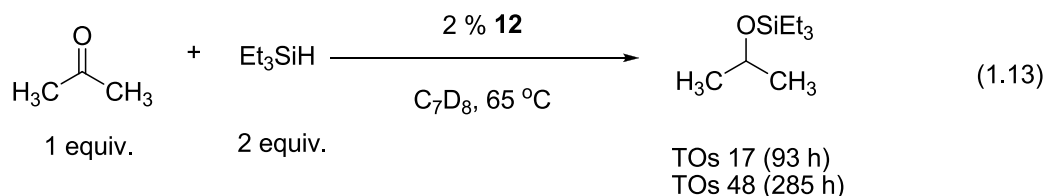
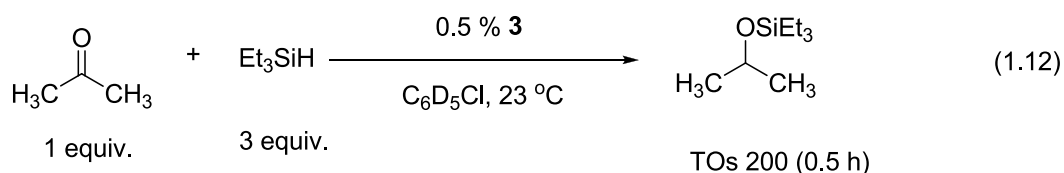
Two additional preliminary studies are shown below to illustrate this concept: catalytic hydrosilation of acetone and hydrodehalogenation of a metal halide.

Scheme 1.9. Application of **3**/Et₃SiH to the Reduction of Other Functional Groups.



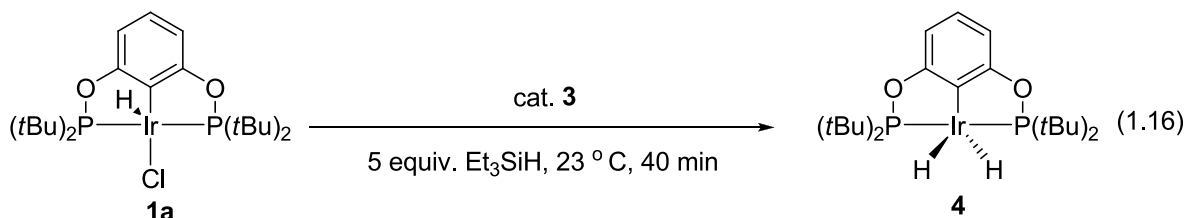
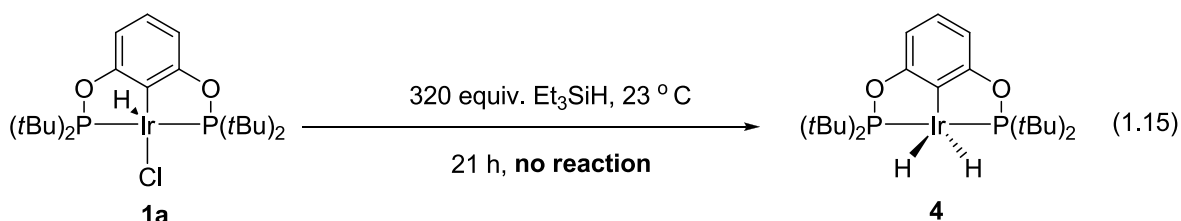
L. Iridium-Catalyzed Hydrosilation of Acetone.

Cationic iridium acetone complex, **3**, catalyzes the hydrosilation of ketones in chlorobenzene. For example, acetone can be rapidly converted to *i*-propyl triethylsilyl ether with 0.5 mol% catalyst loadings at 23 °C (eq 1.12). For comparison, rates and conditions of hydrosilation of ketones catalyzed by iridium silyl hydride **12** and another cationic Rh(I) Lewis acid, **15**, are shown in eq 1.13 and 1.14. It can be seen that **3** is much more active for hydrosilation than its neutral analog and the cationic Rh(I) species, **15**.¹⁶

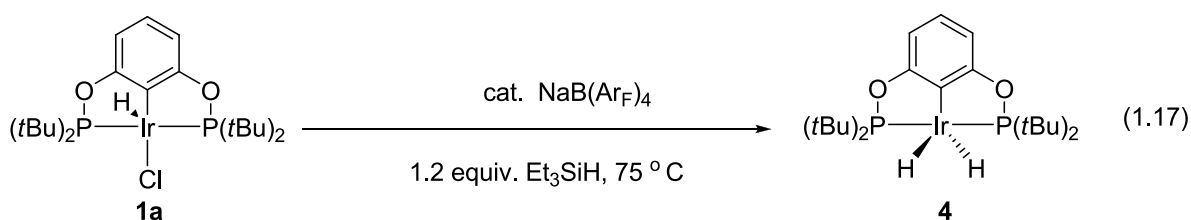


M. Auto-catalysis: Catalytic Hydrodechlorination of **1a** with Et₃SiH

To further broaden the scope of this reduction chemistry, we have extended it to the catalytic hydrodehalogenation of a metal halide, **1a**. While a control experiment shows that there is no appreciable reactivity of iridium hydrochloride **1a** towards excess (320 equiv.) Et₃SiH for 21 h (eq 1.15), it could be readily converted to iridium dihydride **4** in the presence of catalytic amounts of **3** at room temperature in 40 minutes (eq 1.16).



In principle, the cationic iridium hydride species could be formed in situ by treating the starting iridium hydrochloride **1a** with $\text{NaB}(\text{Ar}_\text{F})_4$. Thus a catalytic amount of $\text{NaB}(\text{Ar}_\text{F})_4$ was found to mediate the hydrodechlorination of **1a** with a slightly excess of Et_3SiH in an autocatalytic¹⁷ fashion (eq 1.17).



Summary

As a part of our continuing interest in incorporation of Si-H bond activation chemistry into catalytic cycles we have discovered cationic iridium bis(phosphinite) pincer complexes as highly efficient catalysts for the reduction of primary, secondary and tertiary chlorides, bromides and iodides as well as certain fluorides by triethylsilane. Catalyst loadings as low as 0.03% have proved successful and this process can be carried out in a solvent-free manner,

which may provide an environmentally attractive and safe alternative to currently practiced reductions of alkyl halides.

This novel reduction chemistry has unique selectivities compared with radical based processes, strong Lewis acid catalysis and the $[\text{Ph}_3\text{C}][\text{B}(\text{C}_6\text{F}_5)_4]/\text{Et}_3\text{SiH}$ system. Relative reduction rates of $1^\circ \text{RX} > 2^\circ \text{RX}$ were determined by head-to-head competition experiments with the ratio of initial rates determined to be: $1^\circ \text{RCl} : 2^\circ \text{RCl} = 2.6:1.0$, $1^\circ \text{RBr} : 2^\circ \text{RBr} = 2.0:1.0$, $1^\circ \text{RI} : 2^\circ \text{RI} = 1.6:1.0$. Qualitatively, reactivities follow the unique order of $\text{RBr} > \text{RCl} > \text{RI}$ when reductions are carried out in separate flasks; however, head-to-head competitions establish $\text{RI} > \text{RBr} > \text{RCl}$ when carried out in the “same flask” experiments. Only traces of CD_2HCl were observed during the reduction of CD_2Cl_2 which shows that CD_2HCl is reduced much faster than CD_2Cl_2 .

In-depth mechanistic studies have been carried out which have revealed a unique catalytic cycle. The electrophilic iridium hydride complex binds and activates the silane. This complex transfers “ Et_3Si^{+} ” to the halide forming a highly active bridged halonium ion which is rapidly reduced by the iridium dihydride remaining following silyl transfer and the cationic iridium hydride complex is thus regenerated and the catalytic cycle is closed. All key intermediates have been identified by in situ NMR monitoring and kinetic studies have been completed.

The new mechanism discovered may attract considerable attention in the field of catalysis as the concept can be generalized to other processes. For example, the cationic iridium acetone complex, **1**, is also highly efficient for hydrosilation of acetone and hydrodehalogenation of a metal halide.

Experimental Section

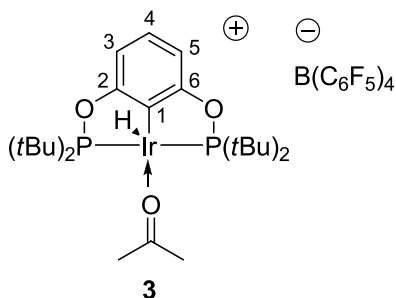
General considerations. All manipulations were carried out using standard Schlenk, high-vacuum and glovebox techniques. Argon and nitrogen were purified by passage through columns of BASF R3-11 catalyst (Chemalog) and 4 Å molecular sieves. THF was distilled under a nitrogen atmosphere from sodium benzophenone ketyl prior to use. Pentane, methylene chloride and toluene were passed through columns of activated alumina¹⁸ and degassed by either freeze-pump-thaw methods or by purging with argon. Benzene and acetone was dried with 4 Å molecular sieves and degassed by freeze-pump-thaw methods. Et₃SiH was dried with LiAlH₄ and vacuum transferred into a sealed flask. Et₃SiD was dried with LiAlD₄ and vacuum transferred into a sealed flask. All the substrates, 1, 3, 5-tris(trifluoromethyl)benzene and all the haloarene solvents were dried with either CaH₂ or 4 Å molecular sieves and vacuum transferred to a sealed flask. NMR spectra were recorded on Bruker spectrometers (DRX-400, AVANCE-400, AMX-300 and DRX-500). ¹H and ¹³C NMR spectra were referenced to residual protio solvent peaks. ³¹P chemical shifts were referenced to an external H₃PO₄ standard. ¹⁹F NMR shifts were referenced to external C₆F₆ (δ ¹⁹F(C₆F₆) = -162.9 vs. CFC₃). ²⁹Si chemical shifts were referenced to external (CH₃)₄Si. K[B(C₆F₅)₄] and NaB(Ar_F)₄ [Ar_F = 3, 5-(CF₃)₂C₆H₃] were purchased from Boulder Scientific and dried *in vacuo* at 120°C for 24 hours. All other reagents were purchased from Sigma-Aldrich or Strem. (POCOP)Ir(H)₂¹⁰, (POCOP)Ir(H)(Cl)^{8a} and [Ph₃C][B(C₆F₅)₄]^{7a} were prepared according to published procedures. GC analysis was performed on an Agilent 6850 Series GC System using a J. & W. Scientific HP-1 column (100% dimethylpolysiloxane,

30m×0.32mm i.d., 0.25 μ m film thickness). Typical temperature program: 10 min isothermal at 33 °C, 20 °C/ min heat up, 10 min isothermal at 300 °C.

Synthesis of [(POCOP)Ir(H)(CH₂Cl₂)]⁺[B(Ar_F)₄]⁻ [Ar_F = **3, 5-(CF₃)₂C₆H₃], **2**.** A flame dried Schlenk flask was charged with (POCOP)Ir(H)(Cl) (**1a**) (200mg, 0.319 mmol), and NaB(Ar_F)₄ (311mg, 0.351 mmol) under argon. Methylene chloride (20 mL) was added and the mixture was stirred at room temperature for 15 hours. The solution was cooled in an ice bath, and NaCl and excess NaB(Ar_F)₄ were removed via cannula filtration. The filtrate was concentrated before pentane (40 mL) was added to precipitate an orange solid. The solid was filtered, washed with pentane (5 mL, three times), and dried *in vacuo* for 2 hours to give 300 mg (65%) of **2** as an orange powder. ¹H NMR (400 MHz, 23°C, CD₂Cl₂): δ 7.72 [s, 8H, B(Ar_F)₄], 7.56 [s, 4H, B(Ar_F)₄], 7.02 (t, 1H), 6.69 (d, 2H), 1.36 (m, 36H, 4 \times *t*Bu), -42.34 (t, 1H, Ir-H). ³¹P{¹H} NMR (162 MHz, 23°C, CD₂Cl₂): δ 179.7. Anal. Calcd for C₅₂H₅₄BF₂₄O₂P₂Ir (1450): C, 42.93; H, 3.54. Found: C, 42.74; H, 3.45.

Synthesis of Iridium Acetone Complex [(POCOP)Ir(H)(acetone)]⁺[B(C₆F₅)₄]⁻, **3.** (POCOP)Ir(H)₂ (**4**) (700 mg, 1.18 mmol) and Ph₃C[B(C₆F₅)₄] (980 mg, 1.07 mmol) were dissolved in acetone (20 mL) and the mixture was allowed to stir at room temperature for 2 hours. The solvent was removed *in vacuo* and the solid obtained was dissolved in a minimum amount of acetone. Pentane was added to precipitate an orange solid. The solid was filtered, washed with pentane and dried *in vacuo* to give 1.33 g (94 %) of complex **3** as an orange powder. ¹H NMR (C₆D₅Cl, 400 MHz): δ 6.83 (t, ³J_{H-H} = 8.0 Hz, 1H, 4-H), 6.62 (d, ³J_{H-H} = 8.0 Hz, 2H, 3- and 5-H), 2.10 (s, 6H, CH₃(CO)CH₃), 1.04 (vt, *J*_{apparent} = 7.6 Hz, 36H, 4 \times *t*Bu),

-42.28 (t, $^2J_{\text{P-H}} = 12.4$ Hz, 1H, IrH). $^{31}\text{P}\{^1\text{H}\}$ NMR ($\text{C}_6\text{D}_5\text{Cl}$, 162 MHz): δ 174.4. $^{13}\text{C}\{^1\text{H}\}$ NMR (CD_2Cl_2 , 100.6 MHz): δ 223.2 (br, $\text{CH}_3(\underline{\text{C}}\text{O})\text{CH}_3$), 167.7 (s, C2 and C6), 148.5 (d, $^1J_{\text{C-F}} = 238.4$ Hz), 138.6 (d, $^1J_{\text{C-F}} = 245.5$ Hz), 136.6 (d, $^1J_{\text{C-F}} = 245.5$ Hz), 129.5 (s, C4), 124.5 (br), 106.3 (s, C3 and C5), 105.2 (C1, tentative), 43.8 and 39.4 [C_q , each, vt each, $J_{\text{P-C}} = 11.9$ and 13.9 Hz, $2 \times \text{P}(t\text{Bu})_2$], 33.7 (br, $\underline{\text{C}}\text{H}_3(\text{CO})\underline{\text{C}}\text{H}_3$), 28.1 and 27.4 [br, CH_3 each, $2 \times \text{P}(t\text{Bu})_2$]. ^{19}F NMR ($\text{C}_6\text{D}_5\text{Cl}$, 376.5 MHz): δ -128.3 (broad, 8F), -158.9 (t, $J_{\text{FF}} = 20.7$ Hz, 4F), -162.7 (broad, 8F). Anal. Calcd for $\text{C}_{49}\text{H}_{46}\text{BF}_{20}\text{O}_3\text{P}_2\text{Ir}$ (1327.82): C, 44.32; H, 3.49. Found: C, 44.21; H, 3.45.



X-ray Structure of $[(\text{POCOP})\text{Ir}(\text{H})(\text{acetone})]^+[\text{B}(\text{C}_6\text{F}_5)_4]^-$, **3.** Crystals of iridium complex **1** were grown by slow diffusion of pentane into an acetone solution of complex **3**. Crystallographic data were collected on a Bruker SMART APEX-2 using Cu-K α radiation. Final agreement indices were R_1 (all) = 3.27% and R_2 (all) = 7.12%, with hydrogen placed in computed positions and included in the refinement using a riding model. All other atoms were refined anisotropically.

Table 1.6. X-ray Crystal Structure Data for Complex **3**.

Formula	C ₄₉ H ₄₆ BF ₂₀ IrO ₃ P ₂
Formula Weight	1327.81
Crystal System	Triclinic
Space Group	P-1
Unit Cell Dimensions	a = 13.4226(6) Å b = 14.0327(6) Å c = 15.1067(7) Å
Volume	2596.0(2) Å ³
Z	2
Absorption Coefficient	6.588 mm ⁻¹
Data/restraints/parameters	7157/ 0 / 703
Final R indices [I>2σ(I)]	R ₁ = 0.0293, wR ₂ = 0.0694

General Procedure for the Reduction of Alkyl Halides in C₆D₅Cl or C₆D₄Cl₂.

Triethylsilane (480 μL, 3.00 mmol, 3 equiv.) was added to a solution of **3** (6.7 mg, 0.005 mmol, 0.5 mol%) in C₆D₅Cl or C₆D₄Cl₂ (0.3 mL) in a medium-walled J. Young NMR tube and the contents were well shaken. The substrate (1.00 mmol, 1 equiv.) was then added and the solution was vigorously shaken. The reactions were allowed to stand at room temperature or heated in an oil bath and the progress was followed by NMR spectroscopy. Conversions were determined by loss of alkyl halides by ¹H NMR spectroscopy (conversions for alkyl fluoride reductions were determined by ¹⁹F NMR spectroscopy). Reduction products were identified using ¹H and ¹³C{¹H} NMR in comparison to literature data or authentic samples.

General Procedure for the Reduction of Alkyl Halides without Solvent. Triethylsilane (480 μL , 3.00 mmol, 3 equiv.) was added to a medium-walled J. Young NMR tube with **3** (6.7 mg, 0.005 mmol, 0.5 mol%) and a sealed capillary tube with C_6D_6 as internal standard. To this suspension was then added the substrate (1.00 mmol, 1 equiv.), and the tube was quickly inverted to ensure complete mixing. The reactions were allowed to stand at room temperature and the progress was monitored by NMR spectroscopy. Conversions were determined by loss of alkyl halides by ^1H NMR spectroscopy. Reduction products were identified using ^1H and $^{13}\text{C}\{^1\text{H}\}$ NMR in comparison to literature data or authentic samples.

Typical Competition Experiments to Determine Relative Reactivities of Primary and Secondary Halides by NMR. A stock solution of **3** (16.7 mM) was prepared in $\text{C}_6\text{D}_4\text{Cl}_2$ in a glovebox. Triethylsilane (480 μL , 3.00 mmol, 6 equiv.) was then added to an aliquot (300 μL , 1 mol% Ir) of this stock solution in a medium-walled J. Young NMR tube and the contents were well shaken. 1-Chloropentane (0.50 mmol, 60.5 μL , 1 equiv.), 2-chloropentane (0.50 mmol, 61.3 μL , 1 equiv.) and 1,3,5-tris(trifluoromethyl)benzene (0.16 mmol, 30.0 μL , 0.32 equiv.; used as an internal standard) were then added and the tube was placed in the NMR probe. The relative reactivities were determined by the ratios of initial rates of substrate loss and the initial rates were obtained from the linear portion of the concentration vs. time curve. Half percent loadings of Ir catalyst were used in the competition experiments of 1-bromopentane and 2-bromopentane due to the rapid reduction of alkyl bromide (Figure 1.8 and 1.9 for RCl , 1.10 and 1.11 for RBr and 1.12 and 1.13 for RI).

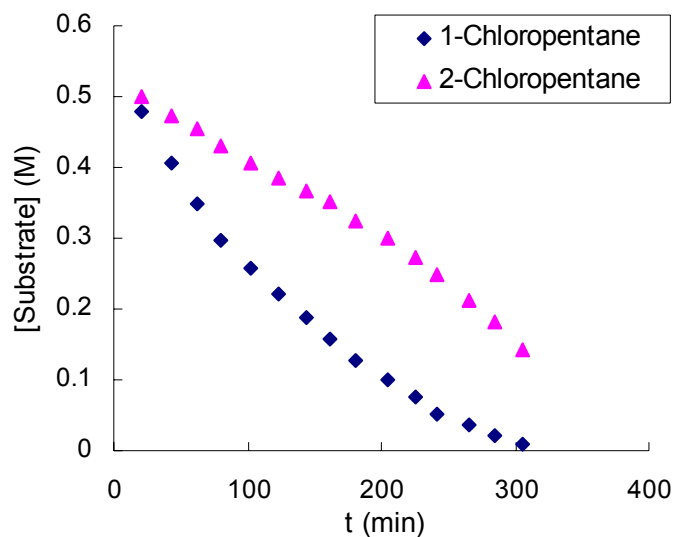
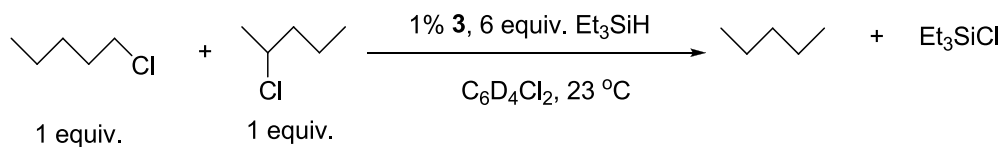


Figure 1.8. Plot of concentration vs. time for the reduction of 1-chloropentane (0.54 M) and 2-chloropentane (0.54 M) with Et_3SiH (3.22 M) and complex **3** (5.4 mM) in $\text{C}_6\text{D}_4\text{Cl}_2$ at 23°C .

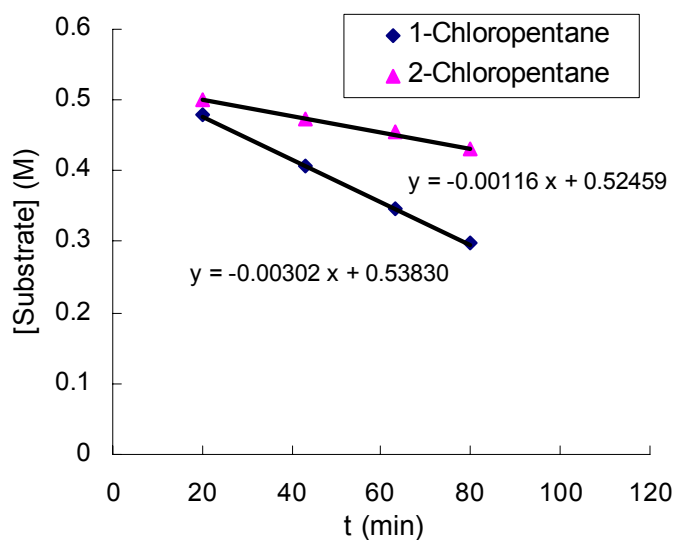


Figure 1.9. Linear portions of the concentration vs. time curve used to determine the initial rates for the reduction of 1-chloropentane and 2-chloropentane.

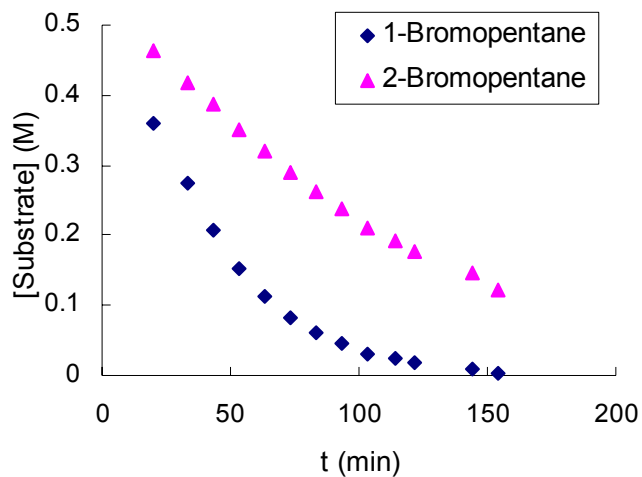
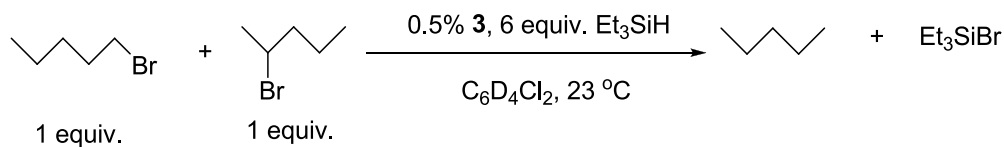


Figure 1.10. Plot of concentration vs. time for the reduction of 1-bromopentane (0.54 M) and 2-bromopentane (0.54 M) with Et_3SiH (3.22 M) and complex **3** (2.7 mM) in $\text{C}_6\text{D}_4\text{Cl}_2$ at 23°C .

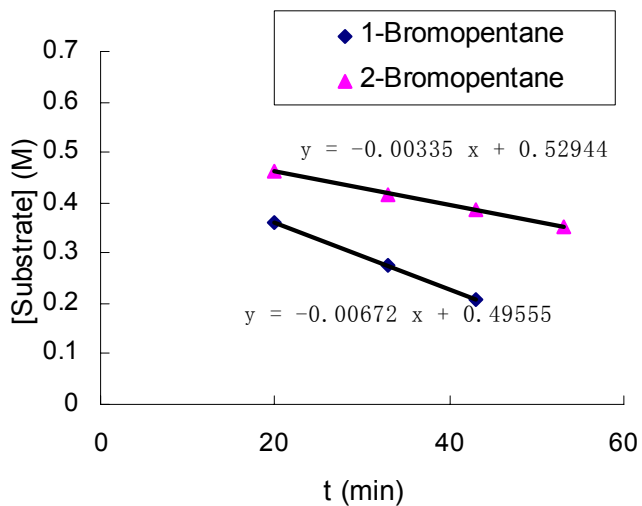


Figure 1.11. Linear portions of the concentration vs. time curve used to determine the initial rates for the reduction of 1-bromopentane and 2-bromopentane.

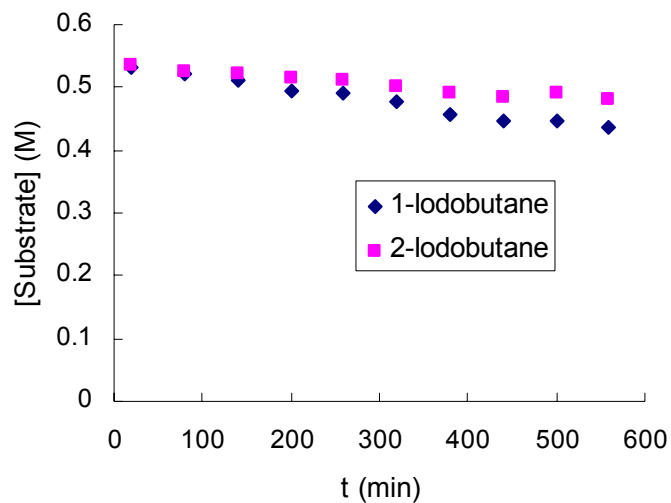
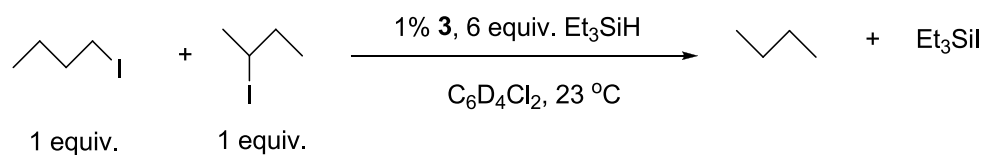


Figure 1.12. Plot of concentration vs. time for the reduction of 1-iodobutane (0.54 M) and 2-iodobutane (0.54 M) with Et_3SiH (3.22 M) and complex **3** (5.4 mM) in $\text{C}_6\text{D}_4\text{Cl}_2$ at 23 $^\circ\text{C}$.

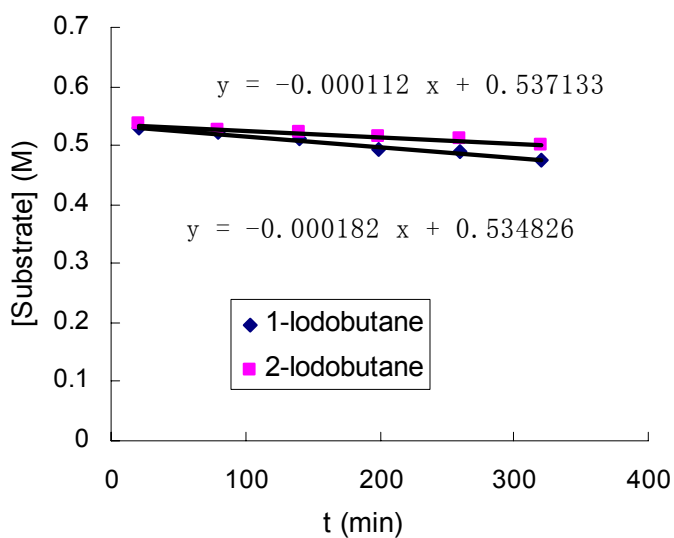


Figure 1.13. Linear portions of the concentration vs. time curve used to determine the initial rate for the reduction of 1-iodobutane and 2-iodobutane.

Typical Competition Experiments to Determine Relative Reactivities of Chloride, Bromide and Iodide by GC. A stock solution of complex **3** (5 mM) was prepared in C₆H₅F in a glovebox. An aliquot (250 μ L, 5 mol% Ir) of this stock solution was then added to a mixture of triethylsilane (120 μ L, 0.75 mmol, 30 equiv.), 1-iodoheptane (4.1 μ L, 0.025 mmol, 1 equiv.), 1-bromohexane (280 μ L, 2 mmol, 80 equiv.) and 1,3,5-tris(trifluoromethyl)benzene (2.0 μ L, 0.011 mol, 0.43 equiv.; used as an internal standard) in a 10 mL screw capped glass vial and the solution was stirred at room temperature. Analysis of heptane and hexane very early in the reaction (less than 2.5 turnovers for heptane formation) by GC established a relative reactivity ratio of 80:1 for 1-iodoheptane: 1-bromohexane (correction has been made for initial concentration ratios). A similar trend was noted at 1% catalyst loading, but accurate quantitative number could not be determined under these conditions.

Reduction of 1-Bromohexane with Et₃SiD catalyzed by **3.** Et₃SiD (160 μ L, 1.00 mmol, 2 equiv.) was added to a solution of **3** (6.7 mg, 0.005 mmol, 1 mol%) in C₆D₄Cl₂ (0.3 mL) in a medium-walled J. Young NMR tube. The contents were well shaken and 1-bromohexane (70.2 μ L, 0.50 mmol, 1 equiv.) was added. The reaction was allowed to stand at room temperature the progress was followed by ¹H and ¹³C{¹H} NMR spectroscopy. CH₃(CH₂)₄CH₂D was the only observable alkane product as determined by ¹³C{¹H} NMR. CH₃(CH₂)₄CH₂D : ¹³C{¹H} NMR (C₆D₄Cl₂, 100.6 MHz): δ 31.71 (s), 31.68 (s), 22.75 (s), 22.66 (s), 14.0 (s), 13.7 (t, J_{D-C} = 19.1 Hz).

Reduction of (Bromomethyl)cyclohexane with Et₃SiD catalyzed by 3. Et₃SiD (240 μ L, 1.50 mmol, 3 equiv.) was added to a solution of **3** (20 mg, 0.015 mmol, 3 mol%) in C₆D₄Cl₂ (0.5 mL) in a medium-walled J. Young NMR tube and the contents were well shaken. (Bromomethyl)cyclohexane (70 μ L, 0.50 mmol, 1 equiv.) was then added. The reaction was allowed to stand at room temperature the progress was followed by ¹H and ¹³C{¹H} NMR spectroscopy. (Deuteriomethyl)cyclohexane was identified as the major alkane product and 1-deuterio-1-methylcyclohexane was the minor one (ca. 6:1 ratio as determined by ¹³C{¹H} NMR spectroscopy). (Deuteriomethyl)cyclohexane: ¹³C{¹H} NMR (C₆D₄Cl₂, 100.6 MHz): δ 35.4 (s), 32.7 (s), 26.5 (s), 26.4 (s), 22.5 (t, J_{D-C} = 19.1 Hz).

Competition Experiments to Determine Relative Reactivities of Primary and Secondary Chlorides in [Ph₃C][B(C₆F₅)₄]/Et₃SiH System. Triethylsilane (480 μ L, 3 mmol, 6 equiv.) was added to a solution of [Ph₃C][B(C₆F₅)₄] (4.6 mg, 0.005 mmol, 1 mol%) in C₆D₄Cl₂ (0.3 mL) in a medium-walled J. Young NMR tube and the contents were well shaken. 1-Chloropentane (60.5 μ L, 0.50 mmol, 1 equiv.) and 2-chloropentane (61.3 μ L, 0.50 mmol, 1 equiv.) were then added. The reaction was allowed to stand at room temperature, and the progress was followed by NMR spectroscopy.

General Procedure for Kinetic Studies (C₆D₄Cl₂). A stock solution of **3** (10 mM) and 1,3,5-tris(trifluoromethyl)benzene (0.16 M; used as an internal standard) was prepared in C₆D₄Cl₂ in a glovebox. Triethylsilane was added to an aliquot (500 μ L) of this stock solution in a medium-walled J. Young NMR tube and the contents were well shaken. Iodomethane was then added by syringe. The reaction was monitored by iodomethane loss relative to the

standard with respect to time. The data were analyzed using the method of initial rates and the initial reduction rates were obtained from the linear portion of the concentration vs. time curve (see Figure 1.14 for example).

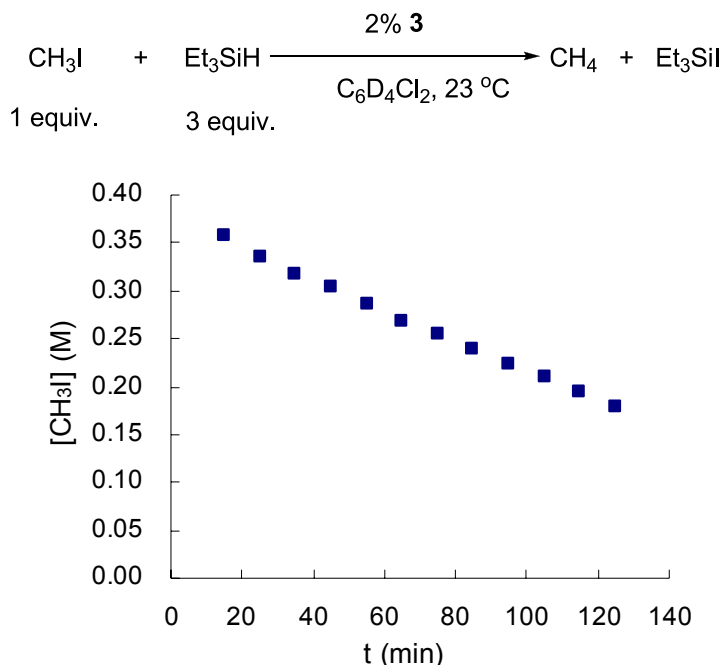


Figure 1.14. Plot of concentration vs. time during the first half life for the reduction of CH_3I (0.39 M) with Et_3SiH (1.18 M) and complex **3** (7.9 mM) in $\text{C}_6\text{D}_4\text{Cl}_2$ at 23 $^\circ\text{C}$.

In Situ Generation of the Iridium Cationic σ -Silane Complex
[(POCOP)Ir(H)(Et₃SiH)]⁺[B(C₆F₅)₄]⁻, **6.** Triethylsilane (240 μL , 1.50 mmol, 300 equiv.) was added to a solution of **3** (6.7 mg, 0.005 mmol, 1 equiv.) in $\text{C}_6\text{D}_5\text{Cl}$ (0.5 mL) in a medium-walled J. Young NMR tube and the solution was vigorously shaken. ^1H NMR ($\text{C}_6\text{D}_5\text{Cl}$, 400 MHz, -40 $^\circ\text{C}$): δ 6.92 (t, $^3J_{\text{H-H}} = 8.0$ Hz, 1H, 4-H), 6.62 (d, $^3J_{\text{H-H}} = 8.0$ Hz, 2H, 3- and 5-H), 1.04 (m, 36H, 4 \times *t*Bu), -5.10 (b, 1H, SiH), -44.25 (b, 1H, IrH). $^{31}\text{P}\{^1\text{H}\}$ NMR ($\text{C}_6\text{D}_5\text{Cl}$, 162 MHz, -40 $^\circ\text{C}$): δ 183.7. $^{31}\text{P}\{^1\text{H}\}$ NMR ($\text{C}_6\text{D}_5\text{Cl}$, 162 MHz, 23 $^\circ\text{C}$): δ 183.2

In Situ Generation of [(POCOP)Ir(H)(C₆D₅Cl)]⁺[B(C₆F₅)₄]⁻, **11.** Complex **11** was generated *in situ* by treatment of (POCOP)Ir(H)₂ (**4**) (5.9 mg, 0.01 mmol, 1 equiv.) with Ph₃C[B(C₆F₅)₄] (9.2 mg, 0.01 mmol, 1 equiv.) in 0.5 mL of C₆D₅Cl at room temperature for 20 min. ¹H NMR (C₆D₅Cl, 400 MHz, 23 °C): δ 6.87 (t, ³J_{H-H} = 8.0 Hz, 1H, 4-H), 6.60 (d, ³J_{H-H} = 8.0 Hz, 2H, 3- and 5-H), 1.00 (m, 36H, 4 × *t*Bu), -42.6 (t, ²J_{P-H} = 11.8 Hz, 1H, IrH). ³¹P{¹H} NMR (C₆D₅Cl, 162 MHz, 23 °C): δ 177.0

General Procedure for the *in Situ* Generation of [(POCOP)Ir(H)(RX)]⁺[B(C₆F₅)₄]⁻, **5, **7**, **8**, **9** and **10**.** (POCOP)Ir(H)₂ (5.9 mg, 0.01 mmol, 1 equiv.) and Ph₃C[B(C₆F₅)₄] (9.2 mg, 0.01 mmol, 1 equiv.) were dissolved in C₆D₅Cl (0.5 mL) in the dry box. After 20 min, the alkyl halide (5-20 equiv. depending on the nature of the halides) was added *via* syringe and the solution was vigorously shaken. ³¹P{¹H} NMR (C₆D₅Cl, 162 MHz, 23 °C): δ 178.6 (complex **5**); δ 178.8 (complex **7**); δ 177.4 (complex **8**); δ 177.6 (complex **9**); δ 177.8 (complex **10**).

In Situ Generation of (POCOP)Ir(H)(SiEt₃), **12.** C₇D₈ (0.5 mL) was added to a mixture of (POCOP)Ir(H)(Cl) (**1a**) (6.3 mg, 0.01 mmol, 1 equiv.) and NaOtBu (1.2 mg, 0.012 mmol, 1.2 equiv.) in a medium-walled J. Young NMR tube. Et₃SiH (20 μL, 0.125 mmol, 12.5 equiv.) was added to this mixture and allowed to react at 55°C for 1 hour. ¹H NMR (C₇D₈, 400 MHz, 23 °C): δ 6.97 (t, ³J_{H-H} = 7.6 Hz, 1H, 4-H), 6.75 (d, ³J_{H-H} = 7.6 Hz, 2H, 3- and 5-H), 1.32 (m, 36H, 4 × *t*Bu), 1.0-1.2 (m, 15H, EtSi, overlap with *t*-Bu and excess Et₃SiH), -15.9 (t, ²J_{P-H} = 5.8 Hz, 1H, IrH) ³¹P{¹H} NMR (C₇D₈, 162 MHz, 23 °C): δ 189.4

Determination of Equilibrium Constants for the Reactions:

$[(\text{POCOP})\text{Ir}(\text{H})(\text{Et}_3\text{SiH})]^+[\text{B}(\text{C}_6\text{F}_5)_4]^- + \text{RX} = [(\text{POCOP})\text{Ir}(\text{H})(\text{RX})]^+[\text{B}(\text{C}_6\text{F}_5)_4]^- + \text{Et}_3\text{SiH}$ (eq 1.6 and eq 1.7). As mentioned earlier, the σ -silane complex is in rapid equilibrium with the halide complexes and this equilibrium is established rapidly relative to reduction, therefore, the equilibrium constants were determined by monitoring the reduction of halides with Et_3SiH by NMR spectroscopy. Concentration ratio of $[(\text{POCOP})\text{Ir}(\text{H})(\text{RX})]^+[\text{B}(\text{C}_6\text{F}_5)_4]^-$ to $[(\text{POCOP})\text{Ir}(\text{H})(\text{Et}_3\text{SiH})]^+[\text{B}(\text{C}_6\text{F}_5)_4]^-$, **6**, was determined by ^{31}P NMR and the concentration ratio of Et_3SiH to RX was determined by ^1H NMR. At several stages of conversion, the equilibrium constants were determined to be: $K_{\text{eq}}(1\text{-C}_6\text{H}_{13}\text{Br}) = 240$, $K_{\text{eq}}(1\text{-C}_5\text{H}_{11}\text{Cl}) = 7.1$. The equilibrium constant between alkyl iodide complexes and the σ -silane complex was not obtainable by NMR spectroscopy due to the very low equilibrium concentrations of the iridium σ -silane complex caused by much tighter binding of alkyl iodide to iridium.

Preliminary Studies on in situ Generation and Dynamics of Triethylsilyl Iodonium Ion, $[\text{Et}_3\text{Si-I-CH}_3][\text{B}(\text{C}_6\text{F}_5)_4]$, **14.** A): synthesis of $[\text{Et}_3\text{Si-H-SiEt}_3][\text{B}(\text{C}_6\text{F}_5)_4]$: triethylsilane (5 mL) was added to a vial with $[\text{Ph}_3\text{C}][\text{B}(\text{C}_6\text{F}_5)_4]$ (400 mg, 0.434 mmol). The suspension was stirred at 25 °C for 52 h in a drybox. The yellow solid was then replaced with a white solid, cooled in an ice bath, filtered, and washed with pentane (5 mL \times 3). The white solid was then dried under vacuum for 1.5 h in an ice bath to give 270 mg of $[\text{Et}_3\text{Si-H-SiEt}_3][\text{B}(\text{C}_6\text{F}_5)_4]$, and stored in freezer in a glovebox. ^1H NMR ($\text{C}_6\text{H}_4\text{F}_2$, 400 MHz, 23 °C): δ 1.5 (s, 1H, Si-H-Si), 0.7-0.8 (m, 30H, Et-). B): in situ generation of **14**: $^{13}\text{CH}_3\text{I}$ (3 μL , 0.048 mmol, 1.4 equiv.) was added by syringe to a solution of

[Et₃Si-H-SiEt₃][B(C₆F₅)₄] (31.7 mg, 0.035 mmol, 1 equiv.) in C₆H₄F₂ (0.6 mL) in a NMR tube at 23 °C. The variable-temperature ¹H NMR dynamic behavior of **14** is discussed in the text.

Reduction of (Chloromethyl)cyclopropane with Et₃SiH Catalyzed by 3. Triethylsilane (120 µL, 0.75 mmol, 3 equiv.) was added to a solution of **3** (6.7 mg, 0.005 mmol, 2 mol%) in C₆D₄Cl₂ (0.4 mL) in a medium-walled J. Young NMR tube. The contents were well shaken and (chloromethyl)cyclopropane (23.1 µL, 0.25 mmol, 1 equiv.) was added. The reaction was allowed to stand at room temperature and the progress was followed by NMR spectroscopy. After 22 h at 23 °C a mixture of chlorocyclobutane, 4-chloro-1-butene, methylcyclopropane, cyclobutane and a small amount of unidentified product were observed by ¹H and ¹³C{¹H} NMR. Chlorocyclobutane: ¹H NMR (C₆D₄Cl₂, 400 MHz): δ 4.20 (m, 1H), 2.30 (m, 2H), 2.13 (m, 2H), 1.77 (m, 1H), 1.55 (m, 1H). ¹³C{¹H} NMR (C₆D₄Cl₂, 100.6 MHz): δ 52.2 (CHCl), 34.9 (CH₂-CH₂-CHCl), 16.6 (CH₂-CH₂-CHCl). 4-Chloro-1-butene: ¹H NMR (C₆D₄Cl₂, 400 MHz): δ 5.64 (m, 1H), 4.98 (m, 1H), 4.97 (m, 1H), 3.34 (t, 2H), 2.30 (m, 2H). ¹³C{¹H} NMR (C₆D₄Cl₂, 100.6 MHz): δ 134.1 (CH₂=CH-), 117.2 (CH₂=CH-), 43.4 (CH₂=CH-CH₂CH₂Cl), 36.9 (CH₂=CH-CH₂CH₂Cl). Methylcyclopropane: ¹H NMR (C₆D₄Cl₂, 400 MHz): δ 0.9 (m, 3H, overlap with Et₃Si- group of Et₃SiCl and Et₃SiH), 0.5 (m, 1H, overlap with Et₃Si- group of Et₃SiCl and Et₃SiH), 0.32 (m, 2H), -0.12 (m, 2H). ¹³C{¹H} NMR (C₆D₄Cl₂, 100.6 MHz): δ 19.3 (CH₃), 5.8 (CH₂), 5.0 (CH). Cyclobutane: ¹H NMR (C₆D₄Cl₂, 400 MHz): δ 1.86 (s, 8H). ¹³C{¹H} NMR (C₆D₄Cl₂, 100.6 MHz): δ 22.8.

Hydrosilation of Acetone with Et₃SiH Catalyzed by 3. Triethylsilane (480 μ L, 3.00 mmol, 3 equiv.) was added to a solution of **3** (6.7 mg, 0.005 mmol, 0.5 mol%) in C₆D₄Cl₂ (0.3 mL) in a medium-walled J. Young NMR tube. The contents were well shaken and dried acetone (73.4 μ L, 1.00 mmol, 1 equiv.) was added. The reaction was allowed to stand at room temperature and monitored by the ¹H and ¹³C{¹H} NMR. Et₃SiOCH(CH₃)₂: ¹H NMR (C₆D₄Cl₂, 400 MHz): δ 3.88 (m, 1H), 1.05 (d, $J_{\text{H-H}} = 6.0$ Hz, 6H), 0.9 (m, 9H), 0.5 (m, 6H). ¹³C{¹H} NMR (C₆D₄Cl₂, 100.6 MHz): δ 64.4 [-OCH(CH₃)₂], 25.7 [-OCH(CH₃)₂], 6.6 [(CH₃CH₂)Si-], 4.9 [(CH₃CH₂)Si-].

Hydrodechlorination of (POCOP)Ir(H)(Cl) (1a) with Et₃SiH Catalyzed by 3. (POCOP)Ir(H)(Cl) (**1a**) (12.52 mg, 0.02 mmol, 1 equiv.) and **3** (6.7 mg, 0.005 mmol, 25 mol%) were dissolved in 0.5 mL of C₆D₅Cl in a J. Young NMR tube. Triethylsilane (16 μ L, 0.1 mmol, 5 equiv.) was added and the contents were well shaken. The reaction was allowed to stand at room temperature and monitored by the ¹H and ³¹P{¹H} NMR. (POCOP)IrH₂ (**4**): ¹H NMR (C₆D₅Cl, 400 MHz, 23 °C): δ 7.08 (t, $^3J_{\text{H-H}} = 7.6$ Hz, 1H, 4-H), 6.87 (d, $^3J_{\text{H-H}} = 7.6$ Hz, 2H, 3- and 5-H), 1.30 (m, 36H, 4 \times *t*Bu), -17.0 (t, $^2J_{\text{P-H}} = 5.8$ Hz, 1H, IrH) ³¹P{¹H} NMR (C₆D₅Cl, 162 MHz, 23 °C): δ 204.8.

References

- (1) a) Neumann, W. P. *Synthesis* **1987**, 665. b) Pereyre, M.; Quintard, J. –P.; Rahm, A. *Tin in Organic Synthesis*; Butterworth: London, **1987**. c) RajanBabu, T. V. *Encyclopedia of Reagents for Organic Synthesis*; Paquette, L., Ed.; Wiley: New York, 1995; Vol. 7, p 5016. d) Alonso, F.; Beletskaya, I. P.; Yus, M. *Chem. Rev.* **2002**, 102, 4009.

- (2) a) Chatgililoglu, C. *Acc. Chem. Res.* **1992**, 25, 188. b) Chatgililoglu, C. *Chem. Rev.* **1995**, 95, 1229.

- (3) a) Clark, K. B.; Griller, D. *Organometallics* **1991**, 10, 746 and references cited therein. b) Giese, B. *Angew. Chem. Int. Ed. Engl.* **1985**, 24, 553 and referenced cited therein.

- (4) a) Daroszewski, J.; Lusztyk, J.; Degueil, M.; Navarro, C.; Maillard, B. *J. Chem. Soc., Chem. Commun.* **1991**, 586. b) Ballestri, M.; Chatgililoglu, C.; Seconi, G. *J. Organomet. Chem.* **1991**, 408. c) Ballestri, M.; Chatgililoglu, C.; Dembech, P.; Guerrini, A.; Seconi, G. In *Sulfur-Centered Reactive Intermediates in Chemistry and Biology*; Chatgililoglu, C.; Asmus, K.-D., Eds.; Plenum: New York, **1990**; pp 319.

- (5) a) Cole, S. J.; Kirwan, J. N.; Roberta, B. P.; Willis, C. R. *J. Chem. Soc., Perkin Trans. I* **1991**, 103. b) Kirwan, J. N.; Roberts, B. P.; Willis, C. R. *Tetrahedron Lett.* **1990**, 31, 5093. c) Allen, R. P.; Roberta, B. P.; Willis, C. R. *J. Chem. Soc., Chem. Commun.* **1989**, 1387.

- (6) a) $\text{AlCl}_3/\text{Et}_3\text{SiH}$ system: Doyle, M. P.; McOsker, C. C.; West, C. T. *J. Org. Chem.* **1976**, 41, 1393. Other reported catalytic systems: b) $\text{Pd(II)}/\text{Et}_3\text{SiH}$ system: Boukherroub, R.; Chatgililoglu, C.; Manuel, G. *Organometallics* **1996**, 15, 1508. c) Catalysis with P,N-chelated Pt(II) complexes and HSiMe_2Ph was reported and the following order of reactivity was observed: $\text{CCl}_4 > \text{CHCl}_3 > \text{CH}_2\text{Cl}_2 > \text{CH}_3\text{Cl}$. Stöhr, F.; Sturmayer, D.; Schubert, U. *Chem. Commun.* **2002**, 2222.

- (7) a) Scott, V. J. Çelenligil-Çetin, R.; Ozerov, O. V. *J. Am. Chem. Soc.* **2005**, 127, 2852. b) Panisch, R.; Bolte, M.; Müller, T. *J. Am. Chem. Soc.* **2006**, 128, 9676.

- (8) a) Goettker-Schnetmann, I.; Brookhart, M. *J. Am. Chem. Soc.* **2004**, 126, 9330. b) Goettker-Schnetmann, I.; White, P.; Brookhart, M. *J. Am. Chem. Soc.* **2004**, 126, 1804.

- (9) Sykes, A. C.; White, P.; Brookhart, M. *Organometallics*, **2006**, 25, 1664.

- (10) Goettker-Schnetmann, I.; White, P.; Brookhart, M. *Organometallics* **2004**, *23*, 1766.
- (11) Yang, J., Brookhart, M. *J. Am. Chem. Soc.* **2007**, *129*, 12656.
- (12) a) Lambert, J. B., Kania, L.; Zhang, S. *Chem. Rev.* **1995**, *95*, 1191. b) Reed, C. A. *Acc. Chem. Res.* **1998**, *31*, 325. c) Hoffmann, S. P.; Kato, T.; Tham, F. S.; Reed, C. A. *Chem. Commun.* **2006**, 767. d) Lambert, J. B.; Zhang, S.; Ciro, S. M. *Organometallics* **1994**, *13*, 2430. e) Lambert, J. B.; Zhang, S.; Stern, C. L.; Huffman, J. C. *Science* **1993**, *260*, 1917.
- (13) Lambert, J. B., Zhao, Y., Wu, H. *J. Org. Chem.* **1999**, *64*, 2729.
- (14) Liu, K. E.; Johnson, C. C.; Newcomb, M. Lippard, S. J. *J. Am. Chem. Soc.* **1993**, *115*, 939.
- (15) Wong, H. N. C.; Hon, M. -Y.; Tse, C. -W.; Yip, Y. -C.; Tanko, J.; Hudlicky, T. *Chem. Rev.* **1989**, *89*, 165.
- (16) Dias, E. L.; Brookhart, M.; White, P. S. *Chem. Commun.* **2001**, 423.
- (17) Recent examples of auto-catalysis: a) Smith, S. E.; Sasaki, J. M.; Bergman, R. G.; Mondloch, J. E.; Finke, R. G. *J. Am. Chem. Soc.* **2008**, *130*, 1839. b) Barrios-Landeros, F.; Carrow, B. P.; Hartwig, J. F. *J. Am. Chem. Soc.* **2008**, *130*, 5842.
- (18) a) Alaimo, P. J.; Peters, D. W.; Arnold, J.; Bergman, R. G. *J. Chem. Educ.* **2001**, *78*, 64. b) Pangborn, A. B.; Giardello, M. A.; Grubbs, R. H.; Rosen, R. K.; Timmers, F. J. *Organometallics* **1996**, *15*, 1518.

CHAPTER TWO

Scope and Mechanism of the Iridium-Catalyzed Cleavage of Alkyl Ethers with Triethylsilane

(Reproduced in part with permission from the American Chemical Society, to be submitted. Unpublished work copyright 2008 American Chemical Society.)

Introduction

Heterolytic activation of H_2 ¹ by several classes of organometallic systems has resulted in catalysts which can perform ionic hydrogenations of aldehydes and ketones.² The basic catalytic mechanism, termed ionic hydrogenation, involves transfer of H^+ and H^- equivalents from the catalyst to the carbonyl group to generate the product alcohol followed by reaction of H_2 with the metal complex to regenerate the active catalyst and close the cycle.² Similar chemistry has been reported for reduction of iminium ions to amines.³ Stephan has recently described phosphinoboranes (termed “frustrated Lewis pairs, FLPs) which heterolytically activate hydrogen to produce phosphonium borate species which perform ionic hydrogenation of imines.⁴

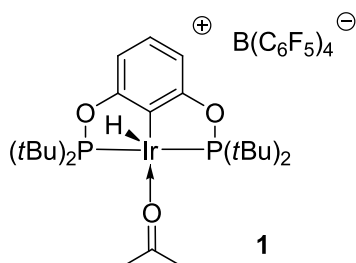
Related hydrosilation chemistry has been reported.⁵⁻⁶ Mechanistic studies by Piers have shown that hydrosilation of carbonyl functionalities catalyzed by $(\text{C}_6\text{F}_5)_3\text{B}^{5\text{a}}$ proceeds by activation of the *silane* by $(\text{C}_6\text{F}_5)_3\text{B}$ and transfer of R_3Si^+ to oxygen to produce $\text{R}_2\text{C}=\text{OSiR}_3^+$ and $\text{H}(\text{C}_6\text{F}_5)_3\text{B}^-$. The catalytic cycle is closed by hydride reduction of $\text{R}_2\text{C}=\text{OSiR}_3^+$.^{5b} Hydrosilation of imines^{5d}, enones and silyl enol ethers^{5e} and olefins^{5f} is reported to occur by a similar mechanism.

The reduction of C-O single bonds⁷ has also been achieved catalytically using the $(\text{C}_6\text{F}_5)_3\text{B}$ /silane system. Gevorgyan and Yamamoto reported that using Et_3SiH as reductant certain alcohols could be converted to alkanes via initial formation and reduction of triethylsilyl alkyl ethers.⁸ Furthermore, alkyl ethers could be reduced to silyl alkyl ethers. Extending this work, McRae demonstrated reduction of ketones and aldehydes as well as primary, secondary and tertiary alcohols to alkanes using either diethylsilane or butylsilane in combination with $(\text{C}_6\text{F}_5)_3\text{B}$.⁹ Mechanistic studies of the reduction of alkyl silyl ethers by $\text{Ph}_2\text{MeSiH}/(\text{C}_6\text{F}_5)_3\text{B}$ have been reported.¹⁰

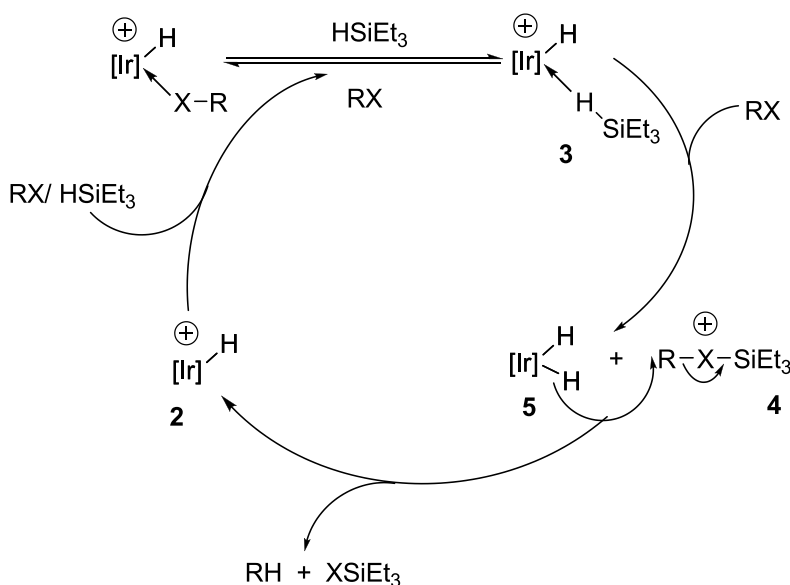
We have discovered that the highly active cationic iridium pincer complex **1** (Chart 2.1) catalyzes the reduction by triethylsilane of primary, secondary and tertiary chlorides, bromides and iodides as well as certain fluorides (see Chapter one).¹¹ In-depth mechanistic studies have been carried out which have revealed a unique catalytic cycle (Scheme 2.1). The electrophilic iridium hydride complex **2** binds and activates the silane to form **3**. This complex transfers “ Et_3Si^+ ” to the halide forming a bridged halonium ion **4** which is rapidly reduced by the iridium dihydride **5** which remains following the silyl transfer. This step regenerates the cationic iridium hydride complex and closes the catalytic cycle. The key Ir(silane) intermediate **3** has been isolated and fully characterized by NMR spectroscopy and

X-ray crystallography, which shows it to be an unprecedented cationic transition metal η^1 -silane complex (see Chapter three).¹²

Chart 2.1. Cationic Iridium Pincer Catalysts **1**.



Scheme 2.1. Proposed Catalytic Cycle for Iridium-Catalyzed Reduction of Alkyl Halides by Triethylsilane

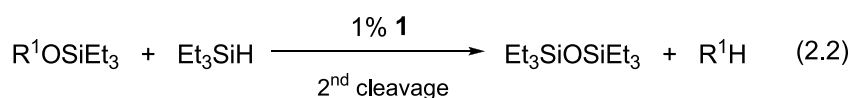
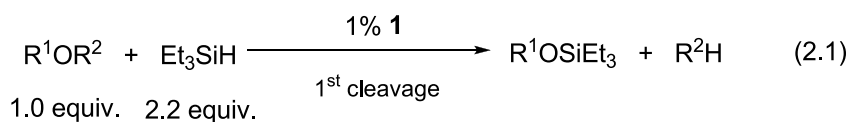


In considering application of this chemistry to other organic functional groups, we have been particularly drawn to the cleavage and reduction of alkyl ethers, due to the potential synthetic applications of this reaction. This Chapter describes the use of cationic iridium pincer catalysts for the room-temperature cleavage and reduction of a broad range of alkyl ethers with triethylsilane, as well as mechanistic details of these novel catalytic

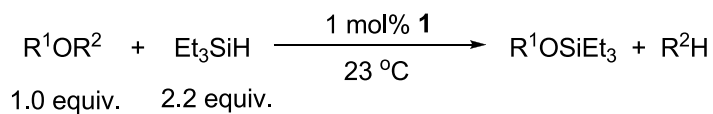
transformations including *isolation* and spectroscopic and structural characterization of the key intermediate diethyl(triethylsilyl)oxonium ion.

Results and Discussion

A. Cleavage of Alkyl Ethers with Et₃SiH Catalyzed by Iridium Complex 1. Alkyl ethers are readily cleaved with Et₃SiH in presence of 1 mol % of iridium complex **1** at room temperature to yield alkyl triethylsilyl ethers and alkane (eq 2.1). In some cases cleavage of the silyl ether can also yield hexaethyldisiloxane and a second equivalent of alkane (eq 2.2).



Dichlorobenzene is generally used as solvent; however, reactions in chlorobenzene, fluorobenzene or neat alkyl ether also proved successful. Results of typical reactions are illustrated in Table 2.1. Conversions are determined by NMR spectroscopy.

Table 2.1. Cleavage of Alkyl Ethers with Et₃SiH Catalyzed by **1**^a

Entry	Cat. [mol %]	Ether	Time (h)	Conversion ^f (%)	Product
1	1.0	Diethyl ether	3	>99	EtOSiEt ₃
		2 nd cleavage	20	>99	Et ₃ SiOSiEt ₃
2	1.0	Diisopropyl ether	43.5	95	<i>i</i> -PrOSiEt ₃
3	1.0	Anisole	3	>99	PhOSiEt ₃
4 ^b	0.1	Anisole	18.5	>99	PhOSiEt ₃
5 ^c	0.25	Anisole	23.2	>99	PhOSiEt ₃
6 ^d	0.5	2,6-Dimethylanisole	10	>99	ArOSiEt ₃
7 ^e	1.0	Benzyl methyl ether	0.3	>99	MeOSiEt ₃ ^g
		2 nd cleavage	5.5	>99	Et ₃ SiOSiEt ₃
8 ^e	1.0	<i>t</i> -Butyl methyl ether	8	>99	Et ₃ SiOSiEt ₃ ^h
9	1.0	<i>n</i> -Butyl methyl ether	0.3	>99	<i>n</i> -BuOSiEt ₃
		2 nd cleavage	69	92	Et ₃ SiOSiEt ₃

^a General reaction conditions: 1 mol% of **1**, 2.2 equiv. of Et₃SiH, C₆D₄Cl₂, 23 °C. ^b Reaction was carried out at 65 °C. ^c in neat anisole. ^d 1.1 equiv. of Et₃SiH was used. ^e 6 equiv. of Et₃SiH was used. ^f Determined by loss of reactant ethers by ¹H NMR spectroscopy. ^g In addition to toluene, some alkylation products were observed. ^h In addition to isobutane, isobutene and H₂ were observed.

Entry 1 shows that rapid cleavage of diethyl ether and formation of ethane and ethoxytriethylsilane (1st cleavage) is accomplished in 3 h at 23 °C with 1% catalyst loading while about 20 h is required for reduction of the formed ethoxytriethylsilane to a second equivalent of ethane and hexaethyldisiloxane (2nd cleavage). Under similar conditions cleavage of secondary alkyl ethers is slow. For example, as shown in entry 2, diisopropyl ether requires ca. 44 h for 95% conversion to propane and isopropyl triethylsilyl ether and resists further reduction to hexaethyldisiloxane (2nd cleavage). Even at longer reaction times (8 days) or elevated reaction temperatures (65 °C, 5 h) only negligible amounts of hexaethyldisiloxane were observed. Similarly, efficient cleavage of alkyl aryl ethers to aryl silyl ethers can be achieved readily. Thus anisole can be cleaved in 4 hours with 1% **1** at 23 °C (entry 3). At 0.1% loading, complete cleavage of anisole is accomplished in 18.5 hours at 65 °C (entry 4). Cleavage reactions can also be carried out in neat anisole and 400 TOs can be readily achieved at 23 °C (entry 5). The bulkier alkyl aryl ether, 2, 6-dimethylanisole, is also cleaved efficiently at 23 °C with a slight excess of Et₃SiH (1.1 equiv.) and 0.5% loading of **1** (entry 6). In the case of aromatic ethers no C(sp²)-O cleavage is ever observed.

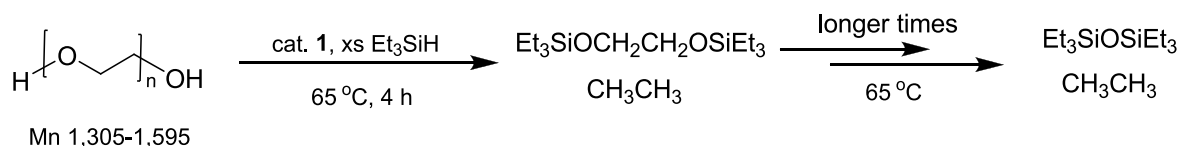
Results of the cleavage of mixed alkyl ethers (R¹OR²) are shown in entries 7-9. Benzyl methyl ether is cleaved to methyl triethylsilyl ether (1st cleavage) in less than 20 minutes with 1% catalyst loading and the formed methyl triethylsilyl ether is further reduced to methane and hexaethyldisiloxane (2nd cleavage) within another 5.5 h. Similarly, *tert*-butyl methyl ether is rapidly cleaved to methyl triethylsilyl ether and a mixture of isobutene, H₂ and isobutane. At longer reaction times, methyl triethylsilyl ether is further reduced to methane and hexaethyldisiloxane while isobutene is hydrogenated to isobutane. The methyl group of *n*-butyl methyl ether is selectively (>95%) and rapidly cleaved to yield *n*-butyl triethylsilyl

ether and methane. At longer reaction times, the formed *n*-butyl triethylsilyl ether can be further reduced to *n*-butane and hexaethyldisiloxane.

In a competition experiment, a mixture of diethyl ether (1 equiv.) and diisopropyl ether (1 equiv.) was treated with Et₃SiH (4.4 equiv.) and 2% **1**. Rapid, exclusive cleavage of diethyl ether resulted in formation of a mixture of ethoxytriethylsilane and unreacted diisopropyl ether. At longer reaction times, reduction of diisopropyl ether occurs faster than reduction of ethoxytriethylsilane. These results indicate that highly chemoselective cleavage of alkyl ethers can be achieved with the **1**/Et₃SiH system.

This C-O cleavage chemistry has also been applied to catalytic fragmentation of poly(ethylene glycol) by triethylsilane. Thus in presence of catalytic amount of **1**, the commercial available poly(ethylene glycol) was readily degraded to Et₃SiOCH₂CH₂OSiEt₃ and ethane at 65 °C (Scheme 2.2).

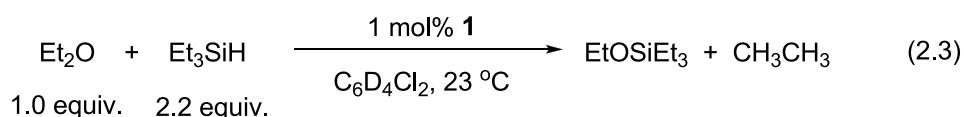
Scheme 2.2. Fragmentation of Poly(ethylene glycol) with **1**/Et₃SiH System.



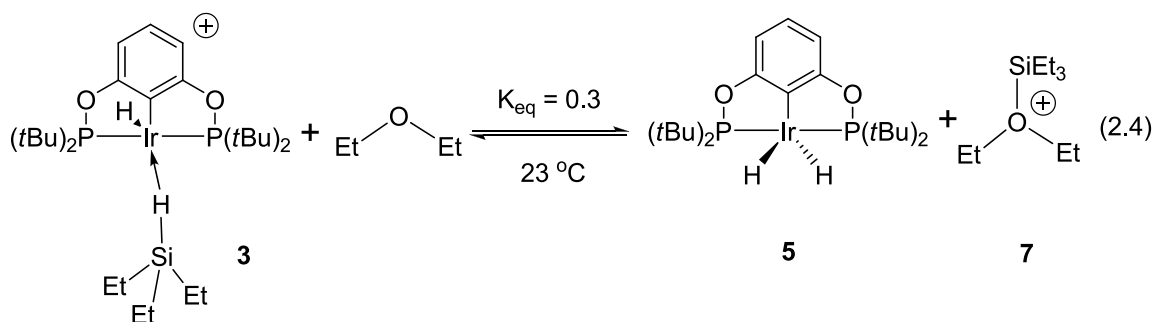
B. In situ ³¹P and ¹H NMR Spectroscopic Monitoring of the Working Catalyst System for Et₂O Reduction: Identification of the Catalytic Resting State and Key Intermediates.

To identify catalyst resting state(s) and key intermediates for this catalytic process, the cleavage of diethyl ether was performed under standard catalytic conditions and monitored by ¹H, ¹³C{¹H} and ³¹P{¹H} NMR spectroscopy. From earlier studies¹¹ we know that complex **1** is rapidly converted to the cationic monohydride complex, **2**, which can bind triethylsilane to form **3**. Following the in situ cleavage of Et₂O at 23 °C with 1 mol % catalyst

loading (eq 2.3), the only iridium species observable initially are the *neutral* iridium dihydride complex¹³, **5**, (ca. 80%) and the neutral silyl hydride complex (POCOP)Ir(H)(SiEt₃) {POCOP = 2, 6-[OP(*t*Bu)₂]₂C₆H₃}, **6**, (ca.20%) (This complex is formed by reaction of **5** with triethylsilane, see below). As the reduction proceeds, Et₂O, **5** and **6** decrease in concentration while the cationic iridium silane complex, **3**, appears and grows in concentration equivalent to the loss of **5** and **6**.

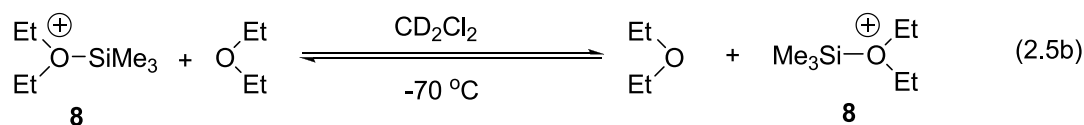
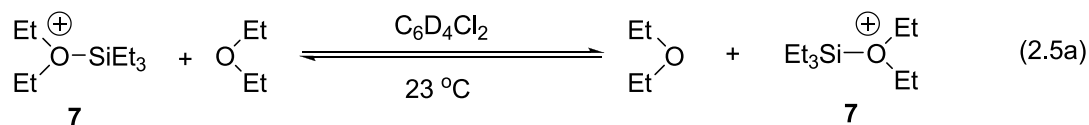


This observation suggests that the iridium silane complex **3** is in equilibrium with the iridium dihydride **5** and diethyl(triethylsilyl)oxonium ion **7** as shown in eq 2.4 and that this equilibrium is established rapidly relative to the rate of reduction. Once the concentration of **3** is sufficient to be measured relative to **5** and Et₂O, the equilibrium constant can be determined by ¹H and ³¹P{¹H} NMR spectroscopy. At several stages of conversion K_{eq} was determined to be 0.3, consistent with the proposition that equilibrium is maintained between **3** and **5** throughout the catalytic reduction.

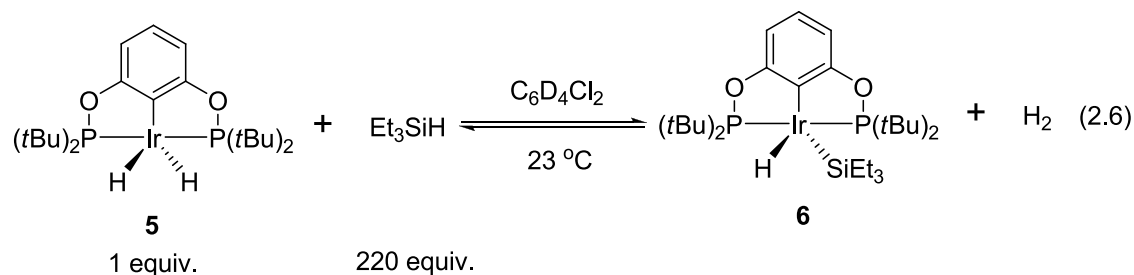


Species **7** cannot be spectroscopically observed at 23 °C. Significant line broadening of the ethyl groups of diethyl ether is observed in both the ¹H and ¹³C NMR spectra which we propose indicates rapid dynamic exchange between **7** and Et₂O (eq 2.5a) . Observations by

Kira, Sakurai and co-workers¹³ support this hypothesis. They showed that in situ generation of $[\text{Et}_2\text{OSiMe}_3]^+[\text{BAr}_\text{F}]^-$ [$\text{Ar}_\text{F} = 3, 5\text{-(CF}_3)_2\text{C}_6\text{H}_3$] in the presence of excess Et_2O at $-70\text{ }^\circ\text{C}$ resulted in a dynamic system described by eq 2.5b as shown by line broadening in the ^1H and ^{13}C NMR spectrum.¹⁴



As noted above, a small quantity (ca. 20% by $^{31}\text{P}\{^1\text{H}\}$ NMR spectroscopy) of an iridium species assigned as the silyl hydride **6** was observed in the working catalytic system. This complex was independently generated by treatment of $(\text{POCOP})\text{Ir}(\text{H})(\text{Cl})$ with NaOtBu in presence of excess Et_3SiH in C_7D_8 and fully characterized by NMR spectroscopy¹¹ (see Chapter one). It can also be generated by treatment of dihydride **5** with a large excess of Et_3SiH in $\text{C}_6\text{D}_4\text{Cl}_2$ in the absence of diethyl ether (eq 2.6). The K_{eq} is not available due to the difficulty of accurately measuring the concentration of H_2 in $\text{C}_6\text{D}_4\text{Cl}_2$ solution.

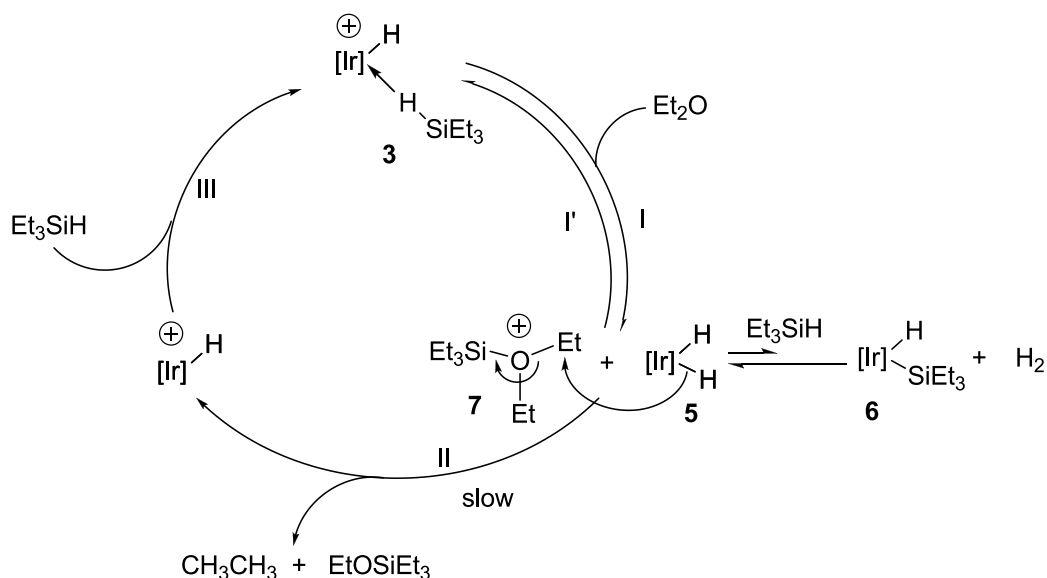


In the working catalyst system for diethyl ether cleavage (eq 2.3), the ratio of **6** to **5** increases with an increase of the initial $\text{Et}_3\text{SiH}:\text{Ir}$ ratio. Thus it is instructive to note that increasing the Et_3SiH concentration while holding the loading of **1** at 1 mol% (relative to

Et₂O) results in a decrease in the rate of the first cleavage. This suggests that dihydride **5** is a much more effective hydride donor for reducing **7** than silyl hydride, **6**.

The above results support the proposed catalytic cycle shown in Scheme 2.3. At high Et₂O concentrations in the initial stages of catalysis equilibrium between **3** plus Et₂O and **5** plus **7** strongly favors **5** plus **7**. The dihydride, **5**, reacts with silane to generate small but observable quantities of silyl hydride, **6**. The dihydride reduces **7** to yield product EtOSiEt₃ and cationic monohydride **2**, which, upon reaction with silane, forms **3** and closes the catalytic cycle. The silyl hydride does not compete with dihydride as a hydride donor. As catalysis proceeds and ether is depleted, the concentration of the silane complex, **3**, increases and becomes observable by NMR spectroscopy. The turnover-limiting step in the cycle is reduction of Et₃SiOEt₂⁺ by the neutral dihydride complex. Two additional experiments were carried out to confirm this catalytic cycle.

Scheme 2.3. Proposed Catalytic Cycle for Cleavage of Et₂O with **1**/Et₃SiH.



C. Effect of Adding Additional Iridium Dihydride, 5. If the turnover-limiting step is reaction of dihydride, **5**, with the oxonium species, **7**, (and knowing dihydride is the catalyst resting state), then addition of **5** to the reaction should result in a proportionate increase in turnover frequency. As expected, addition of 1.0 mol% of iridium dihydride **5** to the catalytic system initiated with 1% Ir (eq. 2.7) was found to increase the initial turnover frequency for an order of 1.8 as can be seen from the data shown in Figure 2.1. If **5** were the sole Ir species present, then a rate increase of 2.0 would be expected. The increase of only 1.8 is attributable to the removal of some **5** from the reaction by formation of the relatively inert **6**. These results further support the mechanistic proposal in Scheme 2.3.

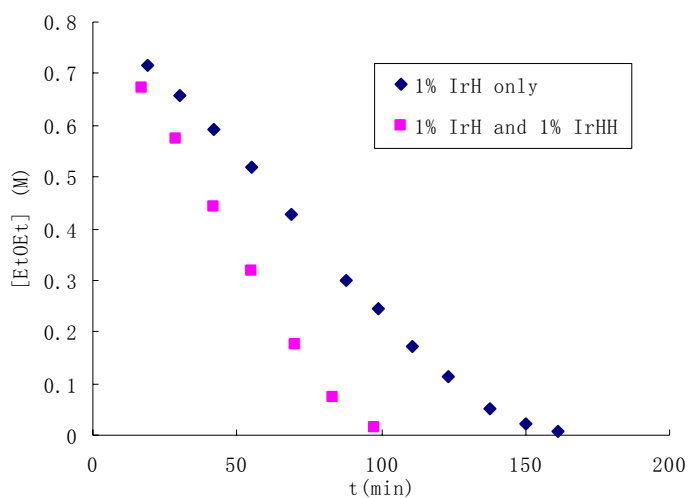
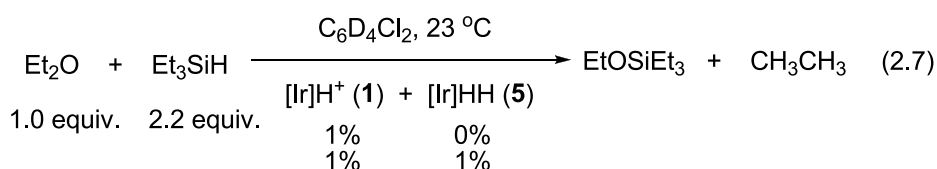


Figure 2.1. Plot of Et₂O concentration vs time for the cleavage of Et₂O with and without adding additional **5**.

D. Generation, Spectroscopic and Structural Characterization and Dynamic Behavior of diethyl(triethylsilyl)oxonium and its Reactivity towards 5. The proposed catalytic intermediate diethyl(triethylsilyl)oxonium ion, $\text{Et}_3\text{SiOEt}_2^+$, **7**, can be independently generated using Lambert methodology^{15,5b} by treating the in situ formed C_6D_6 -stabilized triethylsilyl cation $[\text{Et}_3\text{Si}(\text{C}_6\text{D}_6)]^+[\text{B}(\text{C}_6\text{F}_5)_4]^-$ with diethyl ether in $\text{C}_6\text{D}_5\text{Cl}$ at $-40\text{ }^\circ\text{C}$. The ^1H , $^{13}\text{C}\{^1\text{H}\}$ and $^{29}\text{Si}\{^1\text{H}\}$ NMR spectra confirm clean formation of cation **7**. The ^1H spectrum shows the triethylsilyl group resonances at δ 0.58 (CH_3) and 0.30 (CH_2), and the methyl and methylene protons adjacent to the oxygen at δ 0.82 and 3.53, respectively. The $^{13}\text{C}\{^1\text{H}\}$ shows, in addition to the $\text{B}(\text{C}_6\text{F}_5)_4^-$ counteranion and excess free Et_2O (δ 66.2 and 15.8) and traces of excess Et_3SiH , only four signals corresponding to the methyl and methylene carbons of the EtO- group at δ 75.1 and 12.8, and the triethylsilyl group at δ 3.1 and 5.5. Slight line broadening of the ethyl groups of **7** is seen in the ^1H and $^{13}\text{C}\{^1\text{H}\}$ NMR spectrum, which indicates rapid dynamic exchange with free Et_2O even at $-40\text{ }^\circ\text{C}$. The $^{29}\text{Si}\{^1\text{H}\}$ resonance of **7** appeared as a singlet at δ 68.9. This is downfield compared to free Et_3SiH (δ 0.2) and the iridium $\eta^1\text{-Et}_3\text{SiH}$ complex **3** (δ 30.2)¹², but still upfield of that for the C_6D_6 -stabilized triethylsilyl cation $[\text{Et}_3\text{Si}(\text{C}_6\text{D}_6)]^+$ (δ 92.3).^{15a}

Upon warming up, the ^1H and ^{13}C resonances corresponding to **7** and free Et_2O broaden and coalesce. At $20\text{ }^\circ\text{C}$ the ^1H NMR spectrum shows broad bands at δ 3.4 and 1.0 respectively for the methylene and methyl protons of the $-\text{OCH}_2\text{CH}_3$ group. The methyl and methylene carbons of the EtO- group, however, are too broad to be observed in the $^{13}\text{C}\{^1\text{H}\}$ NMR spectrum due to exchange on the NMR timescale.

An X-ray quality crystal of **7** was obtained by slow diffusion of pentane into a $\text{C}_6\text{D}_5\text{Cl}$ solution of **7** at $-35\text{ }^\circ\text{C}$ under Ar. Complex **7** can also be isolated by crystallization from the

catalytic reaction mixture at -35 °C, which further indicates its intermediacy as a resting state in the working catalyst system. The ORTEP diagram of **7** is shown in Figure 2.2.

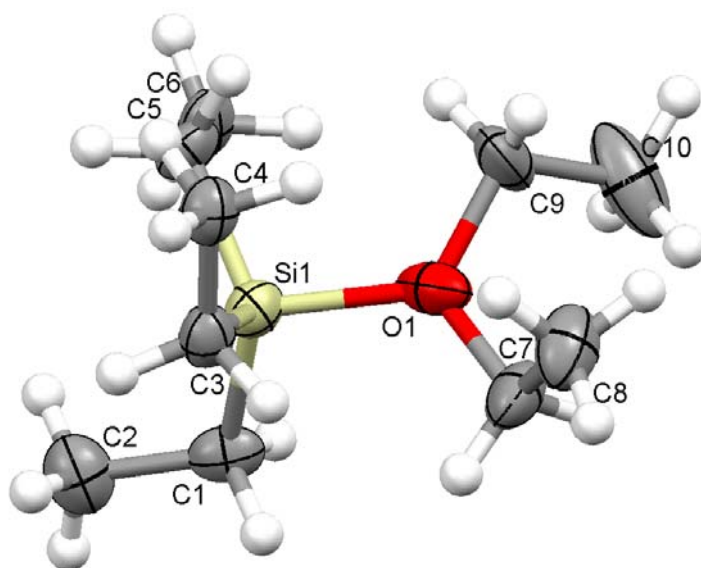
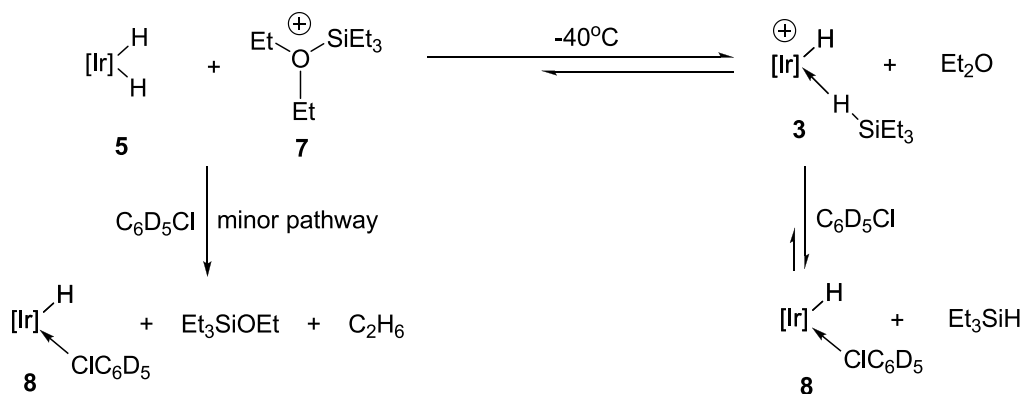


Figure 2.2. An ORTEP diagram of the cation in **7**. Key bond distances (Å) and bond angles (°): Si(1)-O(1) = 1.812(4), Si(1)-C(1) = 1.841(5), Si(1)-C(3) = 1.863(5), Si(1)-C(5) = 1.863(5), O(1)-C(7) = 1.487(7), O(1)-C(9) = 1.494(7), C(1)-C(2) = 1.516(8), C(3)-C(4) = 1.527(8), C(5)-C(6) = 1.534(8), C(7)-C(8) = 1.491(8), C(9)-C(10) = 1.493(11), O(1)-Si(1)-C(1) = 104.2(2), O(1)-Si(1)-C(3) = 104.7(2), O(1)-Si(1)-C(5) = 105.1(2), C(1)-Si(1)-C(3) = 115.3(2), C(1)-Si(1)-C(5) = 112.5(3), C(3)-Si(1)-C(5) = 113.7(2), C(7)-O(1)-C(9) = 116.3(2), C(7)-O(1)-Si(1) = 117.8(3), C(9)-O(1)-Si(1) = 124.0(4).

Addition of iridium dihydride **5** in C₆D₅Cl solution at -40 °C to in situ generated diethyl(triethylsilyl)oxonium ion **7** at -40 °C, results in formation of free Et₃SiH and cationic iridium chlorobenzene-d₅ complex **8** with little formation of cleavage products EtOSiEt₃ and C₂H₆ (Scheme 2.4). This result is consistent with the mechanistic proposal shown in Scheme 2.3 in which there is a rapid pre-equilibrium between **5** and **3** prior to product formation. If

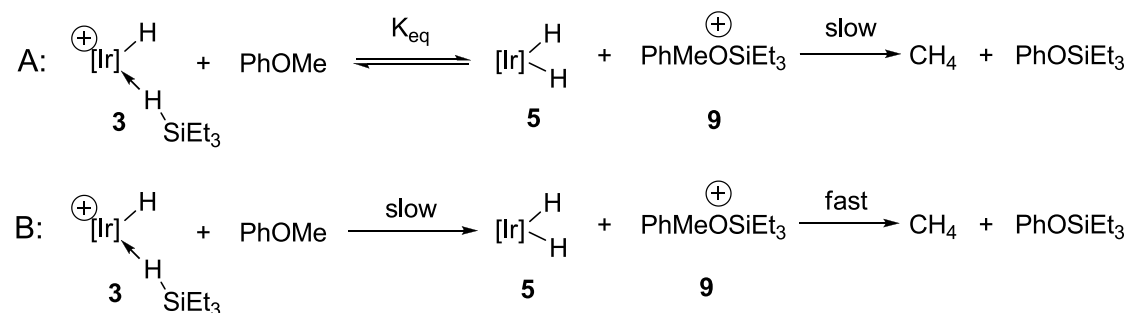
nucleophilic attack of **5** on **7** to yield EtOSiEt₃ is turnover-limiting, then reaction of **5** with **7** should *initially* yield predominantly **3** and Et₂O as observed. (Under these conditions with only one equivalent of silane present per Ir center, we have previously established that silane will be displaced from **3** by solvent to yield the chlorobenzene adduct, **8**.)

Scheme 2.4. Reaction of **7** with **5** at -40 °C



E. Catalytic Cleavage of Less Basic PhOCH₃ with Et₃SiH. Following the in situ NMR monitoring and mechanistic analysis of the diethyl ether cleavage reactions, we turned to investigate a much less basic alkyl aryl ether, anisole. The catalytic cleavage reaction with PhOCH₃ was also monitored by both ¹H and ³¹P{¹H} NMR spectroscopy. Interestingly, the only Ir species present throughout the entire catalytic reaction is the iridium silane complex, **3**. This could be due to (1) the low basicity of anisole, which results in very low equilibrium concentrations (beyond NMR detection limit) of neutral iridium dihydride **5** and methylphenyl(triethylsilyl)oxonium ion **9** (Scheme 2.5A) or (2) the result of slow transfer of “Et₃Si⁺” from **3** to anisole followed by fast reaction of **5** with oxonium species **9** (Scheme 2.5B). However, in either of these two cases, no dependence of the TOF on the concentration of **5** would be expected.

Scheme 2.5. Two Mechanistic Proposals for Ir-catalyzed Cleavage of Anisole with Et₃SiH



Thus addition of 0.5 mol% to 1.5 mol% iridium dihydride **5** to the catalytic reaction mixture (eq 2.8) was found to have no effect on the reaction rate (Figure 2.3), and as expected, under these reaction conditions (eq 2.9), the turnover frequency is zero-order in the concentration of Et₃SiH (Figure 2.4).

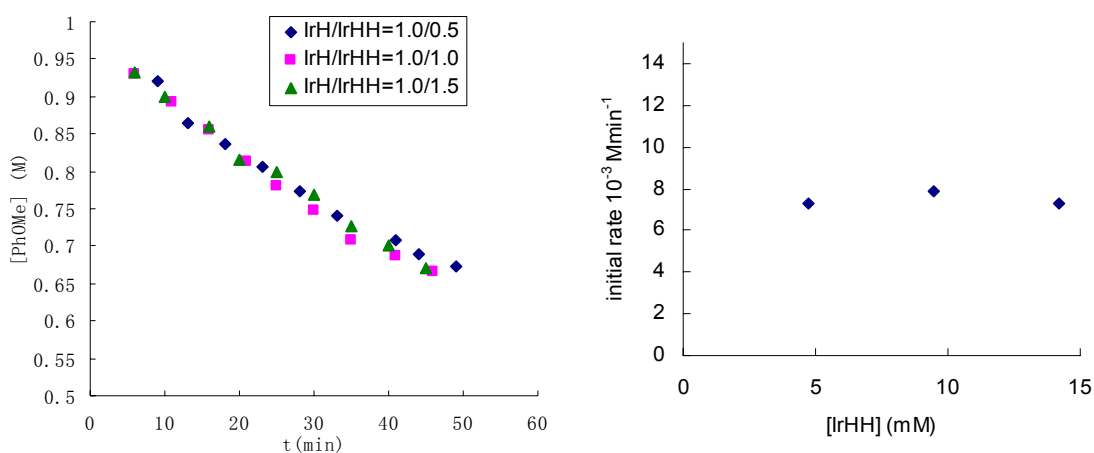
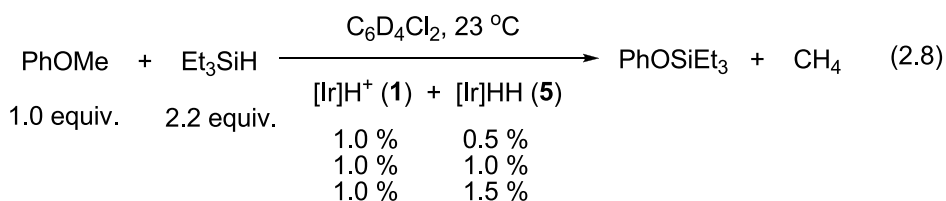


Figure 2.3. (Left): plot of PhOMe concentration vs time for the anisole cleavage catalyzed by **1** and **5**; (right): plot of the initial rate, V_i , vs. concentration of **5** for the cleavage of anisole catalyzed by **1** and **5**.

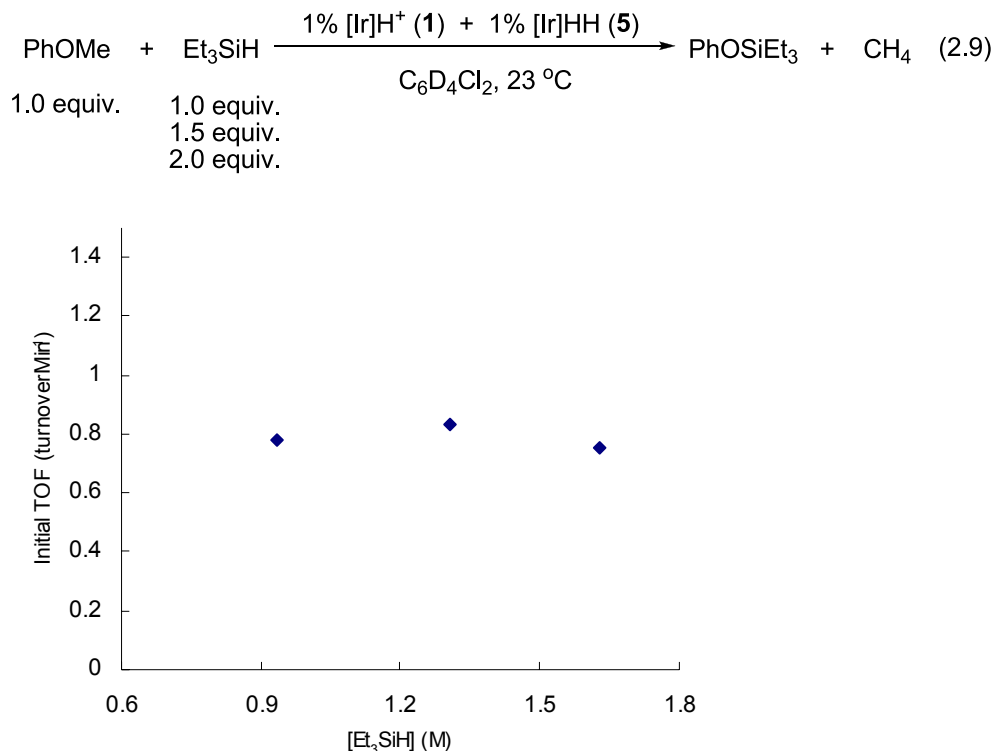
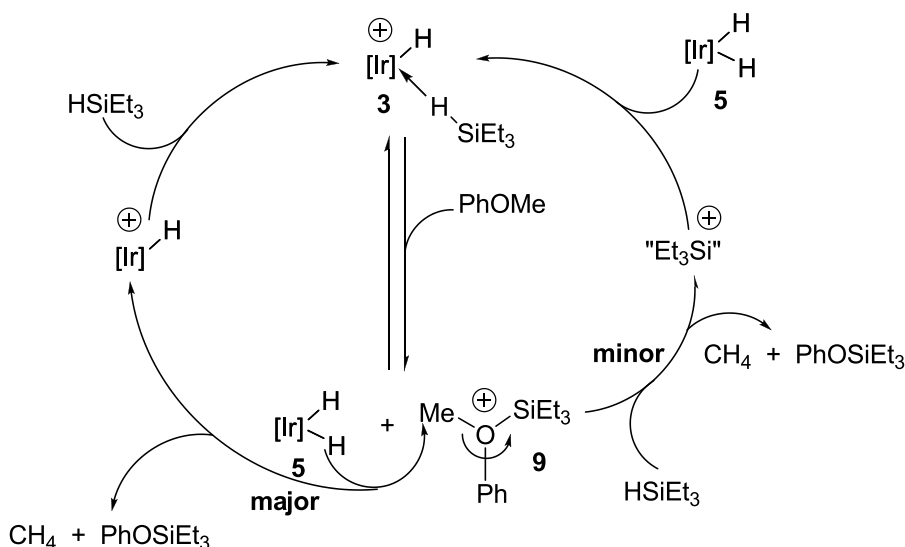


Figure 2.4. Plot of the initial turnover frequency (TOF) vs. Et₃SiH concentration for the cleavage of anisole catalyzed by **1** and **5**.

Under conditions where no additional iridium dihydride **5** is added, there is very little **5** and methylphenyl(triethylsilyl)oxonium ion **9** present. Under these conditions, since the iridium silane complex **3** is the only detectable resting state, triethylsilane, which is present in much higher concentration, could compete with **5** for the reduction of **9** (Scheme 2.6). A complication as noted earlier is that **5** and Et₃SiH are also in equilibrium with iridium silyl hydride **6** and H₂ (eq 2.6). Therefore, fully consistent kinetic results could not be obtained in the absence of additional iridium dihydride. However our preliminary studies favor iridium dihydride **5** as the major hydride donor in the cleavage of anisole.

Scheme 2.6. Proposed Catalytic Cycle for Cleavage of PhOMe



A similar situation occurs in the 2nd step of the cleavage of diethyl ether (conversion of EtOSiEt_3 to $\text{Et}_3\text{SiOSiEt}_3$ and ethane, see eq 2). Like the anisole system, the iridium silane complex, **3**, was observed as the catalyst resting state. Interestingly, in the same reaction pot, addition of **5**, which resulted in a rate increase for the 1st cleavage step of diethyl ether, was found to dramatically retard the 2nd cleavage reaction (94% conversion after 353 h as compared to 97% conversion after 20 h without adding **5**). Kinetic studies show that increasing the Et_3SiH concentration results in an increase in the rate of the second cleavage, which suggests that Et_3SiH may serve as a hydride donor in the second cleavage reactions. Iridium silane complex, **3**, and EtOSiEt_3 are in rapid pre-equilibrium with **5** and $\text{EtO}(\text{SiEt}_3)_2^+$, **10**, and Et_3SiH competes with very low concentrations of **5** for reduction of **10**. Addition of **5** to the catalytic system would decrease the concentration of **10** and thus result in a decrease in the overall rate of the 2nd cleavage. The steric crowding of the $-\text{CH}_2-$ group in $[(\text{Et}_3\text{Si})_2\text{O}-\text{CH}_2\text{CH}_3]^+$ may disfavor reduction by the bulky iridium dihydride, **5**. (A small but observable

amount of neutral iridium silyl hydride, **6**, was also observed in the 2nd cleavage of diethyl ether, which diminished after the reduction was finished.)

F. Comparison of Ir-catalysis with [Ph₃C][B(C₆F₅)₄] for Alkyl Ether Cleavage. The combination of [Ph₃C][B(C₆F₅)₄]/Et₃SiH was reported by Lambert^{15a} for catalytic hydrosilation of diphenylethene and has also been demonstrated recently by Ozerov¹⁶ to be capable of catalytic hydrodefluorination of C(sp³)-F bond presumably via a mechanism involving a carbenium ion intermediate. To gain further mechanistic insight into the system, we have examined the capability of [Ph₃C][B(C₆F₅)₄]/Et₃SiH system for alkyl ether cleavage reactions and compared it with the **1**/Et₃SiH system (eq 10). In the catalytic cleavage of anisole, as shown in Figure 5, iridium complex **1** is less reactive than [Ph₃C][B(C₆F₅)₄] (*t*_{1/2} (23 °C) = 80 min for **1**; *t*_{1/2} (23 °C) = 10 min for [Ph₃C][B(C₆F₅)₄]). However, for catalytic reactions with the more basic alkyl ether Et₂O (Figure 6), iridium complex **1** is much more reactive than [Ph₃C][B(C₆F₅)₄]/Et₃SiH system under same reaction conditions (*t*_{1/2} (23 °C) = 80 min for **1**; *t*_{1/2} (23 °C) = 120 h for [Ph₃C][B(C₆F₅)₄]).

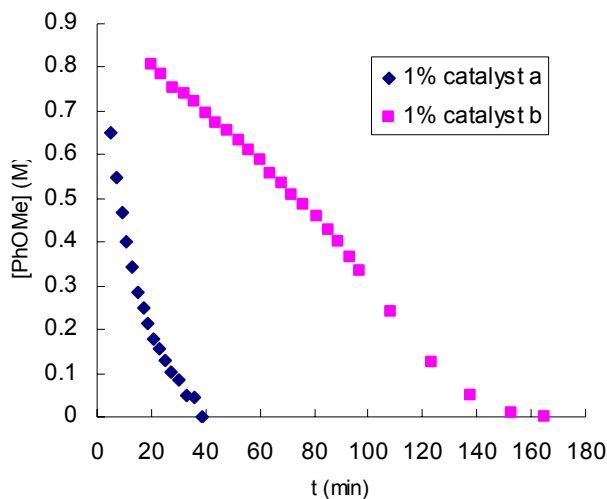
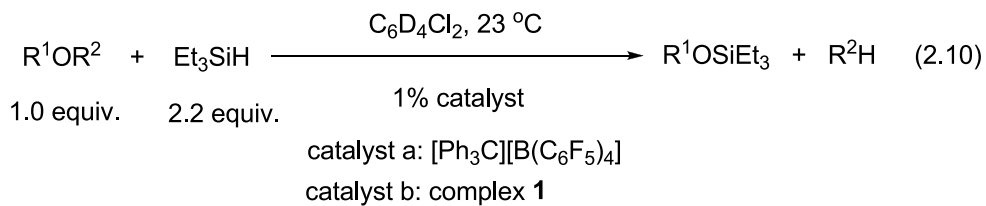


Figure 2.5. Plot of PhOMe concentration vs time for anisole cleavage reactions catalyzed by catalyst a: $[\text{Ph}_3\text{C}][\text{B}(\text{C}_6\text{F}_5)_4]$ and by catalyst b: complex **1**.

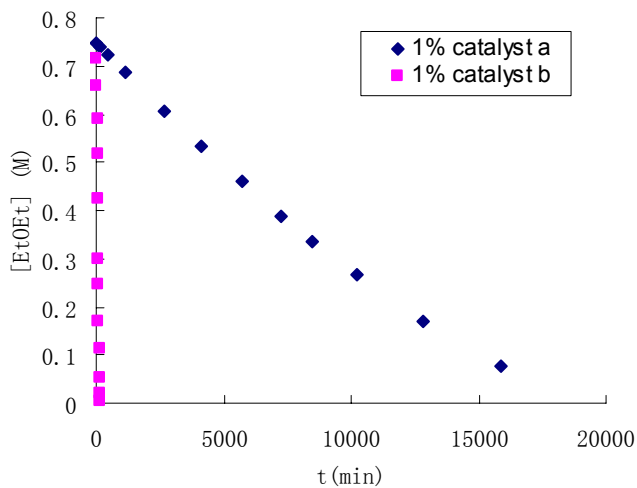
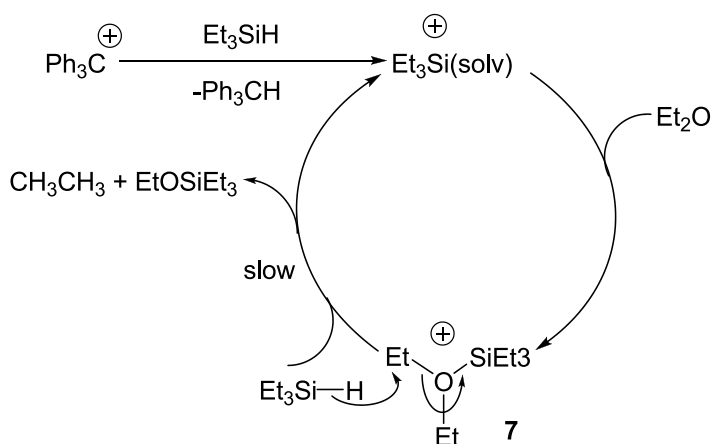


Figure 2.6. Plot of Et₂O concentration vs time for Et₂O cleavage reactions catalyzed by catalyst a: $[\text{Ph}_3\text{C}][\text{B}(\text{C}_6\text{F}_5)_4]$ and by catalyst b: complex **1**.

Scheme 2.7. Proposed Catalytic Cycle for Et₂O Cleavage with [Ph₃C][B(C₆F₅)₄]/Et₃SiH



When the catalytic cleavage of Et₂O with [Ph₃C][B(C₆F₅)₄] was followed by ¹H and ¹³C NMR spectroscopy, similar to the iridium catalytic system, line broadening of the ethyl groups of diethyl ether was observed in the both ¹H and ¹³C NMR spectra. This indicates that diethyl(trimethylsilyl)oxonium ion, **7**, is the resting state in the Et₂O cleavage reaction catalyzed by [Ph₃C][B(C₆F₅)₄] (Scheme 2.7). Indeed **7** can be isolated from this catalytic reaction mixture as well. Although lower in concentration ([**7**]/[Et₃SiH] = 1/250 in Et₂O reduction), iridium dihydride **5** is more nucleophilic than Et₃SiH and potentially a much better hydride donor, therefore, the turn-over limiting hydride transfer step is much faster for iridium-catalysis compared with [Ph₃C][B(C₆F₅)₄]-catalysis in diethyl ether cleavage. Relative rates for hydride reduction of **7** (**5**: Et₃SiH = ca. 30000:1) can be estimated from the ratio of initial reduction rates (V_i(Ir): V_i(Ph₃C⁺) = 105:1) and the relative initial concentration ratio ([**5**]: [Et₃SiH] = 1:270).

However, in the catalytic reaction with less basic PhOCH₃, as discussed earlier, iridium silane complex **3** is the catalyst resting state and results in very low concentrations of iridium dihydride **5** and methylphenyl(trimethylsilyl)oxonium ion **9**, then a slower reaction was

observed as compared to $[\text{Ph}_3\text{C}][\text{B}(\text{C}_6\text{F}_5)_4]$ -catalysis. (In the $[\text{Ph}_3\text{C}][\text{B}(\text{C}_6\text{F}_5)_4]/\text{Et}_3\text{SiH}$ system, the presumably “resting state”, PhMeOSiEt_3^+ , **9**, has also been independently generated according to procedures analogous to **7**, see experimental section for details.)

Summary

The novel reduction chemistry discovered in Chapter one has been applied to the catalytic cleavage and reduction of alkyl ethers due to the potential synthetic applications of this reaction. At room temperature cationic iridium pincer catalyst **1** in combination with Et_3SiH reduces a wide variety of unactivated alkyl ethers including primary, secondary and tertiary alkyl ethers as well as aryl alkyl ethers. For example, diethyl ether can be readily converted to two equivalents of ethane and $\text{Et}_3\text{SiOSiEt}_3$. This C-O cleavage chemistry has also been applied to catalytic fragmentation of poly(ethylene glycol).

Highly chemoselective cleavage of alkyl ethers can be achieved with the **1**/ Et_3SiH system. For example, in a competition experiment, a mixture of diethyl ether and diisopropyl ether was treated with **1**/ Et_3SiH and resulted in the rapid, exclusive cleavage of diethyl ether with formation of a mixture of ethoxytriethylsilane and unreacted diisopropyl ether. At longer reaction times, reduction of diisopropyl ether occurs faster than reduction of ethoxytriethylsilane.

Mechanistic studies have revealed the full details of the catalytic cycle. In the diethyl ether cleavage, iridium $\eta^1\text{-Et}_3\text{SiH}$ (**3**) and Et_2O are in rapid equilibrium with dihydride (**5**) and diethyl(triethylsilyl)oxonium ion (**7**), and the equilibrium strongly favors **5** plus **7**. The turnover-limiting step in the cycle is the reduction of $\text{Et}_3\text{SiOEt}_2^+$ by the neutral dihydride complex, **5**. Addition of **5** into the catalytic system resulted in a proportionate increase in

turnover frequency. The key intermediate diethyl(triethylsilyl)oxonium ion (**7**) was independently generated and isolated by crystallization.

In the cleavage of the less basic ether, anisole, the iridium silane complex (**3**) was found to be the catalyst resting state and resulted in very little **5** and methylphenyl(triethylsilyl)oxonium ion (**9**) present. Triethylsilane is present in much higher concentration, and could compete with **5** for the reduction of **9**. However, our preliminary studies favor iridium dihydride **5** as the major hydride donor in this reaction. Addition of between 0.5 mol% and 1.5 mol% iridium dihydride **5** to the catalytic reaction mixture was found to have no effect on the reaction rate and under these reaction conditions the turnover frequency is zero-order in the concentration of Et₃SiH.

To gain more mechanistic insights, we have compared the catalytic reactivities of **3** with [Ph₃C][B(C₆F₅)₄] for alkyl ethers cleavage. In the catalytic cleavage of anisole, iridium complex **1** is less reactive than [Ph₃C][B(C₆F₅)₄]. However, for catalytic reactions with the more basic diethyl ether, iridium complex **1** is much more reactive than trityl salts under same reaction conditions ($t_{1/2}$ (23 °C) = 77 min for **1**; $t_{1/2}$ (23 °C) = 120 h for [Ph₃C][B(C₆F₅)₄]).

Experimental Section

General considerations. All manipulations were carried out using standard Schlenk, high-vacuum and glovebox techniques. Argon and nitrogen were purified by passage through columns of BASF R3-11 catalyst (Chemalog) and 4 Å molecular sieves. THF and Et₂O were distilled from sodium benzophenone ketyl prior to use. Methylene chloride and toluene were passed through columns of activated alumina¹⁷ and degassed by either freeze-pump-thaw methods or by purging with argon. Benzene and acetone was dried with 4 Å molecular sieves and degassed by freeze-pump-thaw methods. Et₃SiH was dried with LiAlH₄ and vacuum transferred into a sealed flask. All of the other substrates, all the arene solvents (C₆D₅Cl, C₆D₄Cl₂, C₆D₆, C₆H₅F), and pentane were dried with CaH₂ and vacuum transferred to a sealed flask. NMR spectra were recorded on Bruker spectrometers (DRX-400, VANCE-400, AMX-300 and DRX-500). ¹H and ¹³C NMR spectra were referenced to residual protio solvent peaks. ³¹P chemical shifts were referenced to an external H₃PO₄ standard. ²⁹Si chemical shifts were referenced to external (CH₃)₄Si. K[B(C₆F₅)₄] was purchased from Boulder Scientific and dried *in vacuo* at 120°C for 24 hours. All other reagents were purchased from Sigma-Aldrich or Strem., [(POCOP)IrH(acetone)]⁺[B(C₆F₅)₄] (**1**)¹¹, (POCOP)Ir(H)₂ (**5**)¹³ and Ph₃C[B(C₆F₅)₄]¹⁶ were prepared according to published procedures.

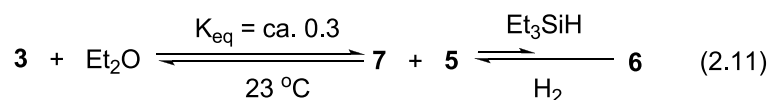
General Procedure for the Cleavage of Alkyl Ethers Catalyzed by Cationic Iridium Acetone Complex, 1. Triethylsilane (175 µL, 1.1 mmol, 2.2 equiv.) was added to a solution of **1** (6.7 mg, 0.005 mmol, 1 mol %) in C₆D₄Cl₂ (0.3 mL) in a medium-walled J. Young NMR tube and the contents were well shaken. The substrate (0.5 mmol, 1.0 equiv.) was then added

and the reactions were allowed to stand at room temperature or heated in an oil bath, and the progress was followed by NMR spectroscopy. Conversions were determined by monitoring the loss of alkyl ethers. Reduction products were identified using ^1H and $^{13}\text{C}\{^1\text{H}\}$ NMR in comparison to literature data or authentic samples.

Cleavage of PhOMe with Et_3SiH Catalyzed by **1 without Solvent.** Triethylsilane (352 μL , 2.2 mmol, 2.2 equiv.) was added to a medium-walled J. Young NMR tube with **1** (3.3 mg, 0.0025 mmol, 0.25 mol%) and a sealed capillary tube with C_6D_6 as internal standard. To this suspension was then added PhOMe (109 μL , 1.0 mmol, 1 equiv.), and the tube was quickly inverted to ensure complete mixing. The reactions were allowed to stand at room temperature and the progress was monitored by NMR spectroscopy. Reduction products (PhOSiEt_3 and CH_4) were identified using ^1H and $^{13}\text{C}\{^1\text{H}\}$ NMR data in comparison to literature data.

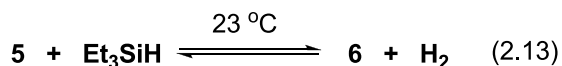
Fragmentation of Poly(ethylene glycol) with Et_3SiH catalyzed by **1.** Catalyst **1** (3.3 mg, 0.0025 mmol) and poly(ethylene glycol) (22 mg, Mw = 1305-1595) were dissolved in $\text{C}_6\text{D}_4\text{Cl}_2$ (0.3 mL) in a J. Young NMR tube. Triethylsilane (240 μL , 1.5 mmol) was added to this solution and the reaction was heated in a 65 $^\circ\text{C}$ oil bath for 4 h. The ^1H and $^{13}\text{C}\{^1\text{H}\}$ NMR spectra show the disappearance of the poly(ethylene glycol) and formation of $\text{Et}_3\text{SiOCH}_2\text{CH}_2\text{OSiEt}_3$ and ethane. $\text{Et}_3\text{SiOCH}_2\text{CH}_2\text{OSiEt}_3$: ^1H NMR ($\text{C}_6\text{D}_4\text{Cl}_2$, 400 MHz, 23 $^\circ\text{C}$): δ 3.60 (s, 4H), 0.9 (m, 9H), 0.5 (m, 6H). $^{13}\text{C}\{^1\text{H}\}$ NMR ($\text{C}_6\text{D}_4\text{Cl}_2$, 100.6 MHz, 23 $^\circ\text{C}$): δ 64.3 (s), 6.5 (s), 4.5 (s). At longer reaction times $\text{Et}_3\text{SiOCH}_2\text{CH}_2\text{OSiEt}_3$ were converted to $\text{Et}_3\text{SiOSiEt}_3$.

Determination of the Equilibrium Constants for Silyl Transfer between 3 and 7 during Diethyl Ether Cleavage. The cleavage of Et₂O was performed under standard catalytic conditions and monitored by ¹H and ³¹P{¹H} NMR spectroscopy. As discussed in the text, a small quantity of 6 was formed by reaction of 5 with triethylsilane (eq 2.11). Thus the concentration of 7 was calculated from the sum of the concentrations of 5 and 6. Once the concentration of 3 was sufficient to be measured relative to 5 and Et₂O, the equilibrium constant was determined by ¹H and ³¹P{¹H} NMR spectroscopy following the formula shown in eq 2.12. At several stages of conversion K_{eq} was determined to be ca. 0.3.



$$K_{\text{eq}} = \frac{[7][5]}{[3][\text{Et}_2\text{O}]} = \frac{([5]+[6])[5]}{[3][\text{Et}_2\text{O}]} \quad (2.12)$$

Reaction of Iridium Dihydride Complex, 5, with Et₃SiH. The iridium silyl hydride, 6, has been previously generated and fully characterized by treatment of (POCOP)Ir(H)(Cl) with NaOtBu in presence of excess Et₃SiH in C₇D₈.¹¹ In current experiment, triethylsilane (175 μL, 1.1 mmol, 220 equiv.) was added to a solution of 5 (3.0 mg, 0.005 mmol, 1 equiv.) in C₆D₄Cl₂ (0.4 mL) in a J. Young NMR tube (eq 2.13). The reaction was allowed to stand at room temperature and the establishment of equilibrium was followed by ¹H and ³¹P{¹H} NMR spectroscopy (eq 2.13). ¹H NMR (C₆D₄Cl₂, 400 MHz, 23 °C): 6, -15.9 (t, 1H, IrH); 5, -17.0 (b, 2H, IrH). ³¹P{¹H} NMR (C₆D₄Cl₂, 162 MHz, 23 °C): 6, δ 189.2; 5, -204.5.



t(min)	6 : 5 (by ^{31}P NMR)
22	0.69:1.00
26	0.87:1.00
36	0.71:1.00
66	0.92:1.00
96	0.93:1.00
116	0.87:1.00
126	0.86:1.00
136	0.86:1.00
1016	0.80:1.00

Cleavage of Et₂O with Et₃SiH Catalyzed by the Mixture of Cationic Complex, 1 and Dihydride Complex, 5. Triethylsilane (175 μL , 1.1 mmol, 2.2 equiv.) and Et₂O (52 μL , 0.5 mmol, 1 equiv.) were added to a solution of **1** (6.7 mg, 0.005 mmol, 1 mol%) and **5** (3.0 mg, 0.005 mmol, 1 mol%) in C₆D₄Cl₂ (0.3 mL) in a medium-walled J. Young NMR tube. The contents were well shaken and the reaction was monitored by Et₂O loss relative to the CH₃CH₂- groups of the silanes [sum of (CH₃CH₂)₃SiH and (CH₃CH₂)₃SiOEt] with respect to time by ^1H NMR spectroscopy.

In situ Generation and Variable-Temperature NMR Spectroscopic Characterization of Diethyl(triethylsilyl)oxonium ion, 7. Dried C₆D₆ (0.5 mL) was added to a screw-cap NMR tube with [Ph₃C][B(C₆F₅)₄] (92 mg, 0.1 mmol, 1.0 equiv.) in drybox. To this suspension was then added triethylsilane (18 μL , 0.113 mmol, 1.13 equiv.), and the tube was quickly inverted to ensure complete mixing. Light brown oil was produced at the bottom.

The clear top phase was removed by syringe and the oil was washed with C₆D₆ (0.1 mL × 2). The oil (ca. 0.1 mL) was dissolved in C₆D₅Cl (0.6 mL) at room temperature and the solution was cooled down to -40 °C. Diethyl ether (20-100 µL, 0.19-0.95 mmol, 1.9-9.5 equiv.) was added by syringe and the NMR tube was then placed in the pre-cooled NMR probe at -40 °C. ¹H NMR (C₆D₅Cl, 400 MHz, -40 °C): δ 3.53 (br, 4H, 4-H), 0.82 (s, 6H), 0.58 (m, 9H), 0.30 (m, 6H). ¹³C{¹H} NMR (C₆D₅Cl, 100.6 MHz, -40 °C): δ 75.1 (br), 12.8 (br), 5.5 (s), 3.1 (s). ²⁹Si{¹H} DEPT 45 (C₆D₅Cl, 79 MHz, -40 °C) δ 68.9. The variable-temperature (-40 to 20 °C) ¹H NMR dynamic behavior of **7** is discussed in the text.

Isolation and X-ray Structure of 7. *Method A:* colorless crystals of **7** can be obtained by slow diffusion of well-dried pentane into the above described solution in C₆D₅Cl at -35 °C. *Method B:* **7** can also be isolated by crystallization from the iridium-catalyzed reaction mixture. Triethylsilane (240 µL, 1.5 mmol, 2.0 equiv.) was added to a solution of **1** (20 mg, 0.015 mmol, 2 mol %) in C₆D₅Cl (0.6 mL) in a J. Young NMR tube. Diethyl ether (78.8 µL, 0.75 mmol, 1.0 equiv.) was then added and the tube was quickly inverted to ensure complete mixing. Oxonium ion **7** crystallized from this reaction mixture at -35 °C. *Method C:* crystals of **7** can be obtained from the [Ph₃C][B(C₆F₅)₄]-catalyzed reaction mixture as well. Triethylsilane (110 µL, 0.69 mmol, 0.97 equiv.) and diethyl ether (75 µL, 0.71 mmol, 1.0 equiv.) were added to a solution of [Ph₃C][B(C₆F₅)₄] (16 mg, 0.0174 mmol, 2.5 mol %) in C₆D₅Cl (0.6 mL) in a J. Young NMR tube. The tube was quickly inverted to ensure complete mixing. The solution was layered with pentane (1-2 mL), and left at room temperature overnight and then -35 °C for a few days to give colorless crystals.

Crystallographic data for **7** were collected on a Bruker SMART APEX-2 using Cu-K α radiation. Final agreement indices were R1 (all) = 9.85 % and R2 (all) = 24.6 %. All atoms were refined anisotropically. Selected crystallographic data appear in Table 2.2.

Table 2.2. X-ray Crystal Structure Data for Complex **7**.

Empirical Formula	C ₃₄ H ₂₅ BF ₂₀ OSi	
Formula Weight	868.44	
Crystal System	Orthorhombic	
Space Group	Pbca	
Unit Cell Dimensions	a = 19.5991(9) Å	$\alpha = 90^\circ$
	b = 17.4575(9) Å	$\beta = 90^\circ$
	c = 21.7621(12) Å	$\gamma = 90^\circ$
Volume	7445.9(7) Å ³	
Z	8	
Absorption Coefficient	0.192 mm ⁻¹	
Density (calculated)	1.549 mg/m ³	
Crystal size	0.30 × 0.30 × 0.10 mm ³	
Data/restraints/parameters	7075/ 0 / 519	
Final R indices [I>2 σ (I)]	R ₁ = 0.0819, wR ₂ = 0.2345	

Reaction of 7 with 5 at Low Temperature. A stock solution of **5** (0.25 M) was prepared in C₆D₅Cl in a glovebox at room temperature. Upon generating **7** in C₆D₅Cl (0.1 mmol, 1.0 equiv.) in a screw-cap NMR tube, an aliquot of the stock solution (400 μ L, 0.1 mmol, 1.0 equiv.) was added by syringe at -40 °C. The NMR tube was then placed in the pre-cooled NMR probe at -40 °C. The progress was monitored by ¹H, ³¹P{¹H} and ¹³C{¹H} NMR spectroscopy.

Typical Procedures for Cleavage of PhOMe Catalyzed by the Mixture of Cationic Complex, 1 and Dihydride Complex, 5. A stock solution (**A**) of **1** (33.3 mM) and a stock solution of **5** (50 mM) (**B**) were respectively prepared in C₆D₄Cl₂ in a glovebox. An aliquot (50-150 μ L, 0.5-1.5 mol% **5**) of stock solution **B** was added by syringe to an aliquot (150 μ L, 1 mol% **1**) of stock solution **A** in a J-Young NMR tube. C₆D₄Cl₂ (100-0 μ L) was added to keep the total amount of C₆D₄Cl₂ as 300 μ L. Triethylsilane (175 μ L, 1.1 mmol, 2.2 equiv.) and anisole (54 μ L, 0.5 mmol, 1 equiv.) were then added to the solution and the contents were well shaken. The reaction was monitored by anisole loss relative to the CH₃CH₂-groups of the silanes [sum of (CH₃CH₂)₃SiH and (CH₃CH₂)₃SiOPh] with respect to time by ¹H NMR spectroscopy. The data were analyzed using the method of initial rates.

Kinetic Studies of Cleavage of PhOMe with Various Amounts of Et₃SiH Catalyzed by 1 and 5. A stock solution of the mixture of **1** (12.5 mM) and **5** (12.5 mM) was prepared in C₆D₄Cl₂ in a glovebox. Triethylsilane (80-160 μ L, 0.5-1.0 mmol, 1-2 equiv.) and anisole (54 μ L, 0.5 mmol, 1 equiv.) were added by syringe to an aliquot (400 μ L) of this stock solution in a J. Young NMR tube and the contents were well shaken. The reaction was monitored by

anisole loss relative to the CH_3CH_2 - groups of the silanes [sum of $(\text{CH}_3\text{CH}_2)_3\text{SiH}$ and $(\text{CH}_3\text{CH}_2)_3\text{SiOPh}$] with respect to time by ^1H NMR spectroscopy.. The data were analyzed using the method of initial rates.

Cleavage of PhOMe with Et_3SiH Catalyzed by $[\text{Ph}_3\text{C}][\text{B}(\text{C}_6\text{F}_5)_4]$. Anisole (54 μL , 0.5 mmol, 1 equiv.) was added to a solution of $[\text{Ph}_3\text{C}][\text{B}(\text{C}_6\text{F}_5)_4]$ (4.6 mg, 0.005 mmol, 1 mol%) in $\text{C}_6\text{D}_4\text{Cl}_2$ (0.3 mL) in a medium-walled J. Young NMR tube. Triethylsilane (175 μL , 1.1 mmol, 2.2 equiv.) was then added and the reaction was allowed to stand at room temperature, and monitored by anisole loss relative to the CH_3CH_2 - groups of silanes [sum of $(\text{CH}_3\text{CH}_2)_3\text{SiH}$ and $(\text{CH}_3\text{CH}_2)_3\text{SiOPh}$] with respect to time by ^1H NMR spectroscopy.

Cleavage of Et_2O with Et_3SiH Catalyzed by $[\text{Ph}_3\text{C}][\text{B}(\text{C}_6\text{F}_5)_4]$. Triethylsilane (175 μL , 1.10 mmol, 2.2 equiv.) was added to a solution of $[\text{Ph}_3\text{C}][\text{B}(\text{C}_6\text{F}_5)_4]$ (4.6 mg, 0.005 mmol, 1 mol%) in $\text{C}_6\text{D}_4\text{Cl}_2$ (0.3 mL) in a medium-walled J. Young NMR tube and the contents were well shaken. Diethyl ether (52 μL , 0.5 mmol, 1 equiv.) was then added and the reaction was allowed to stand at room temperature, and was monitored by Et_2O loss relative to the CH_3CH_2 - groups of the silanes [sum of $(\text{CH}_3\text{CH}_2)_3\text{SiH}$ and $(\text{CH}_3\text{CH}_2)_3\text{SiOEt}$] with respect to time by ^1H NMR spectroscopy.

In situ Generation and NMR Spectroscopic Characterization of Methylphenyl(triethylsilyl)oxonium ion, 9. C_6D_6 (0.5 mL) was added to a screw-cap NMR tube with $[\text{Ph}_3\text{C}][\text{B}(\text{C}_6\text{F}_5)_4]$ (46 mg, 0.05 mmol, 1.0 equiv.) in drybox. To this suspension was then added triethylsilane (9 μL , 0.056 mmol, 1.13 equiv.), and the tube was quickly

inverted to ensure complete mixing. Light brown oil was produced at the bottom. The clear top phase was removed by syringe and the oil was washed with C_6D_6 ($0.1 \text{ mL} \times 2$). The oil was dissolved in $\text{C}_6\text{D}_5\text{Cl}$ (0.6 mL) and the solution was cooled down to -40°C . Anisole ($20 \mu\text{L}$, 0.19 mmol , 3.7 equiv.) was added by syringe and the NMR tube was then placed in the pre-cooled NMR probe at -40°C . Oxonium ion **9** and free anisole coalesce under these conditions due to rapid exchange on the NMR timescale. The ^1H spectrum shows the triethylsilyl group resonances at δ 0.54 (CH_3) and 0.32 (CH_2), and broad bands at δ 3.42 for the methyl protons of the $-\text{OCH}_3$ group. The $^{13}\text{C}\{^1\text{H}\}$ shows, in addition to the $\text{B}(\text{C}_6\text{F}_5)_4^-$ counteranion and PhOMe (line broadenings observed), two signals corresponding to the triethylsilyl group at δ 3.6 and 5.4. ^1H NMR ($\text{C}_6\text{D}_5\text{Cl}$, 500 MHz , -40°C): δ 7.16 (br), 6.96 (br), 6.75 (br), 3.42 (br), 0.54 (m), 0.32 (m). $^{29}\text{Si}\{^1\text{H}\}$ DEPT 45 ($\text{C}_6\text{D}_5\text{Cl}$, 99 MHz , -40°C) δ 77.2.

References

- (1) a) Kubas, G. J. *Metal Dihydrogen and σ -Bond Complexes*, Kluwer Academic/Plenum Publishers, New York, **2001**. b) Kubas, G. J. *Adv. Inorg. Chem.* **2004**, 56, 127.
- (2) a) Bullock, R. M. *Chem. Eur. J.* **2004**, 10, 2366; b) Bullock, R. M. in *Handbook of Homogeneous Hydrogenation* (Eds.: J. G. de Vries, C. J. Elsevier), Wiley-VCH, Weinheim, 2007, Chap. 7.
- (3) a) Guan, H.; Iimura, M.; Magee, M. P.; Norton, J. R.; Zhu, G. *J. Am. Chem. Soc.*; **2005**; 127; 7805. b) Magee, M.; Norton, J. *J. Am. Chem. Soc.*, **2001**, 123, 1778. c) Guan, H.; Saddoughi, S. A.; Shaw, A. P.; Norton, J. R. *Organometallics*; **2005**; 24; 6358.
- (4) a) Stephan, D. W. *Org. Biomol. Chem.* **2008**, 6, 1535. b) Kenward, A. L.; Piers, W. E. *Angew. Chem. Int. Ed. Engl.* **2008**, 47, 38. c) Welch, G. C.; Stephan, D. W. *J. Am. Chem. Soc.* **2007**, 129, 1880. d) Spies, P.; Erker, G.; Kehr, G.; Bergander, K.; Frohlich, R.; Grimme, S.; Stephan, D. W. *Chem. Commun.* **2007**, 5072. e) Chase, P. A.; Welch, G. C.; Jurca T.; Stephan, D. W. *Angew. Chem. Int. Ed.* **2007**, 49, 8050. f) Chase, P. A.; Jurca T.; Stephan, D. W., *Chem. Commun.* **2008**, 1701. g) Welch, G. C.; Cabrera, L.; Chase, P. A.; Hollink, E.; Masuda, J. D.; Wei, P.; Stephan, D. W.; *Dalton Trans.* **2007**, 3407. h) Welch, G. C.; Juan, R. R. S.; Masuda J. D.; Stephan, D. W. *Science* **2006**, 314, 1124.
- (5) a) Piers, W. E. *Adv. Organomet. Chem.* **2005**, 52, 1. b) Parks, D. J.; Blackwell, J. M.; Piers, W. E. *J. Org. Chem.* **2000**, 65, 3090. c) Parks, D. J.; Piers, W. E. *J. Am. Chem. Soc.* **1996**, 118, 9440. d) Blackwell, J. M.; Sonmor, E. R.; Scoccitti T.; Piers, W. E.; *Org. Lett.* **2000**, 2, 3921. e) Blackwell, J. M.; Morrison, D. J.; Piers, W. E. *Tetrahedron* **2002**, 58, 8247. f) Rubin, M.; Schwier, T.; Gevorgyan, V. *J. Org. Chem.* **2002**, 67, 1936.
- (6) a) Du, G.; Fanwick, P. E.; Abu-Omar, M. M. *J. Am. Chem. Soc.* **2007**, 129, 5180. b) Dioumaev, V. K.; Bullock, R. M. *Nature* **2003**, 424, 530.
- (7) It is well known that hydrosilanes are able to reduce alkyl ethers in the presence of stoichiometric amounts of Lewis acids: a) Adlington, M. G.; Orfanopoulos, M.; Fry, J. L. *Tetrahedron Lett.* **1976**, 2955. b) Fry, J. L.; Orfanopoulos, M.; Adlington, M. G.; Dittman, W. R.; Silverman, S. B. *J. Org. Chem.* **1978**, 43, 374. c) Orfanopoulos, M.; Smonou, I. *Synth. Commun.* **1988**, 18, 833. d) Larsen, J. W.; Chang, L. W. *J. Org. Chem.* **1979**, 44, 1168. e) Yato, M.; Ishida, A. *Heterocycles* **1995**, 41, 17. f) Smonou, I. *Synth. Commun.* **1994**, 24, 1999.

- (8) a) Gevorgyan, V.; Rubin, M.; Benson, S.; Liu, J.-X.; Yamamoto, Y. *J. Org. Chem.* **2000**, *65*, 6179. b) Gevorgyan, V.; Liu, J.-X.; Rubin, M.; Benson, S.; Yamamoto, Y. *Tetrahedron Lett.* **1999**, *40*, 8919. Also see: c) Blackwell, J. M.; Foster, K. L.; Beck, V. H.; Piers, W. E. *J. Org. Chem.* **1999**, *64*, 4887. High loadings of Pd(II) salts have been shown to induce Et₃SiH reduction of certain classes of primary and secondary alcohols: Ferreri, C.; Costantino, C.; Chatgililoglu, C.; Boukherroub, R.; Manuel, G. *J. Organomet. Chem.* **1998**, *554*, 135.
- (9) a) Nimmagadda, R. D.; McRae, C. *Tetrahedron Lett.* **2006**, *47*, 5755. For B(C₆F₅)₃-catalyzed reductions of carbonyl functions to the corresponding alkyl functions with Et₃SiH: b) Gevorgyan, V.; Rubin, M.; Liu, J.-X.; Yamamoto, Y. *J. Org. Chem.* **2001**, *66*, 1672. c) Bajracharya, G. B.; Nogami, T.; Jin, T.; Matsuda, K.; Gevorgyan, V.; Yamamoto, Y. *Synthesis* **2004**, 308. With polymethylhydrosiloxane as reductant: d) Chandrasekhar, S.; Reddy, C. R.; Babu, B. N. *J. Org. Chem.* **2002**, *67*, 9080–9082.
- (10) Chojnowski, J.; Rubinsztajn, S.; Cella, J. A.; Fortuniak, W.; Cypryk, M.; Kurjata, J.; Kazmierski, K. *Organometallics* **2005**, *24*, 6077.
- (11) Yang, J.; Brookhart, M. *J. Am. Chem. Soc.* **2007**, *129*, 12656.
- (12) Yang, J.; White, P. S.; Schauer, C. K.; Brookhart, M. *Angew. Chem. Int. Ed. Engl.* **2008**, *47*, 4141.
- (13) Goettker-Schnetmann, I.; White, P.; Brookhart, M. *Organometallics* **2004**, *23*, 1766.
- (14) Kira, M.; Hino, T.; Sakurai, H. *J. Am. Chem. Soc.* **1992**, *114*, 6697.
- (15) a) Lambert, J. B.; Zhao, Y.; Wu, H. *J. Org. Chem.* **1999**, *64*, 2729; b) Lambert, J. B.; Zhang, S.; Ciro, S. M. *Organometallics* **1994**, *13*, 2430. c) Lambert, J. B.; Kania, L.; Zhang, S. *Chem. Rev.* **1995**, *95*, 1191. d) Reed, C. A. *Acc. Chem. Res.* **1998**, *31*, 325. e) Lambert, J. B.; Zhang, S.; Stern, C. L.; Huffman, J. C. *Science* **1993**, *260*, 1917. f) Corey, J. Y. *J. Am. Chem. Soc.* **1975**, *97*, 3237.
- (16) Scott, V. J. Çelenligil-Çetin, R.; Ozerov, O. V. *J. Am. Chem. Soc.* **2005**, *127*, 2852.
- (17) a) Alaimo, P. J.; Peters, D. W.; Arnold, J.; Bergman, R. G. *J. Chem. Educ.* **2001**, *78*, 64; b) Pangborn, A. B.; Giardello, M. A.; Grubbs, R. H.; Rosen, R. K.; Timmers, F. J.

Organometallics **1996**, *15*, 1518.

CHAPTER THREE

Structural and Spectroscopic Characterization and Dynamics of an Unprecedented Cationic Transition Metal η^1 -Silane Complex

(Part of this chapter has been adapted with permission from: Yang, J., White, P. S., Schauer, C. K., Brookhart, M. *Angew. Chem. Int. Ed. Engl.* **2008**, 47, 4141-4143. Copyright 2008 WILEY-VCH. DFT calculation carried out by Professor Cynthia Schauer has been included to provide a full picture and understanding of this unprecedented cationic η^1 -silane complex.)

Introduction

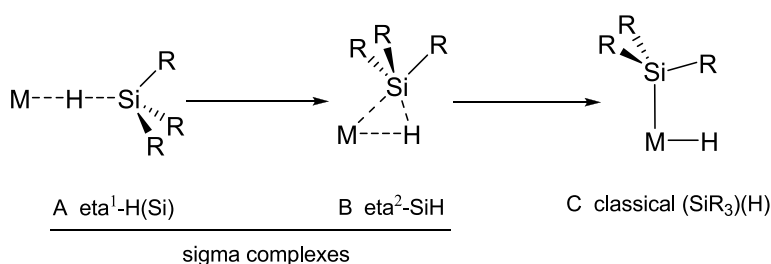
Understanding the coordination chemistry of σ bonds to metal centers is not only of fundamental importance but also provides insights useful for developing metal-catalyzed transformations involving the activation of σ bonds, particularly dihydrogen, silanes, boranes, and alkanes.¹

Sigma complexes between silanes and cationic transition metal compounds possess highly electrophilic silicon centers and are invoked as key intermediates in a number of important catalytic Si-H activation reactions, i. e. silane alcoholysis, hydrosilylation, and more recently reduction of alkyl halides and ethers.^{2, 3} Those reported σ -silane complexes are structurally characterized or generally proposed to be η^2 -silane complexes (Scheme 1, **B**) in which the silane is bound side-on with significant metal-silicon interaction.⁴ Calculations have

previously identified possible transition metal complexes with decreased Si-M interactions, but supporting experimental evidence is lacking.^{5, 6}

While there are numerous examples of neutral σ -silane complexes with X-ray structures, isolable cationic analogs are scarce.⁴ This scarcity reflects the extreme sensitivity of the electrophilic Si center towards nucleophiles, like adventitious moisture, dichloromethane or even fluoride from certain anions.^{3d} Kubas et al. reported a cationic Re(I) η^2 -Et₃SiH complex with tied-back phosphite ligands, where a solid-state structure could not be obtained due to a highly disordered X-ray structure.⁷ More recently, Lemke has described a structurally characterized cationic Ru η^2 -silane complex with a short Ru-H and a long Si-H bond which was proposed to model the latter stage of oxidative addition of a silane to metal fragments.⁸

Scheme 3.1. Interactions of R₃SiH with Transition Metal Complexes.

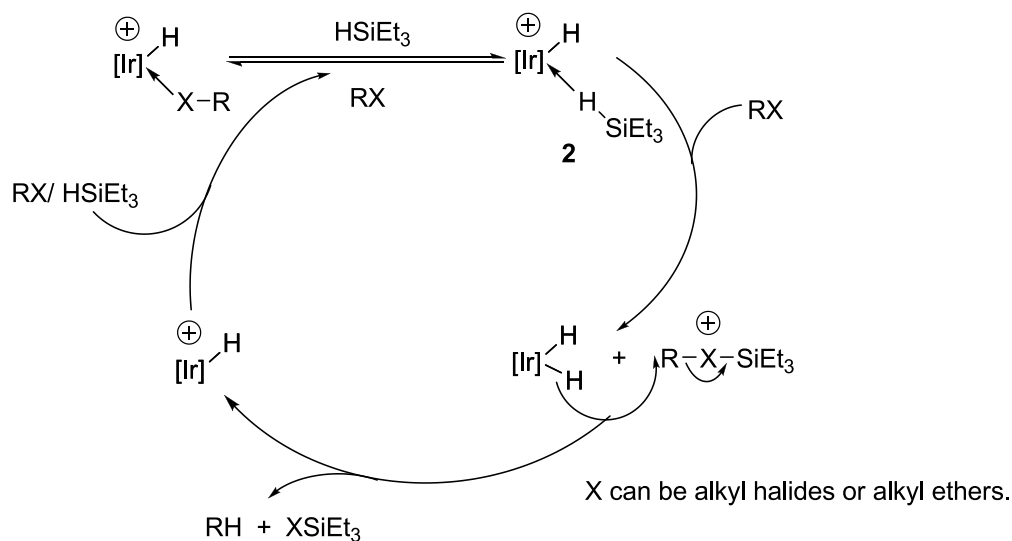


Previously in our lab the cationic POCOP iridium pincer complex [(POCOP)Ir(H)(H₂)] [BAr_F] [Ar_F = 3, 5-(CF₃)₂C₆H₃] has been synthesized and spectroscopically characterized which shows it to be an η^2 -dihydrogen complex.⁹ At 23 °C, the hydrogens are in fast exchange and appear as a broad singlet at ca. -14 ppm by ¹H NMR spectroscopy. At -100 °C, the hydrogens are seen at 0.033 and -41.9 ppm in a 2:1 ratio in the ¹H NMR spectrum. Using a one dimensional HMQC experiment at -100 °C, Dr. Alison Sykes was able to measure the H-D coupling constant as 33 Hz, supporting the proposal that

H-D is bound in an η^2 fashion. The first-order rate constant for exchange of the hydride and dihydrogen ligand was estimated as 168 s^{-1} at -81°C , corresponding to a ΔG^\ddagger ca. 9.1 kcal/mol .

During our mechanistic studies of iridium-catalyzed reduction of C-X bonds ($\text{X} = \text{F}, \text{Cl}, \text{Br}, \text{I}, \text{O}$) by triethylsilane, a cationic iridium $\sigma\text{-Et}_3\text{SiH}$ complex was invoked as a key intermediate (Scheme 3.2).^{2a} In this chapter we will describe studies on the generation, spectroscopic characterization and dynamic behavior of this unique cationic silane complex. Importantly, a crystal structure of this species has also been obtained which shows the first example of a cationic transition metal η^1 -silane complex in which the silane is bound to a metal center in an unprecedented end-on fashion through the Si-H bond with no appreciable metal-silicon interaction (Scheme 3.1, **A**).

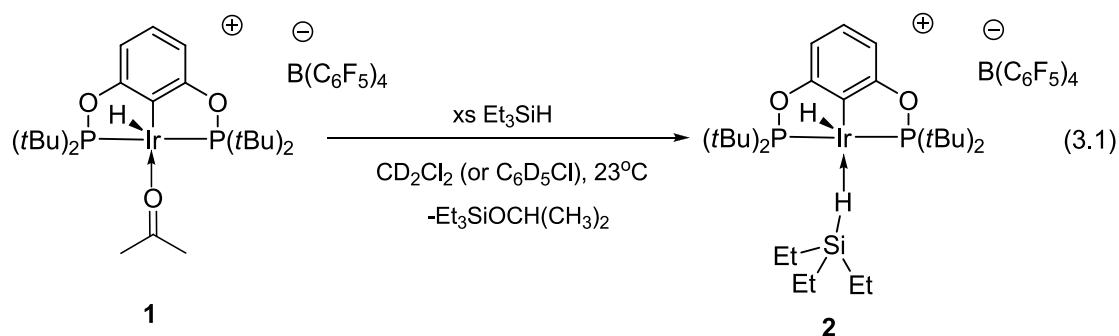
Scheme 3.2. Proposed Catalytic Cycle for Iridium-Catalyzed Reduction of C-X Bonds.



Results and Discussion

A. In Situ Generation and Spectroscopic Characterization of the Iridium σ -Et₃SiH complex [(POCOP)Ir(H)(Et₃SiH)]⁺[B(C₆F₅)₄]⁻

This Iridium σ -Et₃SiH complex can be generated in situ by treatment of [(POCOP)Ir(H)(acetone)]⁺[B(C₆F₅)₄]⁻ {POCOP = 2, 6-[OP(*t*Bu)₂]₂C₆H₃} (**1**) with excess Et₃SiH in CD₂Cl₂ at 23 °C (eq 3.1). The ³¹P{¹H} NMR spectrum of **2** at 23 °C exhibits a major singlet at δ 183.2 ppm, but ¹H NMR resonances for the terminal (Ir-H) and bridging (Ir-H-Si) hydrides are too broad to be observed at 23 °C due to exchange on the NMR timescale. At -70 °C, the static spectrum is obtained which shows two hydride resonances in a 1:1 ratio. The singlet at δ -4.9 with ²⁹Si satellites (¹J_{Si-H} = 79 Hz) is assigned to a bridging (Ir-H-Si) hydride while the triplet at δ -44.2 (²J_{P-H} = 11.6 Hz) is assigned to a terminal (Ir-H) hydride. Based on the resonance frequency of similar POCOP iridium pincer complexes,¹⁰ the very high upfield shift of -44.2 ppm is indicative of a hydride *trans* to a vacant coordination site. These NMR data, especially the J_{Si-H} value, suggest that **2** is a square-pyramidal Et₃SiH σ -complex with an apical hydride and with silane bound in the square plane *trans* to the aryl ligand.¹¹



B. X-ray Crystallography of **2**

An X-ray quality crystal of **2** was obtained by slow diffusion of pentane into a C₆H₅F solution of **1** and excess Et₃SiH at 25 °C under Ar. The ORTEP diagram of **2** is shown in Figure 3.1. Et₃SiH is coordinated *trans* to the ipso carbon of the tridentate POCOP backbone. The hydrogens bound to Ir were located in the final difference map, and their refined positions are consistent with a square-pyramidal geometry at Ir assigned using ¹H NMR data. The most striking structural feature of **2** is the orientation of the coordinated silane ligand characterized by a long Ir...Si distance of 3.346(1) Å (0.97 Å greater than the sum of the covalent radii of Ir and Si¹²) and an Ir-H-Si angle of 157°, both indicative of an end-on η¹-H(Si) coordination mode of the silane. In η²-SiH complexes, the M-Si distances remain relatively short.⁴ For example, the Mn-Si distance in the manganese derivatives Cp''L(CO)Mn(η²-HSiR₃) (L= CO or 2-electron donor; Cp''=Cp, Cp' or Cp*) is only slightly longer than those in Mn(I)-SiR₃ complexes (at most a 4% lengthening).^{4c} Given the rarity of isolated cationic silane σ-complexes, one example for direct comparison is the aforementioned complex reported by Lemke, [Ru(η²-HSiCl₃)(PMe₃)₂Cp][B(Ar_F)₄], in which the Ru-Si bond (2.329 Å) is elongated by only about 0.064 Å compared with that of a model silyl complex, Ru(SiCl₃)(PMe₃)₂Cp(2.265 Å).⁸

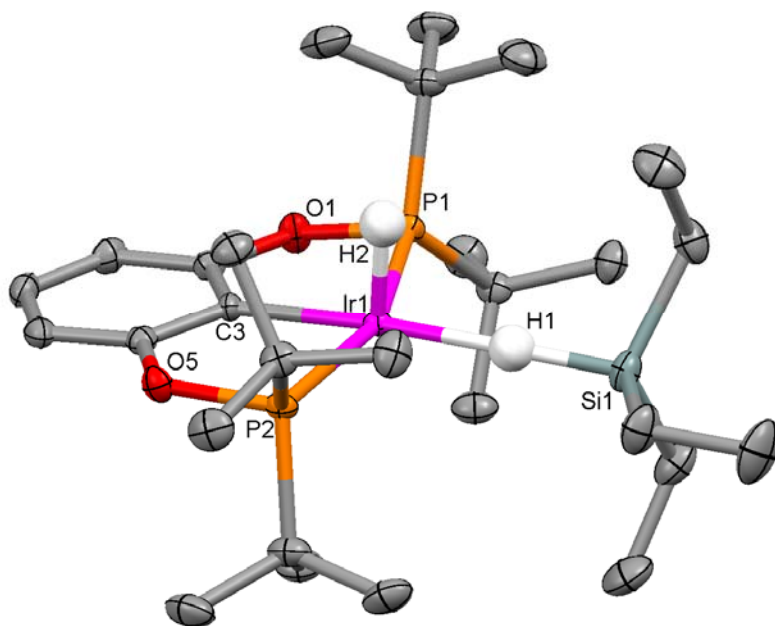
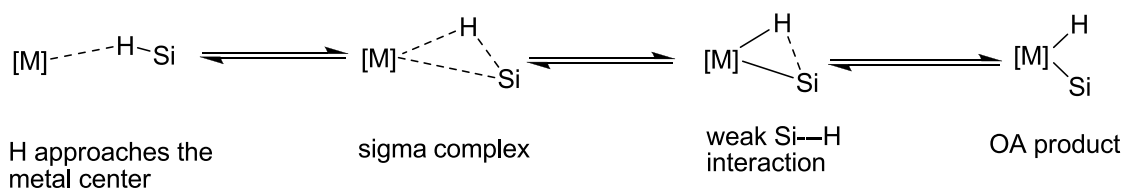


Figure 3.1. An ORTEP diagram of the cation in **2** (hydrogens omitted). Key bond distances (Å) and bond angles (°): Ir(1)-C(3) = 2.015(2), Ir(1)-P(2) = 2.3091(6), Ir(1)-P(1) = 2.3470(6), Ir(1)-H(1) = 1.94(3), Ir(1)-H(2) = 1.425(18), Si(1)-H(1) = 1.48(3), Ir(1)···Si(1) = 3.346(1), Ir(1)-H(1)-Si(1) = 157(1), P(2)-Ir(1)-P(1) = 158.06(2).

Schubert has proposed that the oxidative addition of hydrosilanes to metal fragments is initiated when the H atom of the Si-H bond approaches the metal center.^{4c} The Si-H component then pivots to place the Si atom close to the metal, thus interaction between metal and Si is increased and the Si-H bond is weakened. In characterized silane complexes, the reaction coordinate seems “arrested” mostly in the latter stage of this pathway.⁴ The structural characteristics of **2** suggest that it may serve as a model for the early stage of the oxidative addition of silanes to unsaturated metal centers as proposed by Schubert. This η^1 -silane structure is unique, elusive, and informative.

Scheme 3.3. A Proposed Pathway for the Reaction of Silanes with Metal Fragment^{4c}



C. Density Functional Theory (DFT) Studies of Structure and Bonding of 2.

To provide insight into the structural and bonding features of the $\eta^1\text{-H}(\text{Si})$ binding mode, DFT studies¹³ were performed on the HSiMe_3 analogue of **2** (**3**), as well as the HSiMe_3 complex of model systems in which Me replaces all four *t*Bu groups (**4**), and Me replaces two *cis t*Bu groups distal to the hydride ligand (**5**). Selected metric parameters for the calculated minima are listed in Table 3.1 and selected minima for **3** and **4** are shown in Figure 3.2. The potential energy surfaces for the silane complexes show multiple minima corresponding to different rotamers about the Ir-H and Si-H bonds. For each complex, structural data are presented for two distinct minima in which the SiMe_3 group is oriented proximal and distal to the hydride ligand (eg., Figure 3.2, **4p** and **4d**, respectively). The calculated structure for **3d** agrees well with expectations based on X-ray data. The hydride ligand occupies the apical site in the square pyramid ($\text{Ir-H} = 1.54 \text{ \AA}$). The hydrogen of the silane is positioned approximately trans to C (aryl) ($\text{Ir-H}(\text{-Si}) = 1.87 \text{ \AA}$). The Si-H distance of 1.57 \AA is ca 0.08 \AA longer than the calculated Si-H distance in the parent silane, reflecting activation of the Si-H bond. The calculated $\text{Ir}\cdots\text{Si}$ non-bonding distance of 3.38 \AA for **3d** is similar to the X-ray distance of 3.35 \AA . The corresponding Ir-H1-Si angle is 161° . An Ir-H1-Si angle of 180° might be expected for an $\eta^1\text{-H}(\text{Si})$ interaction. The space-filling diagram for **3d** (Figure 3.2) shows close contact between the Si-Me groups and the Me groups on the *t*Bu

substituents, and these interactions, together with similar close interactions on the opposite face apparently dictate the Ir-H1-Si angle adopted in **2**.

Table 3.1. Selected bond lengths (Å) and angles (°) and energies from DFT studies.

Cmpd	Ir-H1	Si-H1 ^a	Ir...Si	Ir-H1-Si	Relative E (kcal mol ⁻¹) ^b
3p	1.865	1.572	3.379	158.7	0.0
3d	1.870	1.572	3.395	161.0	-0.2
4p	1.785	1.576	3.169	141.1	0.0
4d	1.753	1.605	2.887	118.5	-1.0
4d'	1.751	1.653	2.619	100.5	-1.9
5d	1.757	1.609	2.871	117.0	0.0
5d'	1.752	1.646	2.626	101.2	-0.9

^a The calculated Si-H distance in HSiMe₃ is 1.493 Å. ^b Difference in electronic energies.

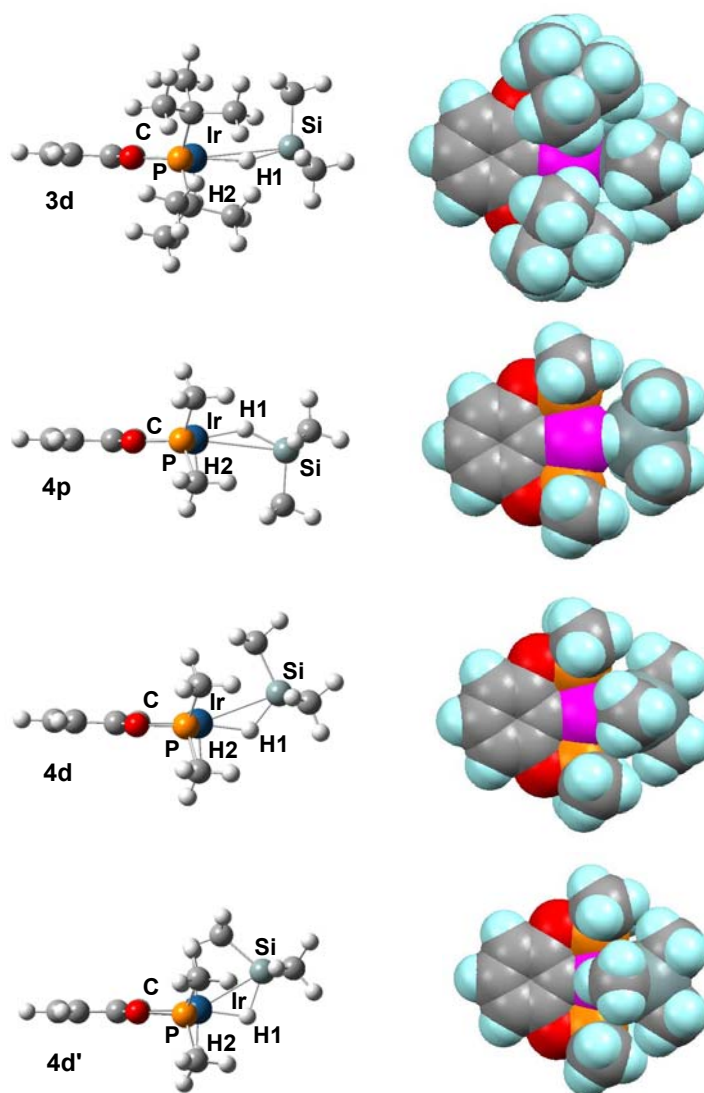


Figure 3.2. Selected minima for **3** and **4**, and corresponding space-filling diagrams (top view).

The reduced ligand steric bulk in trimmed **4** allows the silicon in **4d** to more closely approach Ir ($\text{Ir}\cdots\text{Si} = 2.89 \text{ \AA}$). Moreover, **4** shows a distinct minimum (**4d'**) with an even shorter Ir-Si distance ($\text{Ir}\cdots\text{Si} = 2.62 \text{ \AA}$), in which the silane coordination is assisted by the formation of an axial agostic interaction with a Si-Me group (Fig. 3.2) ($\text{H}\cdots\text{Ir} = 2.25 \text{ \AA}$). The

development of the η^2 -SiH interaction is demonstrated by the structural parameters of the series of complexes, **4p**, **4d**, and **4d'**, with progressively longer H1-Si distances, shorter Ir-H1 and Ir-Si distances, and smaller Ir-H1-Si angles along the series (see Table 3.1). The relative energies of **4p**, **4d**, and **4d'** are 0, -1.0, and -1.9 kcal mol⁻¹, respectively, indicating that the stabilization afforded by the η^2 -SiH interaction is small. Trimmed **5** is electronically intermediate between **3** and **4**. The similar structural parameters and energetics of the **d** and **d'** minima for **4** and **5** are consistent with the assertion that the steric properties of the ligand are driving the structural changes in the trimmed complexes.

Table 3.2. Natural charges and NBO populations in the silane complexes.^a

	Natural Charges				NBO populations		
	Ir	Si	H(Si)	Si-H	. * Ir-C	Ir(d *)	. * Si-H
3p	0.021	1.563	-0.281	1.796	0.313	1.952	0.063
3d	0.011	1.554	-0.275	1.796	0.313	1.954	0.063
4p	-0.011	1.540	-0.255	1.763	0.336	1.947	0.071
4d	-0.051	1.476	-0.175	1.712	0.380	1.931	0.084
4d'	-0.116	1.441	-0.115	1.673	0.426	1.916	0.093
5d	-0.038	1.490	-0.180	1.720	0.376	1.933	0.079
5d'	-0.123	1.449	-0.115	1.674	0.429	1.916	0.092

^a In HSiMe₃, the natural charges on Si and H are 1.345 and -0.196.

An NBO analysis¹⁴ was conducted on the silane complexes, and the natural charges are shown in Table 3.2. Formation of the η^1 -H(Si) silane complex increases the polarization of the Si-H bond, with an accompanying increase in charge on silicon by ca 0.2 in comparison to the free silane, and a decrease in the charge on hydrogen. Adoption of the η^2 -SiH

coordination mode reduces the positive charge on silicon, and increases the charge on hydrogen. Therefore the $\eta^1\text{-H}(\text{Si})$ coordinated silane, with little Ir to Si-H σ^* backbonding, is expected to be a more potent source of electrophilic silicon than an $\eta^2\text{-SiH}$ complex. The NBO populations of the relevant orbitals for interaction with the silane (Figure 3.3) are summarized in Table 3.2. The NBO populations are consistent with greater donation from σ Si-H to σ^* Ir-C and greater back-donation from $d\pi^*$ Ir to σ^* Si-H as the silane coordination geometry changes from **4p**, **4d**, to **4d'**.

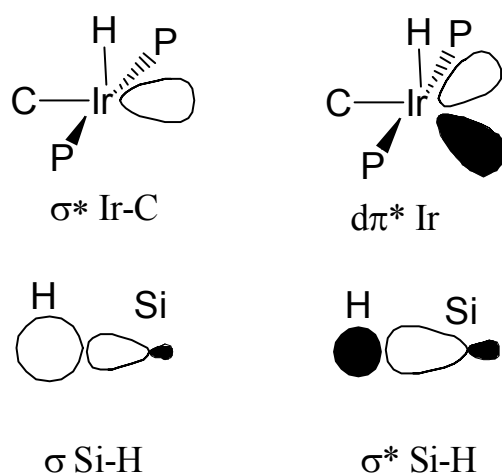


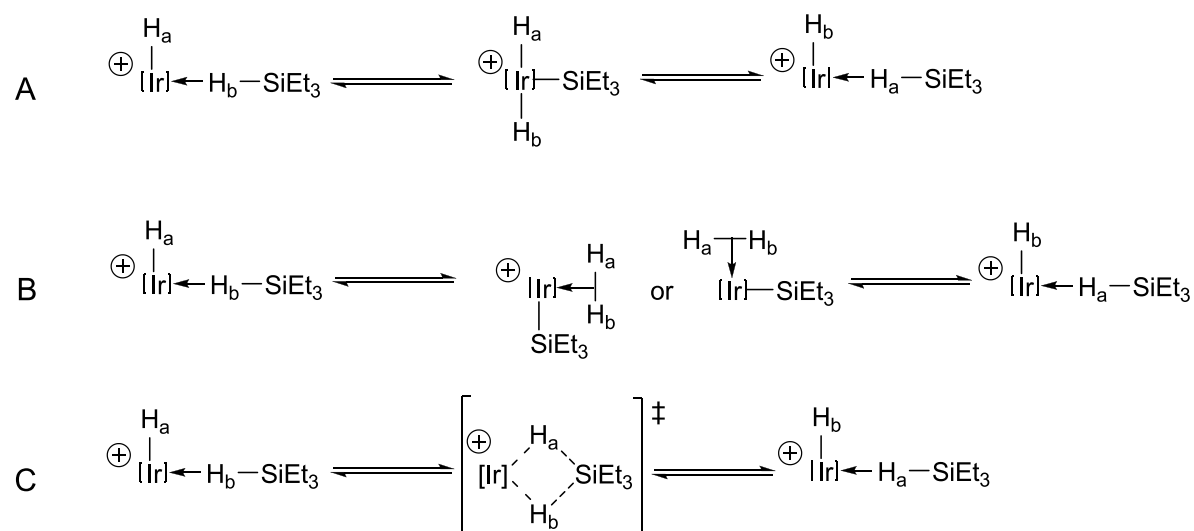
Figure 3.3. Relevant orbitals for interaction between silane and iridium in **2**

D. Dynamics of **2** and Hydride Exchange Mechanisms.

Three possible mechanisms for exchange of the terminal (Ir-H) and bridging (Ir-H-Si) hydrides in the cationic iridium silane complex **2** are shown in Scheme 3.4. Mechanism **A** is the oxidative addition of Et_3SiH to the iridium center, formation of cationic Ir(V) silyl dihydride intermediate and then reductive coupling of Et_3SiH to regenerate the iridium $\eta^1\text{-Et}_3\text{SiH}$ complex. The second possibility involves the intermediacy of the iridium silyl $\eta^2\text{-H}_2$

complex followed by rotation of the η^2 -dihydrogen ligand which interchanges H_a and H_b (Scheme 3.4, **B**). Mechanism **C** is the transfer of triethylsilyl from the end-on bound triethylsilane to the terminal hydride (“silyl slide”)^{2b} through a transition state which adopts a symmetric geometry with the silicon occupies the central position trans to ipso carbon of the tridentate POCOP backbone.

Scheme 3.4. Possible Mechanisms of Scrambling Hydrides in **2**



Through line-broadening studies, the first-order rate constant for exchange of the terminal and bridging hydrides was estimated as $k_{ex} = 31.3 \text{ s}^{-1}$ at -55°C , corresponding to a ΔG^\ddagger of ca. 11.2 kcal/mol (Figure 3.4). At 23°C only one triplet is seen for the average of two *t*-butyl groups. At low temperature it is evident that the resonance decoalesces into two triplets of nearly equal intensity. The barrier for this process can be roughly estimated from the coalescence temperature (ca. -55°C) to be ca. 10.9 kcal/mol. It is approximately equal to the barrier for the exchange between terminal and bridging hydrides, which indicates that the same mechanism accounts for both averaging processes. Thus it is suggested that the transition state for equilibration of the terminal and bridging hydrides appears to adopt a

symmetric geometry, thus mechanism **B** is not a viable option. However, experimental data alone can not distinguish between mechanism **A** and **C** under these reaction conditions.

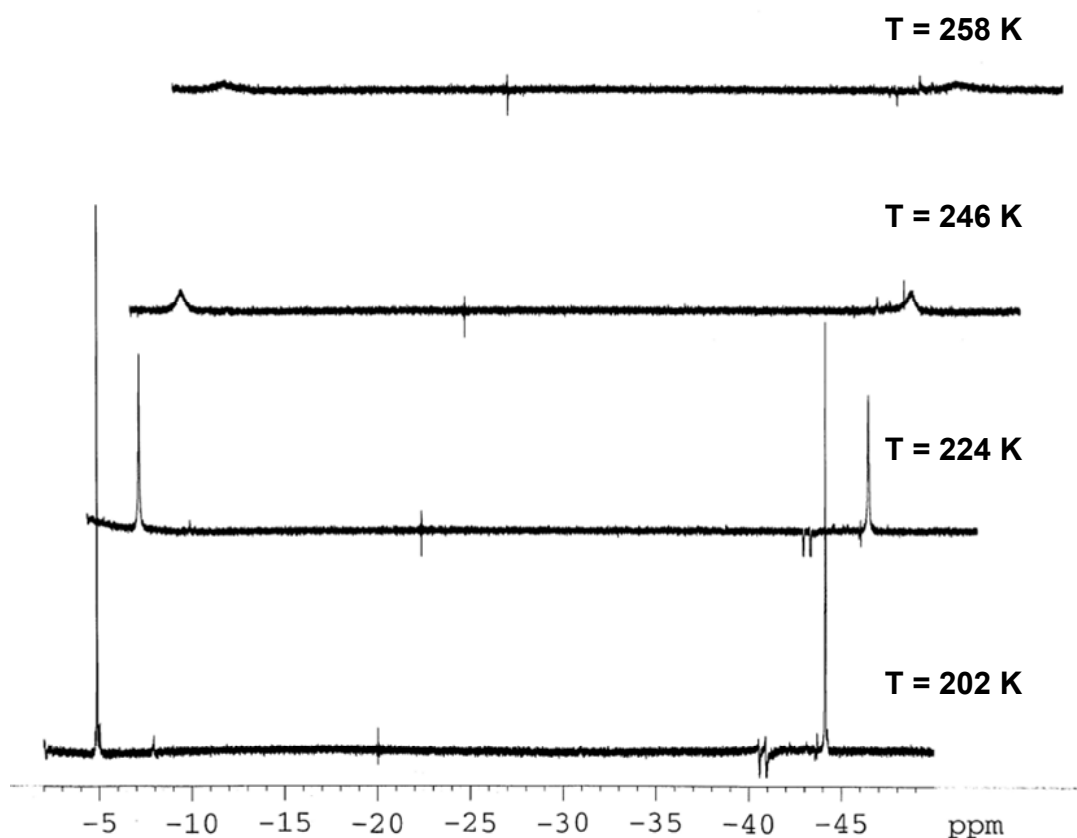


Figure 3.4. Variable temperature stacked ¹H NMR spectra of **2** (hydride region)

Results from DFT calculations are consistent with this deduction. The lowest energy transition state for exchange of the terminal and bridging hydrides in the trimmed complex **4** (the *t*Bu groups on the POCOP ligand were replaced by Me) adopts a symmetric geometry, and lies 9.2 kcal/mol higher in energy than **4** (Figure 3.5). The silicon occupies the central position, *trans* to C, with an Ir-Si distance of 2.72 Å. The Si-H distances of ca. 1.93 Å are considerable longer than in the silane complexes (1.57–1.65 Å). A similar “open-direct” transition state was found to be the lowest energy pathway for exchange of the hydride and

dihydrogen ligands in $cis\text{-}[\text{Fe}(\text{PR}_3)_4(\text{H})(\eta^2\text{-H}_2)]^+$ ¹⁵ and also found for the exchange of the hydride ligand and the silane hydrogen in $\text{TpRu}(\text{PPh}_3)(\text{H})(\eta^2\text{-HSiR}_3)$ ¹⁶. Alternate mechanisms involving the oxidative addition of Et_3SiH (Scheme 3.4, **A**) or intermediacy of an $\eta^2\text{-H}_2$ complex (Scheme 3.4, **B**) were found to have much higher barriers. The general structural features for the transition state in the untrimmed complex, **2**, are very similar to **4**, but much more crowded, as reflected in a longer Ir-Si distance of 2.80 Å and a higher transition state energy of 16.7 kcal/mol.

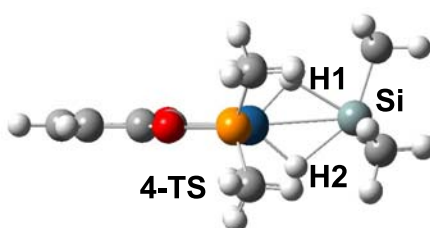


Figure 3.5. Calculated lowest energy transition state for exchange of the terminal and bridging hydrides in the trimmed complex **4**

These hydride exchange reactions are examples of degenerate σ -complex assisted metathesis processes (the σ -CAM process coined in ref. 3a). Importantly, for the $\eta^1\text{-HSiEt}_3$ complex **2**, there is no significant interaction between Ir and Si in the ground state. An interaction between Ir and Si then develops in transition state (like **4-TS** in Figure 3.5) to productively carry out the exchange reaction, indicating that formation of an η^2 -sigma complex is *not* a requirement for carrying out metathesis.

Summary

The key cationic σ -silane intermediate (**1**) for iridium-catalyzed reduction of C-X bonds (X = F, Cl, Br, I, O) with Et₃SiH has been generated, isolated, and spectroscopically and structurally characterized. X-ray crystallography shows it to be the first example of a transition metal η^1 -silane complex in which the silane is bound to an iridium(III) center in an unprecedented end-on fashion through the Si-H bond with no appreciable metal-silicon interaction.

DFT studies on the model Me₃SiH σ -complex and analogues with trimmed ligands indicate that the bulky substituents on phosphorus in the POCOP ligand dictate the coordination mode of the silane and in complexes with trimmed ligands η^2 -SiH conformers are energy minima. The small energy difference between η^1 -H(Si) and η^2 -SiH conformers suggests that backbonding from Ir to Si-H σ^* in these cationic complexes is not a very important stabilizing interaction.

At 23 °C, the ¹H NMR resonances for the terminal (Ir-H) and bridging (Ir-H-Si) hydrides are too broad to be observed due to exchange. At -70 °C, the static spectrum is obtained which shows two hydride resonances in a 1:1 ratio. Through line-broadening studies, the first-order rate constant for exchange of the terminal and bridging hydrides was estimated as $k_{\text{ex}} = 31.3 \text{ s}^{-1}$ at -55 °C, corresponding to a ΔG^\ddagger of ca. 11.2 kcal/mol, a slightly higher barrier than the similar exchange in the dihydrogen analog, [(POCOP)Ir(H)(H₂)] [BAr_F] [Ar_F = 3, 5-(CF₃)₂C₆H₃] (ΔG^\ddagger ca. 9.1 kcal/mol).⁹

Combining the analysis of the dynamic NMR spectrum and DFT studies, we found that the scrambling mechanism surprisingly does not involve an η^2 -H₂ intermediate. The scrambling mechanism appears to involve the transfer of triethylsilyl from the end-on bound

triethylsilane to the terminal hydride (“silyl slide”) through a transition state which adopts a symmetric geometry where the silicon occupies the central position trans to the ipso carbon of the tridentate POCOP backbone.

Computational studies⁵ have previously identified possible transition metal silane complexes with minima showing weak Si-M interactions but supporting experimental evidence is lacking. Thus the isolation and full characterization of the first example of a cationic transition metal η^1 -silane complex (**1**) is of fundamental importance. On the basis of the structural characteristics, **1** may be considered as a model for the early stage of the oxidative addition of silanes to unsaturated metal centers, which is extremely rare.^{4c}

Perhaps equally significant is the mechanism of scrambling of hydrides in **1** and its η^2 -H₂ analog. These hydride exchange reactions are important examples of degenerate σ -complex assisted metathesis processes (σ -CAM) and in a certain sense they mimic the σ -bond metathesis of d⁰ metals on late transition metal centers.^{3a} Therefore, now at the end of this dissertation, I predict this system and other related or similar complexes exhibiting such structure and dynamic processes will find their way in future catalytic transformation.

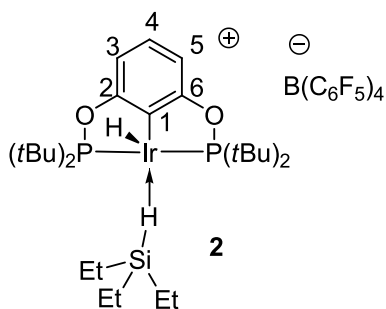
Experimental Section

General Considerations. All manipulations were carried out using standard Schlenk, high-vacuum and glovebox techniques. Argon and nitrogen were purified by passage through columns of BASF R3-11 catalyst (Chemalog) and 4 Å molecular sieves. Pentane, methylene chloride and toluene were passed through columns of activated alumina and degassed by

freeze-pump-thaw methods. Acetone was dried with 4 Å molecular sieves for 18 hours and degassed by freeze-pump-thaw methods. Et₃SiH was dried with LiAlH₄ and vacuum transferred into a sealed flask. C₆D₅Cl, C₆D₄Cl₂ and CD₂Cl₂ were purchased from Cambridge Isotope Laboratories, Inc., dried with CaH₂, and vacuum transferred to a sealed flask. C₆H₅F was dried with CaH₂ and vacuum transferred to a sealed flask. NMR spectra were recorded on Bruker spectrometers (DRX-400, AVANCE-400, AMX-300 and DRX-500). ¹H NMR spectra were referenced to residual protio solvent peaks. ³¹P chemical shifts were referenced to an external 85% H₃PO₄ standard. ²⁹Si chemical shifts were referenced to external (CH₃)₄Si. K[B(C₆F₅)₄] were purchased from Boulder Scientific and dried *in vacuo* at 120°C for 24 hours. All other reagents were purchased from Sigma-Aldrich or Strem. Complex **1**, [(POCOP)IrH(acetone)]⁺[B(C₆F₅)₄]⁻ was prepared according to published procedures.

In situ Generation of [(POCOP)Ir(H)(η¹-Et₃SiH)]⁺[B(C₆F₅)₄]⁻ in CD₂Cl₂, **2.** The in situ generation of iridium η¹-Et₃SiH complex **2** in C₆D₅Cl has been described previously in the experimental section of Chapter One. In order to get a static spectrum, the procedure was reproduced in CD₂Cl₂. Triethylsilane (160 mL, 1.00 mmol, 100 equiv.) was added to a solution of **1** (13.3 mg, 0.01 mmol, 1 equiv.) in CD₂Cl₂ (0.8 mL) in a medium-walled J. Young NMR tube. ¹H NMR (CD₂Cl₂, 500 MHz, -70 °C): δ 7.01 (t, ³J_{H-H} = 8.0 Hz, 1H, 4-H), 6.66 (d, ³J_{H-H} = 8.0 Hz, 2H, 3- and 5-H), 1.27 and 1.22 [vt each, 36H, 2 × P(*t*Bu)₂], -4.91 (s, 1H, SiH, J_{Si-H} = 79 Hz), -44.17 (t, ²J_{P-H} = 11.6 Hz, 1H, IrH). ³¹P{¹H} NMR (CD₂Cl₂, 162 MHz, -70 °C): δ 183.9. ³¹P{¹H} NMR (CD₂Cl₂, 162 MHz, 23 °C): δ 183.2. ²⁹Si{¹H} DEPT 45 (C₆D₄Cl₂, 79 MHz, 23 °C) δ 30.2. The NMR probe temperature was calibrated with neat

methanol, and the variable-temperature ^1H NMR dynamic behavior of **2** is discussed in the text.



Isolation and X-ray Crystallography of 2. Crystals of **2** were grown by slow diffusion of pentane into a $\text{C}_6\text{H}_5\text{F}$ solution of **1** and excess Et_3SiH at room temperature under Ar. Crystallographic data were collected on a Bruker SMART APEX-2 using Cu-K α radiation. Final agreement indices were R_1 (all) = 2.48% and R_2 (all) = 6.21%, with H1 and H2 found in difference maps and refined. All other atoms were refined anisotropically. Selected crystallographic data appear in Table 3.3.

Table 3.3. X-ray Crystal Structure Data for Complex **2**.

Empirical Formula	$\text{C}_{52}\text{H}_{56}\text{BF}_{20}\text{IrO}_2\text{P}_2\text{Si}$	
Formula Weight	1386.01	
Crystal System	Triclinic	
Space Group	P-1	
Unit Cell Dimensions	$a = 12.4133(7) \text{ \AA}$	$\alpha = 70.938(2)^\circ$
	$b = 13.9005(8) \text{ \AA}$	$\beta = 87.821(2)^\circ$
	$c = 17.0525(9) \text{ \AA}$	$\gamma = 88.840(2)^\circ$
Volume	$2779.0(3) \text{ \AA}^3$	
Z	2	
Absorption Coefficient	6.366 mm^{-1}	
Density (calculated)	1.656 mg/m^3	
Crystal size	$0.25 \times 0.25 \times 0.05 \text{ mm}^3$	
Data/restraints/parameters	10084/ 1 / 735	
Final R indices $[I > 2\sigma(I)]$	$R_1 = 0.0246, wR_2 = 0.0620$	

References

- (1) a) Kubas, G. J. *Metal Dihydrogen and σ -Bond Complexes*, Kluwer Academic/Plenum Publishers, New York, **2001**. b) Bercaw, J. E.; Labinger, J. A. *Proc. Natl. Acad. Sci. U.S.A.* **2007**, *104*, 6899, and the following articles in this special feature "Coordination Chemistry of Saturated Molecules".
- (2) a) Yang, J.; Brookhart, M. *J. Am. Chem. Soc.* **2007**, *129*, 12656. b) Doherty, M. D.; Grant, B.; White, P. S.; Brookhart, M. *Organometallics* **2007**, *26*, 5950.
- (3) a) Perutz, R. N.; Sabo-Etienne, S. *Angew. Chem. Int. Ed. Engl.* **2007**, *46*, 2578. b) Matthews, S. L.; Pons, V.; Heinekey, D. M. *Inorg. Chem.* **2006**, *45*, 6453. c) Kubas, G. J. *Catal. Lett.* **2005**, *104*, 79. d) Kubas, G. J. *Adv. Inorg. Chem.* **2004**, *56*, 127. e) Buhl, M.; Mauschick, F. T. *Organometallics* **2003**, *22*, 1422. f) Fang, X.; Huhmann-Vincent, J.; Scott, B. L.; Kubas, G. J. *J. Organometal. Chem.* **2000**, *609*, 95. g) Chang, S.; Scharrer, E.; Brookhart, M. *J. Mol. Catal. A.* **1998**, *130*, 107. h) Scharrer, E.; Chang, S.; Brookhart, M. *Organometallics* **1995**, *14*, 5686. i) Brookhart, M.; Grant, B. E. *J. Am. Chem. Soc.* **1993**, *115*, 2151. j) Luo, X. -L.; Crabtree, R. H. *J. Am. Chem. Soc.* **1989**, *115*, 2527.
- (4) For reviews: a) Nikonov, G. *Adv. Organomet. Chem.* **2005**, *53*, 217. b) Corey, J. Y.; Braddock-Wilking, J. *Chem. Rev.* **1999**, *99*, 175. c) Schubert, U. *Adv. Organomet. Chem.* **1990**, *30*, 151. d) Lachaize, S.; Sabo-Etienne, S. *Eur. J. Inorg. Chem.* **2006**, 2115. e) Lin, Z. *Chem. Soc. Rev.* **2002**, *31*, 239. f) Schneider, J. J. *Angew. Chem. Int. Ed. Engl.* **1996**, *35*, 1068. g) Crabtree, R. H. *Angew. Chem. Int. Ed. Engl.* **1993**, *32*, 789.
- (5) Calculations have identified complexes with minima showing smaller Si-M interactions: a) Nagaraja, C. M.; Parameswaran, P.; Jemmis, E. D.; Jagirdar, B. R. *J. Am. Chem. Soc.* **2007**, *129*, 5587. b) Vyboishchikov, S. F.; Nikonov, G. I. *Organometallics* **2007**, *26*, 4160. c) Ignatov, S. K.; Rees, N. H.; Tyrrell, B. R.; Duberley, S. R.; Razuvaev, A. G.; Mountford, P.; Nikonov, G. I. *Chem. Eur. J.* **2004**, *10*, 4991. d) Rabaâ, H.; Saillard, J. -Y.; Schubert, U. *J. Organomet. Chem.* **1987**, *330*, 397.
- (6) A neutral Zr dimer with a linear Si-H-Zr interaction has been observed in solid state but does not persist in solution: Ciruelo, G.; Cuenca, T.; Gómez, R.; Gomez-Sal, R.; Martin, A. *J. Chem. Soc., Dalton Trans.* **2001**, 1657.
- (7) Fang, X.; Scott, B. L.; John, K. D.; Kubas, G. J. *Organometallics* **2000**, *19*, 4141.
- (8) Freeman, S. T. N.; Lemke, F. R.; Brammer, L. *Organometallics* **2002**, *21*, 2030.

- (9) Sykes, A.; Brookhart, M. unpublished work.
- (10) a) Goettker-Schnetmann, I.; Brookhart, M. *J. Am. Chem. Soc.* **2004**, *126*, 9330. b) Goettker-Schnetmann, I.; White, P.; Brookhart, M. *J. Am. Chem. Soc.* **2004**, *126*, 1804. c) Goettker-Schnetmann, I.; White, P.; Brookhart, M. *Organometallics* **2004**, *23*, 1766.
- (11) Usually $J_{\text{Si-H}} < 20\text{Hz}$ for classical H-M-Si interactions, see ref. 3; $J_{\text{Si-H}} = 175\text{ Hz}$ for free Et_3SiH .
- (12) For example, Ir-Si = 2.390(1) Å in $\text{Cp}^*\text{Ir}(\text{H})_2(\text{SiEt}_3)_2$: Ricci, J. S.; Koetzle, T. F.; Fernandez, M. J.; Maitlis, P. M.; Green, J. C. *J. Organomet. Chem.* **1986**, *299*, 383.
- (13) Gaussian 03, Revision D.02; B3LYP; LANL2DZ on Ir(+f polarization); 6-311G** on other atoms.
- (14) a) Reed, A. E.; Curtiss, L. A.; Weinhold, F. *Chem. Rev.* **1988**, *88*, 899. b) Reed, A. E.; Weinstock, R. B.; Weinhold, F. *J. Chem. Phys.* **1985**, *83*, 735.
- (15) Maseras, F.; Duran, M.; Lledós, A.; Bertran, F. *J. Am. Chem. Soc.* **1992**, *114*, 2922.
- (16) Ng, S. M.; Lau, C. P.; Fan, M. -F.; Lin, Z. *Organometallics* **1999**, *18*, 2484.